Design of emulsion-based adjuvants for animal vaccines

by

Yulia Burakova

B.S./M.S., Mendeleev University of Chemical Technology of Russia, 2010

AN ABSTRACT OF A DISSERTATION

submitted in partial fulfillment of the requirements for the degree

DOCTOR OF PHILOSOPHY

Department of Chemical Engineering
College of Engineering

KANSAS STATE UNIVERSITY
Manhattan, Kansas

2018

Abstract

Vaccination is one of the most essential steps in controlling and preventing economically important infectious diseases in livestock. Vaccines need to be effective at producing a high level of immune responses that protect the animal from future encounters with infectious agents. Additional requirements for veterinary vaccines include safety, inexpensive components, and feasibility for large-scale production. These factors make emulsions attractive vaccine adjuvants. The use of emulsions as adjuvants (substances that help to amplify the immune responses to the antigen) has been explored for decades. However, emulsions are commonly produced with expensive and energy-demanding devices which impact the price of the adjuvant, therefore, affecting the price of the final product.

This study examined low-energy emulsification methods to meet the requirements for a simple and low-cost vaccine manufacture that avoided utilizing complicated equipment. Spontaneous emulsification (SE) and phase inversion composition (PIC) was explored to formulate stable emulsions with nanometer droplet sizes. The study on the impact of oil composition on the formation of emulsions produced by SE revealed that addition of medium-chain triglycerides into the oil phase is beneficial for droplet size reduction and stability of emulsions. Box-Behnken design (BBD) was used to develop mathematical relationships between formulation variables and droplet size, polydispersity, zeta potential, and stability of emulsions formulated via SE. The BBD allowed the study of a simultaneous effect of multiple variables and formulate emulsions with certain physical characteristics, an effect that suggested that there was a more effective approach in designing complex systems like emulsions.

New adjuvants containing mixtures of oils and surfactants were developed to produce emulsions with nanoscale droplet diameters and multiple water-in-oil-in-water structures via the

PIC approach. The strong antibody responses and the absence of injection site side effects were observed in animals that received emulsion vaccines with experimental adjuvants.

Additionally, inexpensive food-grade saponin extract was examined for stabilizing and increasing immunostimulatory activity of oil-in-water emulsion-based adjuvants. The adjuvants demonstrated high immune responses in pigs after co-administration with a subunit protein antigen.

Design of emulsion-based adjuvants for animal vaccines

by

Yulia Burakova

B.S./M.S., Mendeleev University of Chemical Technology of Russia, 2010

A DISSERTATION

submitted in partial fulfillment of the requirements for the degree

DOCTOR OF PHILOSOPHY

Department of Chemical Engineering
College of Engineering

KANSAS STATE UNIVERSITY
Manhattan, Kansas

2018

Approved by:

Co-Major Professor
Dr. John Schlup

Approved by:

Co-Major Professor
Dr. Jishu Shi

Copyright

Abstract

Vaccination is one of the most essential steps in controlling and preventing economically important infectious diseases in livestock. Vaccines need to be effective at producing a high level of immune responses that protect the animal from future encounters with infectious agents. Additional requirements for veterinary vaccines include safety, inexpensive components, and feasibility for large-scale production. These factors make emulsions attractive vaccine adjuvants. The use of emulsions as adjuvants (substances that help to amplify the immune responses to the antigen) has been explored for decades. However, emulsions are commonly produced with expensive and energy-demanding devices which impact the price of the adjuvant, therefore, affecting the price of the final product.

This study examined low-energy emulsification methods to meet the requirements for a simple and low-cost vaccine manufacture that avoided utilizing complicated equipment. Spontaneous emulsification (SE) and phase inversion composition (PIC) was explored to formulate stable emulsions with nanometer droplet sizes. The study on the impact of oil composition on the formation of emulsions produced by SE revealed that addition of medium-chain triglycerides into the oil phase is beneficial for droplet size reduction and stability of emulsions. Box-Behnken design (BBD) was used to develop mathematical relationships between formulation variables and droplet size, polydispersity, zeta potential, and stability of emulsions formulated via SE. The BBD allowed the study of a simultaneous effect of multiple variables and formulate emulsions with certain physical characteristics, an effect that suggested that there was a more effective approach in designing complex systems like emulsions.

New adjuvants containing mixtures of oils and surfactants were developed to produce emulsions with nanoscale droplet diameters and multiple water-in-oil-in-water structures via the

PIC approach. The strong antibody responses and the absence of injection site side effects were observed in animals that received emulsion vaccines with experimental adjuvants.

Additionally, inexpensive food-grade saponin extract was examined for stabilizing and increasing immunostimulatory activity of oil-in-water emulsion-based adjuvants. The adjuvants demonstrated high immune responses in pigs after co-administration with a subunit protein antigen.

Table of Contents

List of Figures

List of Tables

Acknowledgments

I want to express my gratitude and appreciation to both my advisors Dr. John Schlup and Dr. Jishu Shi, and thank them for their infinite support, understanding, and many helpful suggestions and discussions. Thank you to Dr. Ryan Hansen, Dr. Urara Hasegawa, and Dr. Michael Apley for finding time and serving on my committee.

I also want to thank all current and former members of Shi group. I especially grateful to Dr. Rachel Madera, Dr. Lihua Wang, Dr. Wenjie Gong, Sterling Buist, Karen Lleellish, Nathan Witters, Calla Reilley, and Chase Cunningham for their help, friendship, and many fun moments and ice-cream breaks that we had throughout all these years. Additionally, I would like to thank Keleigh Schettler who helped me with editing this dissertation.

I want to recognize the assistance of my undergraduate workers Maggie Meyer, Rachel Anstaett, and Megan Clapp. Chapter 3 and 5 contain the data that both Maggie and Rachel helped me to obtain.

I am thankful to Dr. Maggie Behnke, Dr. Brooke Bloomberg, and Dr. Sally Olson from Comparative Medicine Group for their assistance with animal studies. In addition, I want to thank veterinary pathologists Dr. Jamie Henningson and Dr. Ada Cino-Ozuna who found time in their busy schedules and helped us with animal examinations.

I also would like to thank to Dr. Dan Boyle from Department of Biology at Kansas State University and Ravi Thakkar from Nanotechnology Innovation Center of Kansas State for their professional help with TEM imaging of emulsions.

Finally, I want to thank my family who always supported and encouraged me to pursue my studies in graduate school. Especially I want to thank my husband Iskandar. You are my soulmate, my best friend, and my rock. Without you, none of this would be possible.

Dedication

To my mom. For everything I am now. I know you would be proud of me.

Chapter 1 - Introduction and Background

Introduction

Every year livestock industries worldwide lose billions of dollars from the outbreaks of devastating animal diseases. Vaccination is among the most important approaches to control and prevent economically important infectious diseases. Design and selection of suitable adjuvants are essential steps in the development of non-live vaccines. Adjuvants are substances or systems administered together with the pathogen/antigen to help amplify host immune responses to the antigen. Several factors shall be considered in the development of adjuvants for veterinary vaccines including but not limited to safety, cost of materials, and feasibility for large-scale production.

This research was devoted to the development of inexpensive and effective animal vaccine adjuvants that will form emulsions after mixing with an antigenic aqueous phase. To achieve simplicity of vaccine preparation, the emphasis was given to low-energy emulsification methods, such as phase inversion and spontaneous or self-emulsification (SE). Due to this emphasis, effects of oil composition on the formation and stability of emulsions produced by SE is studied in Chapter 2 of this thesis. The combination of medium chain triglycerides and paraffin oil has been demonstrated as the most effective way for droplet size reduction and increased stability of emulsions obtained via SE. Simultaneous impact of multiple formulation variables, including the surfactant-to-oil ratio on physical characteristics of self-emulsified emulsions using the design of experiment (DOE) approach, is investigated in Chapter 3. The DOE allowed for identification of a mathematical relationship between formulation parameters and responses, such as average size, polydispersity, zeta potential, and stability of emulsion droplets. This method is a promising

systematic approach towards optimizing emulsions that have characteristics required for the vaccine industry.

Application of phase inversion composition (PIC) for low-energy emulsification is explored in Chapter 4 and Chapter 5. Additionally, the possibility to use inexpensive food-grade saponin extract as an emulsifier and immunostimulant in an emulsion-based adjuvant is studied in Chapter 4. Emulsions formulated with food-grade saponins were stable for a prolonged time at elevated temperatures and elicited strong immune responses in pigs after co-administration with a subunit protein as an antigen.

The production of vaccines containing water-in-oil-in-water emulsions via an energy-efficient PIC method is described in Chapter 5. There, novel mixtures of oils and surfactants forming stable emulsions after mixing with an aqueous phase are presented. The nanoscale size and multiple structure of emulsion droplets were confirmed with dynamic light scattering and transmission electron microscopy. These oil-surfactant mixtures were tested in vaccine formulations demonstrating strong antibody responses in animals. In addition, experimental vaccines did not cause health issues nor significant adverse reactions at injection sites.

Finally, the summary of this thesis and suggestions for future directions are given in Chapter 7.

Background

Adjuvants for veterinary vaccines[1]

In the early 20th century, French veterinarian, Gaston Ramon, observed that the addition of different substances, such as calcium chloride, saponins, starch, vegetable oil, and bacteria to the ‘‘anatoxine diphte´rique’’ vaccine for horses promoted inflammation at the vaccine injection sites, a reaction that is responsible for the enhanced production of antibodies against toxins *(1)* . Since then, adjuvants have played a very important role in vaccine technology for both animals and humans. The development of safe, highly purified subunit and inactivated vaccines requires safe and potent adjuvants because the antigens in these types of vaccines are usually less immunogenic compared with modified live microbes *(2)*. To date, numerous compounds of organic, inorganic, synthetic, and natural origin demonstrate an ability to form potent adjuvant properties to stimulate immune responses *(3)*. These substances can be broadly divided in two different groups: immunostimulants (saponins, Toll-like receptor (TLR) agonists, cytokines] and delivery agents (emulsions, microparticles, mineral salts) *(4, 5)*. Immunostimulants stimulate the antigen-presenting cells (APCs) and promote the secretion of various cytokines. Delivery agents help to preserve the conformation of antigens (Ag) for proper presentation to APCs and provide a slow release for continuing immune stimulation. For instance, TLR agonists and other immunostimulatory substances can enhance immune cell recruitment and cytokine secretion, whereas emulsions and mineral salts can produce a depot effect at the injection site with a prolonged release of the antigen and continued stimulation of immune cells.

[1] This section was partially reproduced from Burakova Y., et al, Adjuvants for animal vaccines in Viral Immunology, 2018, Vol.31(1), pp.11-22. Final publication is available from Mary Ann Liebert, Inc., publishers http://doi.org/10.1089/vim.2017.0049.

Vaccine development for food animals differs from that of human and companion animals. In humans, the health and well-being of the individual are of paramount importance, whereas disease control measures for farm animals must be cost-effective. While human vaccines can be marketed at more than a $100 per dose, the price for vaccines used in the livestock industry is usually no more than a couple of dollars per dose *(6, 7)*. Therefore, less financial resources are available for research and development of animal vaccines compared with that for human vaccines. On the other hand, livestock vaccine technology has fewer regulatory restrictions compared with the development of human vaccines *(7)*. Thus, due to safety restrictions, some compounds are prohibited for use in a human vaccine (Quil-A®, mineral oil-based emulsions), but are successfully employed in vaccines for livestock species. For more information about differences between human and veterinary vaccine research and development, the readers are referred to the review by Knight-Jones et al. *(6)*.

Emulsions

Emulsions have been employed as adjuvant systems in animal vaccines for a long time and are a good choice for animal vaccines because they are relatively simple to produce, cost-effective, and demonstrate good efficacy in the production of antibody responses *(4)*.

Classification of emulsions

Emulsions are the mixture of two immiscible liquids, one of which is organized into droplets, stabilized by an interfacial surfactant layer, and dispersed into the other. Thus, the dispersion of an organic liquid such as oil in water is called an oil-in-water (o/w) emulsion, while water droplets dispersed in a continuous oil phase are called water-in-oil (w/o) emulsions *(8)*. In addition, there are multiple or double emulsions, such as water-in-oil-in-water (w/o/w) or oil-in-water-in-oil (o/w/o). These systems are occasionally referred to as “emulsions of emulsions” as

they, in the case of w/o/w emulsions, contain water droplets within the oil droplets, which, at the same time, are dispersed into a continuous water phase.

Conventional emulsions are thermodynamically unstable, meaning they will eventually separate into their oil and water phases over time. They can be macroemulsions with droplet sizes in 1 to 5 μm range and nanoemulsions with diameters of droplets less than 1 μm *(9)*. A lot of attention has recently been given to thermodynamically stable emulsions denoted micellar emulsions or microemulsions. Microemulsions are generally in the 5-50 nm size range and are stable until the introduction of the external energy input *(10)*.

The difference between conventional emulsions and microemulsions can be better described using the concept of the free energy of emulsion formation (G_{EF}). Thus, according to the second law of thermodynamics, change in the free energy of emulsion formation will be equal to the interfacial free energy minus the configurational entropy *(10)*:

$$\Delta G_{EF} = \gamma_{IE} \Delta A - T \Delta S \qquad (1.1)$$

where ΔG_{EF} – the change in the free energy of emulsion formation (J), γ_{IE} - interfacial tension (J m^{-2}), T- temperature (K), ΔA – change in the interfacial area (m^2), and ΔS - change in the entropy (J K^{-1}) all due to the emulsification procedure.

In the case of conventional emulsions, the interfacial free energy term will be significantly larger than the configurational entropy, resulting in a positive ΔG_{EF} *(11)*. Therefore, to form an emulsion, energy needs to be introduced to render the system thermodynamically unstable. However, an energy barrier between emulsion droplets can be created by the surfactant providing the kinetical stability to the system *(10, 11)*.

On the contrary, ΔG_{EF} is negative when the interfacial free energy is very low. This results in formation of thermodynamically stable emulsions or microemulsions. The free energy of emulsion formation is also negative in spontaneous emulsification, which will be explored later in

this chapter. Usually, a high ratio of surfactant to oil is required to achieve very low interfacial tension and, as a result, thermodynamically stable emulsions *(10, 11)*.

Surfactants and the Hydrophilic-Lipophilic Balance (HLB) concept

Surface active-agents, or surfactants, help to achieve kinetic stability of emulsions and are amphiphilic substances composed of hydrophilic and hydrophobic moieties. The hydrophilic portion is usually a water-soluble polar or ionic group while the hydrophobic portion of the surfactant is usually a hydrocarbon or fatty acid chain insoluble in the water phase. This structure allows a surfactant molecule to absorb at the interface of two phases, lowering the surface tension between them *(9)*.

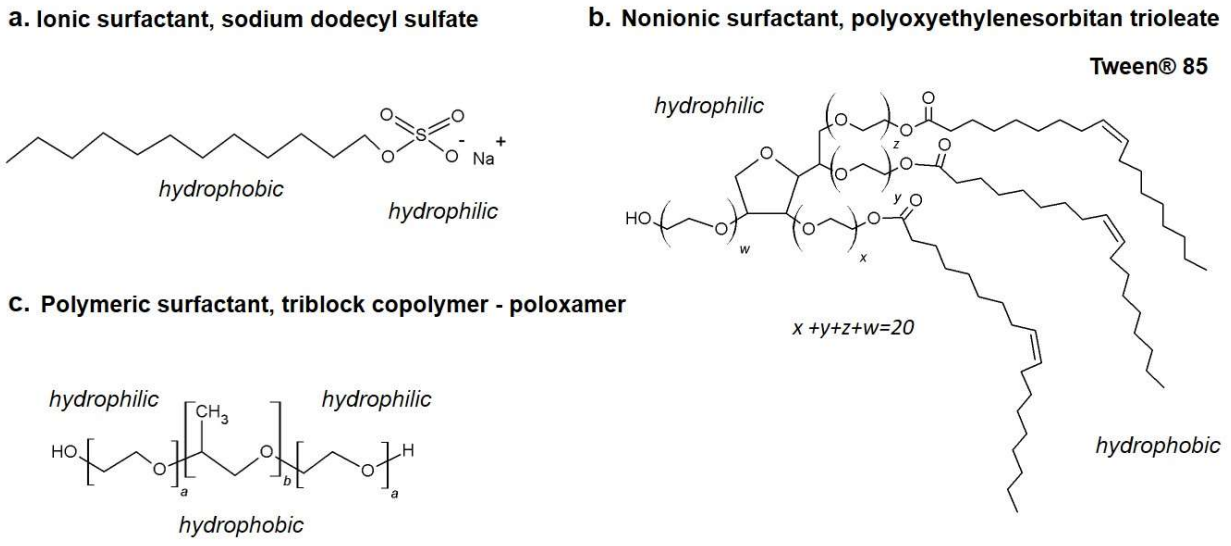

Figure 1.1 Chemical structure of different types of surfactants.

Depending on the type of hydrophilic part of a molecule, surfactants can be ionic (anionic and cationic) or nonionic, and can further be classified as monomeric or polymeric substances (Fig 1.1) *(12)*. For example, sodium dodecyl sulfate (SDS) is an anionic surfactant commonly used as a detergent in hygienic and other cleaning products *(13)*. SDS is composed of a water-insoluble hydrocarbon tail and a water-soluble (anionic) sulfonate group, which dissociates in water on an

amphiphilic anion and Na^+ cation (Fig. 1.1a). In contrast to ionic surfactants, nonionic surfactants do not undergo ionization after dissolving in water. The sorbitan esters and their ethoxylates are typical nonionic surfactants commonly used in food and pharmaceuticals due to their lower toxicity when compared with ionic surfactants *(14)*. Figure 1.1b demonstrates the structure of nonionic polyoxyethylenesorbitan trioleate (Tween® 85) surfactant, which is a product of ethoxylation of sorbitan trioleate (Span® 85) that is obtained after dehydration of sorbitol followed by esterification with oleic acid *(15)*. Polymeric surfactants are also nonionic in nature and are composed of high-molecular hydrophilic and hydrophobic blocks. Figure 1.1c shows an example of a typical polymeric surfactant – poloxamer, triblock co-polymer. Poloxamer is composed of a central hydrophobic poly(propylene oxide) with two hydrophilic chains of poly(ethylene oxide) on each end *(16)*.

The Hydrophilic-Lipophilic Balance (HLB) concept, introduced by Griffin, suggests that the proportion between hydrophilic and hydrophobic groups in the surfactant molecules can indicate behavior of the surfactant *(17, 18)*. According to Griffin, an HLB value of a surfactant can be obtained using the following empirical equation *(18)*:

$$HLB = 20 * \frac{M_h}{M} \qquad (1.2)$$

where M_h– molecular weight of the hydrophilic group in surfactant (g mol^{-1}) and M – molecular weight of the surfactant (g mol^{-1}). Surfactants that are hydrophilic in nature will have high HLB numbers (>10), while surfactants that are lipophilic will have low HLB numbers (<10). The HLB concept is commonly used among formulation scientists for the characterization of surfactant properties and their selections for an application (Table 1.1) *(17, 19)*.

Table 1.1 HLB range and different classes of surfactants.

HLB value	Surfactant
< 10	Hydrophobic (water-insoluble)
> 10	Hydrophilic (oil-insoluble)
1-3	Anti-foaming agent
4-6	W/o emulsifier
7-9	Wetting agent
8-16	O/w emulsifier
13-16	Detergent
16-18	Solubiliser

Emulsion production methods

Emulsions can be formed with different equipment and approaches (Fig. 1.2). The pharmaceutical industry routinely uses high-pressure valve homogenizers and microfluidizers. These systems deliver high throughput of emulsions with average droplet sizes around 0.2 μm and narrow size distributions *(20)*. To provide emulsions with fine droplets, these devices force a liquid sample through a valve or interaction chamber with microchannels (in the case of microfluidizer) which results in the disruption of droplets due to the high shear, pressure drop, and cavitation *(21, 22)*. Among the disadvantages of these machines, the significant power demand and high stress on the sample, including elevated temperatures that can affect the physical characteristics of emulsions as well as other active ingredients in the formulation *(21)*.

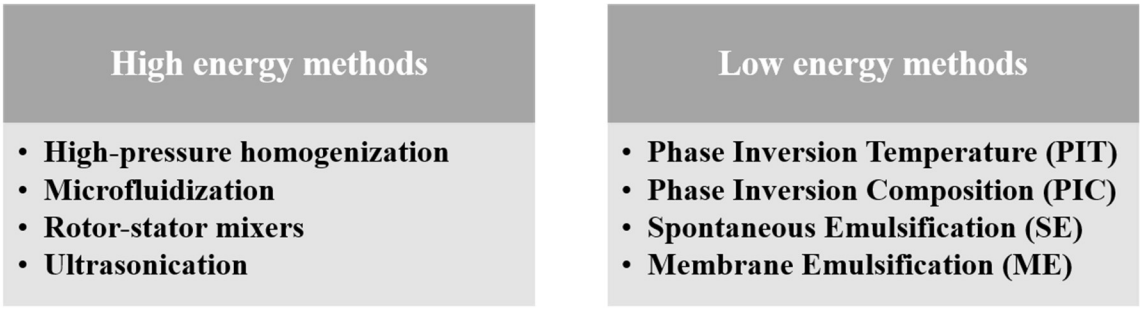

Figure 1.2 Methods of emulsification.

Rotor-stator mixers are also commonly employed in the industrial and laboratory settings and allow users to obtain emulsions with droplet diameters between 2 to 20 μm by high sheer mixing generated by the rotor *(23)*. Although the ultrasonic generators can form emulsions with droplets less than 1 μm in diameter (due to the low product throughput), these devices are usually used in laboratory settings only *(21)*. They generate high-intensity ultrasonic waves to create microturbulences and cavitation for dispersing from one phase into another *(24)*.

The formation of emulsions by low-energy approaches, such as phase inversion and spontaneous emulsification (SE), has recently become popular in pharmaceutical and food industries because of low energy demand and simplified equipment *(25)*. Additionally, these methods allow obtaining emulsion droplets that are nanometers in size, have a low polydispersity, and a prolonged stability. However, the right selection of surfactants and oils are key factors for successful self-emulsification and phase inversion, usually requiring high concentrations of surfactants to achieve small droplets and extended stability of the emulsions *(26)*.

Phase inversion refers to the emulsification procedures occurring when an oil-in-water emulsion inverts into a water-in-oil emulsion, or vice versa, because of a change in temperature (PIT) or composition (PIC). During the PIT, temperature changes affect the surfactant's affinity for the two phases, thus making it more hydrophilic or lipophilic *(27)*; the dispersed phase becomes the continuous phase and vice versa. Phase inversion composition (PIC) involves the gradual addition of water to the oil-surfactant mixture to obtain an o/w emulsion through the initial formation of a w/o emulsion *(25)*. The mechanism of PIC, also called catastrophic phase inversion, is similar to PIT as it involves the hydration-driven change of interfacial curvature when water is added. This reaction leads to reduced oil solubilization, supersaturation, and droplet nucleation *(28)*.

Spontaneous emulsification, or self-emulsification, occurs when an oil phase is introduced into a water phase, producing a fine emulsion without any energy input due to the negative values of free energy of emulsion formation *(29)*. In contrast to phase inversion, there is no change in the surfactant interfacial curvature. The surfactant molecules diffuse from the oil (dispersed) phase and into the water (continuous) phase followed by nucleation and growth of emulsion droplets *(29)*. This approach has become very popular in the pharmaceutical industry for production of so-called self-emulsifying drug delivery systems (SEDDS): solid, semi-solid or liquid mixtures of oils, surfactants, and active ingredients that self-emulsify in the gastro-intestinal tract after pre-oral administration *(30)*.

Another low-energy approach, membrane emulsification (ME), occurs by forcing a dispersed phase into a continuous phase through a microporous membrane that produces highly monodispersed droplets with a controlled size distribution *(31)*. The low throughput in ME limits its industrial application, however, this method is suitable for production of emulsions for subsequent use as templates for fabrication of particles with complex and non-spherical structures *(31)*.

Breakdown and degradation pathways in emulsions

As mentioned previously, conventional emulsions are unstable and tend to separate into oil and water over time in order to minimize the interfacial area and free energy of formation. Stability of emulsions is determined by the resistance of droplets to coalesce. Coalescence occurs due to the strong Van der Waals attraction forces, which bring two droplets so close to each other that the liquid film between them ruptures resulting in their fusion into one big droplet; this ultimately leads to complete phase separation *(32)*. Different degradation pathways can result in coalescence and emulsion breakdown (Fig. 1.3). Among them, creaming and sedimentation occurs due to gravitational forces that overpower the Brownian motion. Due to density differences, larger

droplets will move to the top (creaming) or deposit on the bottom of the vessel (sedimentation) *(9, 12)*. One way to prevent creaming and sedimentation is to use oil with a density similar to the density of water. However, in practice, the more reliable approach is reduction of the droplet size or by addition of a thickener agent to increase viscosity of the continuous phase *(9)*.

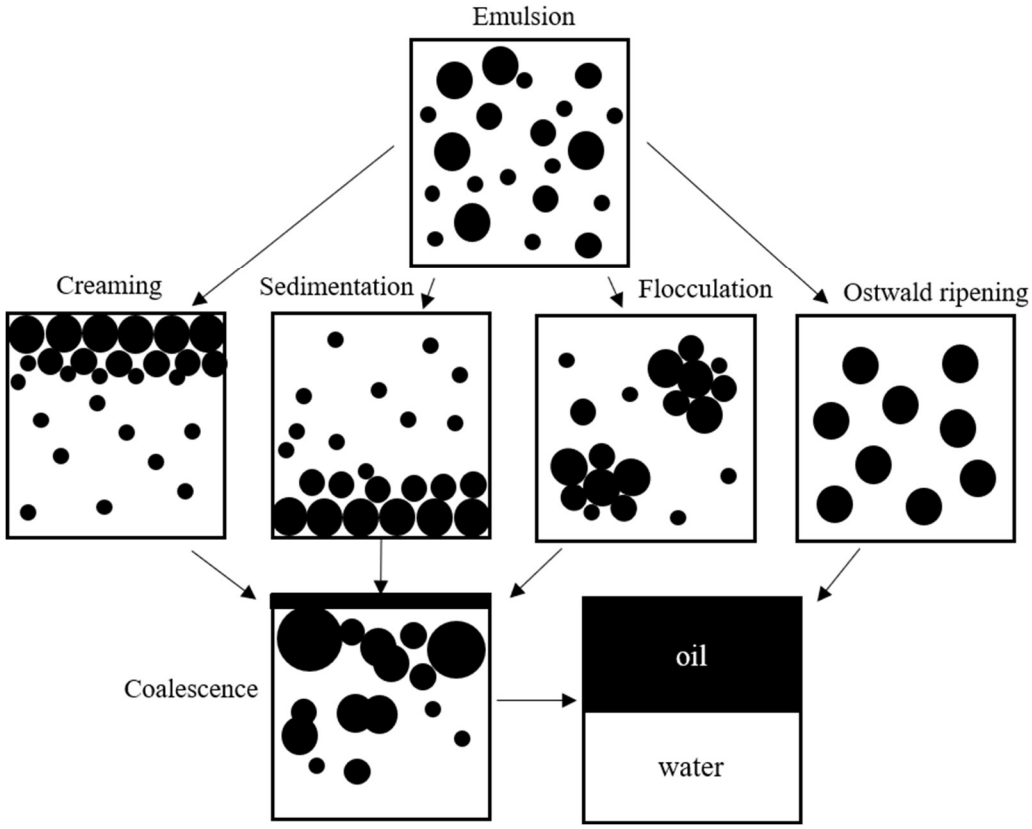

Figure 1.3 Schematic illustration of emulsion degradation processes.

Flocculation, the phenomenon where emulsion droplets form clusters, occurs when the repulsion between droplets is weaker than Van der Waals attraction forces (Fig. 1.3). Because of flocculation, accumulations of the droplets will move to the top or precipitate on the bottom, depending on the density. Flocculation can also lead to the coalescence of droplets *(9, 33)*. To offset Van der Waals attraction forces and prevent, or slow, both flocculation and coalescence,

stronger repulsive forces between the emulsion droplets must be created. This can be achieved by creation of either an electrostatic or steric barrier.

Electrostatic repulsion (V_R) between particles is a function of the zeta potential *(34)*:

$$V_R = 2\pi\varepsilon_r\varepsilon_0 R\zeta^2 \exp(-\kappa D) \qquad (1.3)$$

where R - radius of the particle (m), ε_r – dielectric constant of the solvent ($CV^{-1}m^{-1}$), ε_0 - permittivity of the vacuum ($C^2\ J^{-1}m^{-1}$), ζ - zeta potential (V), and κ - Debye-Hückel parameter related to the "thickness" of the double layer (m^{-1}), D – separation distance (m). From this equation, the higher magnitude of the zeta potential, the stronger the repulsion and more stable the system becomes. Zeta potential is a potential difference between the droplet and the stationary layer of the continuous phase attached to that droplet. Therefore, it is a function of surface charge of the particle, which arises from the absorbed layer of the surfactant. In the case of ionic surfactants, the amphiphilic ion determines the sign of the surface charge *(19)*. For nonionic surfactants, the charge on the droplet appears from hydroxyl ions absorbed from the aqueous phase *(35)*. Zeta potential depends on the nature and composition of the continuous phase, which includes pH and ionic strength of the solution.

Steric stabilization between emulsion droplets can be created by nonionic and polymeric surfactants. The repulsion produced by steric stabilization is related to the thermodynamic behavior of polymeric chains in solutions. Loss of configurational entropy of the chains in the compressed absorbed layer of two particles increases the Gibbs free energy, which is unfavorable; therefore, steric interaction is always repulsive *(36)*.

Finally, Ostwald ripening can also lead to emulsion degradation and usually occurs in nanoemulsions. Although an emulsion is usually formed from two immiscible liquids, occasionally, their mutual solubility cannot be ignored. Consequently, smaller droplets that have a larger solubility will dissolve over time, and their molecules will re-deposit onto bigger droplets;

this results in an increase of the average size of emulsion droplets. Ostwald ripening can be reduced by using less soluble oil. In addition, polymeric emulsifiers can help to create a thick layer at the oil/water interface, further inhibiting the movement of oil molecules to and from droplets *(33)*.

Emulsions as adjuvants[2]

Different types of emulsions have different mechanisms of action in vaccine formulations (Fig. 1.4). A water-in-oil (w/o) emulsion is a dispersion of water droplets within a continuous oil phase (Fig. 1.4a). The antigen is entrapped in the water phase surrounded by a continuous oil phase and slowly released upon breakdown of oil after injection *(37)*. The depot effect at the injection site preserves the antigen from fast clearance by phagocytosis and the liver and, therefore, extends the time available for immune cell recruitment and antigen processing *(4)*.

The most well-known example of w/o emulsion adjuvants is Freund's adjuvants *(38)*. Based on the paraffin oil and heat-killed and dried mycobacteria (Freund's complete adjuvant, FCA) or without mycobacteria (Freund's incomplete adjuvant, FIA), these adjuvants are very efficient in inducing high-titer antibody responses. However, Freund's adjuvants produce strong adverse reactions, such as local inflammatory lesions, pain, and distress, which have prevented their use in animal and human vaccines *(39)*. Successfully commercialized w/o emulsions are available under the brand name Montanide™ Incomplete Seppic Adjuvants (ISA) (Seppic, France). These adjuvants show effectiveness on the level of FIA, but have fewer side effects *(40, 41)* and are utilized in veterinary vaccines. ISA contain purified mineral or squalene oil and mannitol esters as emulsifiers. W/o Montanide adjuvants have been used in vaccines for Newcastle disease in chickens *(42)*, subunit vaccine for Mycoplasma hyopneumoniae in pigs *(43)*, inactivated

[2] This section was partially reproduced from Burakova Y., et al, Adjuvants for animal vaccines in Viral Immunology, 2018. Final publication is available from Mary Ann Liebert, Inc., publishers http://doi.org/10.1089/vim.2017.0049.

vaccine for foot-and-mouth disease (FMD) in swine *(44)* and cattle *(45, 46)*, and farmed fish vaccines for various viral and bacterial infections *(47, 48)*.

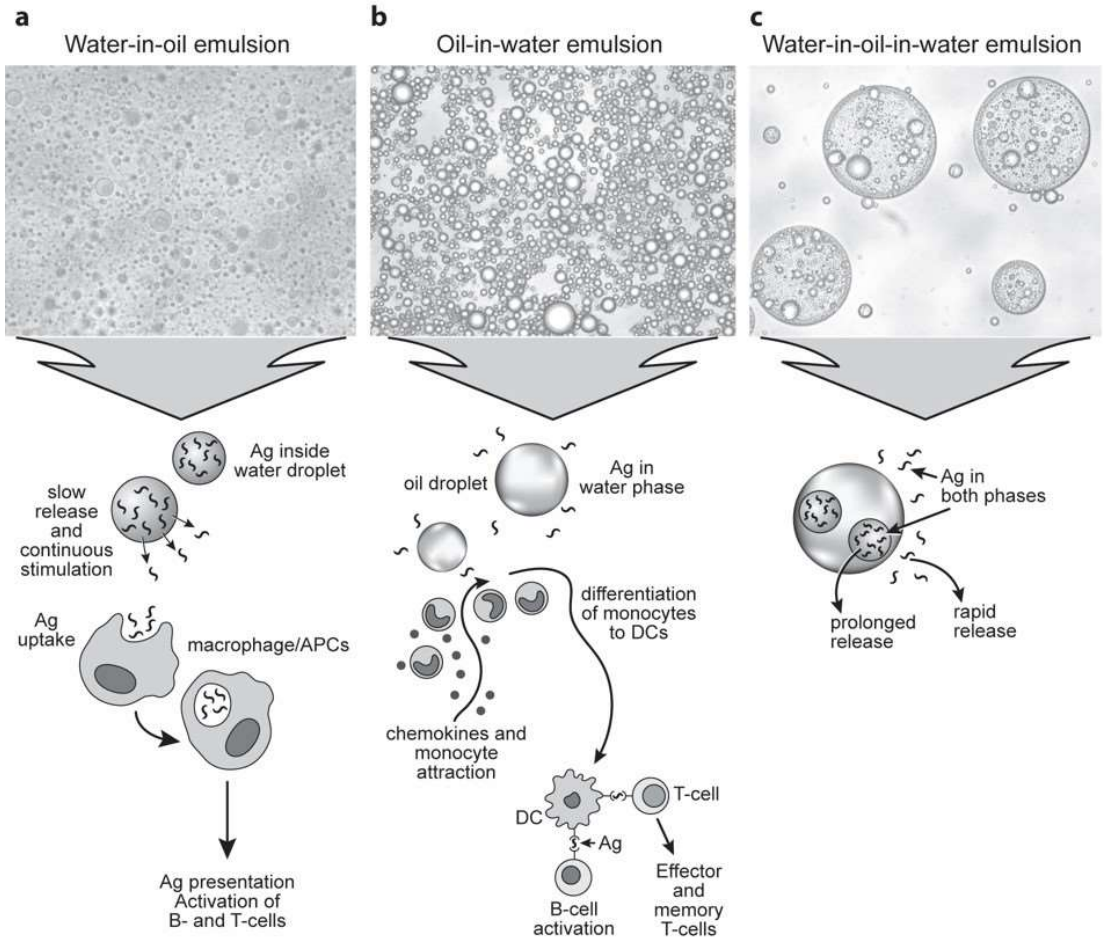

Figure 1.4 Microscopic images of different types of emulsions and their mechanisms of action as immunological adjuvants.

Another type of emulsion utilized in vaccines is oil-in-water (o/w) emulsions, formed by the dispersion of oil droplets in the aqueous phase (Fig. 1.4b). Studies on MF59 (a squalene o/w vaccine adjuvant) has shed some light on how o/w emulsions induce immune responses *(49)*. Unlike w/o emulsions, o/w emulsion-based adjuvant does not form an antigen depot at the injection site. Instead, the oil droplets facilitate the chemokine-driven immune cell recruitment and the differentiation of macrophages and dendritic cells (DCs) *(50, 51)*. MF59 demonstrated better adjuvanticity in stimulating a cell-mediated immune response against influenza virus than

aluminum hydroxide or calcium phosphate *(52)*. For veterinary applications, several commercially available o/w adjuvants exist under the brands of Montanide ISA, Emulsigen® (MVP Technologies, USA), and Meta-Stim® (Fort Dodge Laboratories, USA). These adjuvants are used in livestock vaccines against various economically important bacterial and viral antigens *(53-57)*. For example, MetaStim coformulated with inactivated equine influenza virus stimulated higher expression of IL-12 and interferon-c (IFN-c) than the vaccine with aluminum phosphate as adjuvant *(55)*. Recently, a new o/w emulsion adjuvant based on mineral oil and an inexpensive food-grade plant-based emulsifier was shown to be effective in vaccine formulations against swine influenza virus, M. hyopneumoniae, and classical swine fever (CSF) virus *(58, 59)*. These research findings suggest that o/w emulsions are more suitable adjuvants for vaccines against viral pathogens than mineral salts.

In attempts to overcome the issues with local reactions and high viscosity associated with w/o emulsions, research efforts have been devoted to developing multiphasic water-in-oil-in-water (w/o/w) emulsions (Fig. 1.4c) as vaccine adjuvants *(60-62)*. In w/o/w emulsions, oil droplets containing internal water droplets are dispersed into continuous water phase. It has been speculated that w/o/w emulsions may provide both fast release of antigens from the external water phase and prolonged release from the internal water droplets. Thus, this type of vaccine may quickly and continuously stimulate immune cells *(60)*. Multiple emulsions have a very fragile structure and their formulations present great challenges. Currently, only few w/o/w emulsion adjuvants are available on the market. Oil-based formulations, Montanide ISA 201 and 206, produce multiple emulsions after gentle mixing with antigenic aqueous phase. These adjuvants demonstrate effectiveness and provide protection for different livestock species against several economically important pathogens, including influenza and FMD viruses *(63-65)*.

The design of emulsions for adjuvant application involves several parameters. The nature and the concentration of emulsion components have a significant impact, not only on the physical and chemical stability of the final products, but also on the level of immune response and adverse reactions after vaccination *(66, 67)*. The choice of oil for the emulsion should also be considered. Several studies demonstrate that poorly metabolized mineral oil has superior efficacy in vaccine formulation compared with plant-derived oils *(66, 68)*. In addition, the proper concentration of surfactants should be determined to produce a stable emulsion, avoiding excessive amounts. Adverse reactions have been reported after vaccination with high concentrations of surfactants in emulsions *(67)*.

The insufficient knowledge in the relationship between the size of emulsion droplets and the quality and quantity of immune responses is a major limiting factor for rational design of emulsion-based adjuvants. Recently, one study has demonstrated that emulsions with droplet size of 160 nm produce significantly higher antibody responses in mice than emulsions with 20 nm droplet diameter *(69)*. However, another report speculates that particles with a size range of 10 – 200 nm can move faster and enter the lymphatic system and target the immune cells more efficiently *(70)*.

Emulsion-based adjuvants are a very attractive selection for livestock vaccine formulations. These adjuvants can be formulated using inexpensive, readily available components such as mineral oil and food-grade emulsifiers. Further investigation is needed to fully understand the relationship between physical characteristics of emulsions and their ability to induce immune responses in animals.

References

1. Ramon, G. Sur la toxine et sur l'anatoxine diphtheriques. *Ann. Inst. Pasteur* **1924**, *38*, 1-10.

2. Kallerup, R. S.; Foged, C. In *Classification of vaccines;* Foged, C., Rades, T., Perrie, Y. and Hook, S., Eds.; Subunit vaccine delivery; Springer-Verlag: New York, USA, **2015**; pp 15-29.

3. Vogel, F. R.; Powell, M. F. A compendium of vaccine adjuvants and excipients. *Pharm. Biotechnol.* **1995**, *6*, 141-228.

4. Cox, J. C.; Coulter, A. R. Adjuvants—a classification and review of their modes of action. *Vaccine* **1997**, *15*, 248-256.

5. O'Hagan, D. T. New-Generation Vaccine Adjuvants. *eLS* **2015**, 1-7.

6. Knight-Jones, T.; Edmond, K.; Gubbins, S.; Paton, D. J. Veterinary and human vaccine evaluation methods. *Proc. R. Soc. Lond. [Biol]* **2014**, *281*, 20132839.

7. Meeusen, E.; Walker, J.; Peters, A.; Pastoret, P. P.; Jungersen, G. Current status of veterinary vaccines. *Clin. Microbiol. Rev.* **2007**, *20*, 489-510.

8. Israelachvili, J. The science and applications of emulsions — an overview. *Colloids Surf. Physicochem. Eng. Aspects* **1994**, *91*, 1-8.

9. Tadros, T. F. In *Emulsion Formation, Stability, and Rheology;* Emulsion Formation and Stability; Wiley-VCH Verlag GmbH & Co. KGaA: **2013**; pp 1-75.

10. Mcclements, D. J. Nanoemulsions versus microemulsions: terminology, differences, and similarities. *Soft Matter; Soft Matter* **2012**, *8*, 1719-1729.

11. Sharma, M. K.; Shah, D. O. In *Introduction to macro- and microemulsions;* ACS Symposium Series; American Chemical Society: Washington, DC, **1985**.

12. Rosen, M. J.; Kunjappu, J. T. In *Emulsification by Surfactants;* Surfactants and Interfacial Phenomena; Wiley: USA, **2012**; Vol. 8, pp 336.

13. National Center for Biotechnology Information. PubChem Compound Database Sodium dodecyl sulfate. https://pubchem.ncbi.nlm.nih.gov/compound/3423265 (accessed 9/17, 2018).

14. Marti-Mestres, G.; Nielloud, F. In *Main surfactants used in the pharmaceutical field;* Nielloud, F., Marti-Mestres, G., Eds.; Pharmaceutical emulsions and suspensions; Marcel Dekker, Inc: New York, USA, **2000**; pp 2.

15. Chemical Book Non-ionic surfactants. https://www.chemicalbook.com/ProductCatalog_EN/1812.htm (accessed 9/27, 2018).

16. Schmolka, I. United States Patent US3740421 (A), **1973**.

17. Griffin, W. C. Classification of surface-active agents by HLB. *J. Soc. Cosmet. Chem.* **1949***, 1*, 311-326.

18. Griffin, W. C. Calculation of HLB values of non-ionic surfactants. *Am Perf Essent Oil Rev* **1955***, 65 (5)*, 26-29.

19. Tadros, T. F. In *Selection of emulsifiers;* Tadros, T. F., Ed.; Emulsion formation and stability; Wiley-VCH Verlag GmbH & Co.: Germany, **2013**; pp 26.

20. Floyd, A. G. Top ten considerations in the development of parenteral emulsions. *Pharm. Sci. Technol. Today* **1999***, 2*, 134-143.

21. Schultz, S.; Wagner, G.; Urban, K.; Ulrich, J. High- Pressure Homogenization as a Process for Emulsion Formation. *Chem. Eng. Technol.* **2004***, 27*, 361-368.

22. Anton, N.; Benoit, J.; Saulnier, P. Design and production of nanoparticles formulated from nano-emulsion templates—A review. *Journal of Controlled Release* **2008***, 128*, 185-199.

23. Pacek, A. W.; Hall, S.; Cooke, M.; Kowalski, A. J. In *Emulsification in rotor–stator mixers;* Tadros, T. F., Ed.; Emulsion Formation and Stability; Wiley-VCH Verlag GmbH & Co.: Germany, **2013**; pp 127.

24. Canselier, J. P.; Delmas, H.; Wilhelm, A. M.; Abismail, B. Ultrasound emulsification - an overview. *J. Dispersion Sci. Technol.* **2002***, 23*, 333-349.

25. Solans, C.; Solé, I. Nano-emulsions: Formation by low-energy methods. *Current Opinion in Colloid & Interface Science* **2012***, 17*, 246-254.

26. Yang, Y.; Marshall-Breton, C.; Leser, M. E.; Sher, A. A.; Mcclements, D. J. Fabrication of ultrafine edible emulsions: Comparison of high- energy and low- energy homogenization methods. *Food Hydrocoll.* **2012***, 29*, 398-406.

27. Shinoda, K.; Saito, H. The effect of temperature on the phase equilibria and the types of dispersions of the ternary system composed of water, cyclohexane, and nonionic surfactant. *Journal of Colloid and Interface Science* **1968***, 26*, 70-74.

28. Perazzo, A.; Preziosi, V. In *Chapter 3 - Catastrophic Phase Inversion Techniques for Nanoemulsification;* Jafari, S. M., McClements, D. J., Eds.; Nanoemulsions; Academic Press: **2018**; pp 53-76.

29. Solans, C.; Morales, D.; Homs, M. Spontaneous emulsification. *Curr. Opin. Colloid Interface Sci.* **2016***, 22*, 88-93.

30. Pouton, C. W. Formulation of self- emulsifying drug delivery systems. *Adv. Drug Deliv. Rev.* **1997***, 25*, 47-58.

31. Vladisavljević, G. T.; Kobayashi, I.; Nakajima, M. In *Emulsion Formation in Membrane and Microfluidic Devices;* Tadros, T. F., Ed.; Emulsion formation and stability; Wiley-VCH Verlag GmbH & Co.: Germany, **2013**; pp 77.

32. Rosen, M. J. *Surfactants and interfacial phenomena;* Hoboken, N.J. : Wiley: Hoboken, N.J., **2012**.

33. Taylor, P. Ostwald ripening in emulsions. *Adv. Colloid Interface Sci.* **1998***, 75*, 107-163.

34. Hiemenz, P. C.; Rajagopalan, R., Eds.; In *Principles of Colloid and Surface Chemistry;* Marcel Dekker, Inc: New York, **1997**; pp 650.

35. Marinova, K. G.; Alargova, R. G.; Denkov, N. D.; Velev, O. D.; Petsev, D. N.; Ivanov, I. B.; Borwankar, R. P. Charging of Oil-Water Interfaces Due to Spontaneous Adsorption of Hydroxyl Ions. *Langmuir* **1996***, 12*, 2045-2051.

36. Tadros, T. In *Electrostatic and steric stabilization of colloidal dispersions;* Ohshima, H., Ed.; Electrical Phenomena at Interfaces and Biointerfaces: Fundamentals and Applications in Nano-, Bio-, and Environmental Sciences; Wiley: Hoboken, **2012**; pp 153-172.

37. Herbert, W. J. The mode of action of mineral- oil emulsion adjuvants on antibody production in mice. *Immunology* **1968***, 14*, 301-318.

38. Freund, J.; Casals, J.; Hosmer, E. P. Sensitization and Antibody Formation after Injection of Tubercle Bacilli and Paraffin Oil. *Proc. Soc. Exp. Biol. Med.* **1937***, 37*, 509-513.

39. Stills, H. F. Adjuvants and Antibody Production: Dispelling the Myths Associated with Freund's Complete and Other Adjuvants. *ILAR Journal* **2005***, 46*, 280-293.

40. Johnston, B. A.; Eisen, H.; Fry, D. An evaluation of several adjuvant emulsion regimens for the production of polyclonal antisera in rabbits. *Lab. Anim. Sci.* **1991***, 41*, 15.

41. Leenaars, P. P. A. M.; Hendriksen, C. F. M.; Angulo, A. F.; Koedam, M. A.; Claassen, E. Evaluation of several adjuvants as alternatives to the use of Freund's adjuvant in rabbits. *Vet. Immunol. Immunopathol.* **1994***, 40*, 225-241.

42. Arous, J. B.; Deville, S.; Pal, J. K.; Baksi, S.; Bertrand, F.; Dupuis, L. Reduction of Newcastle Disease Vaccine Dose Using a Novel Adjuvant for Cellular Immune Response in Poultry. *Procedia Vaccinol* **2013***, 7*, 28-33.

43. Jorge, S.; de Oliveira, N. R.; Marchioro, S. B.; Fisch, A.; Gomes, C. K.; Hartleben, C. P.; Conceição, F. R.; Dellagostin, O. A. The Mycoplasma hyopneumoniae recombinant heat shock protein P42 induces an immune response in pigs under field conditions. *Comp. Immunol. Microbiol. Infect. Dis.* **2014***, 37*, 229-236.

44. Ibrahim, E. E.; Gamal, W. M.; Hassan, A. I.; Mahdy, S. E.; Hegazy, A. Z.; Abdel-Atty, M. Comparative study on the immunopotentiator effect of ISA 201, ISA 61, ISA 50, ISA 206

used in trivalent foot and mouth disease vaccine.(RESEARCH ARTICLE). *Veterinary World* **2015***, 8*, 1189.

45. Iyer, A. V.; Ghosh, S.; Singh, S. N.; Deshmukh, R. A. Evaluation of three 'ready to formulate' oil adjuvants for foot-and-mouth disease vaccine production. *Vaccine* **2000***, 19*, 1097-1105.

46. Khorasani, A.; Madadgar, O.; Soleimanjahi, H.; Keyvanfar, H.; Mahravani, H. Evaluation of the efficacy of a new oil-based adjuvant ISA 61 VG FMD vaccine as a potential vaccine for cattle. *Iranian Journal of Veterinary Research* **2015***, 17*, 8-12.

47. Tafalla, C.; Bøgwald, J.; Dalmo, R. A. Adjuvants and immunostimulants in fish vaccines: Current knowledge and future perspectives. *Fish Shellfish Immunol.* **2013***, 35*, 1740-1750.

48. Veenstra, K. A.; Tubbs, L.; Ben Arous, J.; Secombes, C. J. Immune responses in rainbow trout (Oncorhynchus mykiss) following the administration of cell-mediated and humoral W/O adjuvanted vaccines post-vaccination and post-challenge. *Fish Shellfish Immunol.* **2016***, 53*, 67-67.

49. O'Hagan, D. T.; Ott, G. S.; De Gregorio, E.; Seubert, A. The mechanism of action of MF59 – An innately attractive adjuvant formulation. *Vaccine* **2012***, 30*, 4341-4348.

50. Dupuis, M.; Denis-Mize, K.; LaBarbara, A.; Peters, W.; Charo, I.; McDonald, D.; Ott, G. Immunization with the adjuvant MF59 induces macrophage trafficking and apoptosis. *Eur. J. Immunol.* **2001***, 31*, 2910-2918.

51. Seubert, A.; Monaci, E.; Pizza, M.; O'Hagan, D. T.; Wack, A. The Adjuvants Aluminum Hydroxide and MF59 Induce Monocyte and Granulocyte Chemoattractants and Enhance Monocyte Differentiation toward Dendritic Cells. *J. Immunol.* **2008***, 180*, 5402-5412.

52. Wack, A.; Baudner, B. C.; Hilbert, A. K.; Manini, I.; Nuti, S.; Tavarini, S.; Scheffczik, H.; Ugozzoli, M.; Singh, M.; Kazzaz, J.; Montomoli, E.; Del Giudice, G.; Rappuoli, R.; O'hagan, D. T. Combination adjuvants for the induction of potent, long- lasting antibody and T- cell responses to influenza vaccine in mice. *Vaccine* **2008***, 26*, 552-561.

53. Arous, J. B.; Bertrand, F.; Gaucheron, J.; Verkhovsky, O. A.; Kotelnikov, A. P.; Shemelkov, E. V.; Alekseev, K. P.; Dupuis, L. Adjuvant Formulations Designed to Improve Swine Vaccine Stability: Application to PCV2 Vaccines. *Procedia Vaccinol* **2013***, 7*, 34-39.

54. Barnett, P. V.; Pullen, L.; Williams, L.; Doel, T. R. International bank for foot-and-mouth disease vaccine: assessment of Montanide ISA 25 and ISA 206, two commercially available oil adjuvants. *Vaccine* **1996***, 14*, 1187-1198.

55. Horohov, D. W.; Dunham, J.; Liu, C.; Betancourt, A.; Stewart, J. C.; Page, A. E.; Chambers, T. M. Characterization of the in situ immunological responses to vaccine adjuvants. *Vet. Immunol. Immunopathol.* **2015***, 164*, 24-29.

56. Lankester, F.; Lugelo, A.; Werling, D.; Mnyambwa, N.; Keyyu, J.; Kazwala, R.; Grant, D.; Smith, S.; Parameswaran, N.; Cleaveland, S.; Russell, G.; Haig, D. The efficacy of alcelaphine herpesvirus-1 (AlHV-1) immunization with the adjuvants Emulsigen(Â®) and the monomeric TLR5 ligand FliC in zebu cattle against AlHV-1 malignant catarrhal fever induced by experimental virus challenge. *Vet. Microbiol.* **2016***, 195*, 144-153.

57. Wallace, M. D. An advancement in veterinary adjuvant technology. *Equine Pract* **1996***, 18*, 15-18.

58. Galliher-Beckley, A.; Pappan, L. K.; Madera, R.; Burakova, Y.; Waters, A.; Nickles, M.; Li, X.; Nietfeld, J.; Schlup, J. R.; Zhong, Q.; Mcvey, S.; Dritz, S. S.; Shi, J. Characterization of a novel oil-in-water emulsion adjuvant for swine influenza virus and Mycoplasma hyopneumoniae vaccines. *Vaccine* **2015***, 33*, 2903-2908.

59. Madera, R.; Gong, W.; Wang, L.; Burakova, Y.; Lleellish, K.; Galliher-Beckley, A.; Nietfeld, J.; Henningson, J.; Jia, K.; Li, P.; Bai, J.; Schlup, J.; McVey, S.; Tu, C.; Shi, J. Pigs immunized with a novel E2 subunit vaccine are protected from subgenotype heterologous classical swine fever virus challenge.(Report). *BMC Vet. Res.* **2016***, 12:197*.

60. Bozkir, A.; Hayta, G. Preparation and evaluation of multiple emulsions water-in-oil-in-water (w/o/w) as delivery system for influenza virus antigens. *J. Drug Target.* **2004***, 12*, 157-164.

61. Fukanoki, S.; Iwakura, T.; Iwaki, S.; Matsumoto, K.; Takeda, R.; Ikeda, K.; Shi, Z.; Mori, H. Safety and efficacy of water-in-oil-in-water emulsion vaccines containing Newcastle disease virus haemagglutinin-neuraminidase glycoprotein. *Avian Pathol.* **2001***, 30*, 509-516.

62. Leclercq, S. Y.; dos Santos, Roberta Márcia Marques; Macedo, L. B.; Campos, P. C.; Ferreira, T. C.; de Almeida, J. G.; Seniuk, J. G. T.; Serakides, R.; Silva-Cunha, A.; Fialho, S. Evaluation of water-in-oil-in-water multiple emulsion and microemulsion as potential adjuvants for immunization with rabies antigen. *European Journal of Pharmaceutical Sciences* **2011***, 43*, 378-385.

63. Bouguyon, E.; Goncalves, E.; Shevtsov, A.; Maisonnasse, P.; Remyga, S.; Goryushev, O.; Deville, S.; Bertho, N.; Ben Arous, J. A New Adjuvant Combined with Inactivated Influenza Enhances Specific CD8 T Cell Response in Mice and Decreases Symptoms in Swine Upon Challenge. *Viral Immunol.* **2015***, 28*, 524-531.

64. Hunter, P. The performance of southern African territories serotypes of foot and mouth disease antigen in oil-adjuvanted vaccines. *Rev. - Off. Int. Epizoot.* **1996***, 15*, 913.

65. Maree, F. F.; Nsamba, P.; Mutowembwa, P.; Rotherham, L. S.; Esterhuysen, J.; Scott, K. Intra-serotype SAT2 chimeric foot-and-mouth disease vaccine protects cattle against FMDV challenge. *Vaccine* **2015***, 33*, 2909-2916.

66. Jansen, T.; Hofmans, M. P. M.; Theelen, M. J. G.; Manders, F.; Schijns, V. E. J. C. Structure- and oil type-based efficacy of emulsion adjuvants. *Vaccine* **2006***, 24*, 5400-5405.

67. Oda, K.; Tsukahara, F.; Kubota, S.; Kida, K.; Kitajima, T.; Hashimoto, S. Emulsifier content and side effects of oil-based adjuvant vaccine in swine. *Res. Vet. Sci.* **2006***, 81*, 51-57.

68. Stone, H. D. Newcastle Disease Oil Emulsion Vaccines Prepared with Animal, Vegetable, and Synthetic Oils. *Avian Dis.* **1997***, 41*, 591-597.

69. Shah, R. R.; Dodd, S.; Schaefer, M.; Ugozzoli, M.; Singh, M.; Otten, G. R.; Amiji, M. M.; O'hagan, D. T.; Brito, L. A. The Development of Self-Emulsifying Oil-in-Water Emulsion Adjuvant and an Evaluation of the Impact of Droplet Size on Performance. *J. Pharm. Sci.* **2015***, 104*, 1352-1361.

70. Manolova, V.; Flace, A.; Bauer, M.; Schwarz, K.; Saudan, P.; Bachmann, M. Nanoparticles target distinct dendritic cell populations according to their size. *Eur. J. Immunol.* **2008***, 38*, 1404-1413.

Chapter 2 - Impact of Oil Composition on Formation and Stability of Emulsions Produced by Spontaneous Emulsification[3]

Abstract

In this study, triglycerides of different chain lengths were mixed with paraffin oil, and their effectiveness in forming emulsions produced by spontaneous emulsification upon the addition of water was investigated. Dependence of the emulsions droplet size exhibited similar trends as a function of the triglyceride/paraffin oil composition for medium chain (C8-C10) and long chain (C18) triglycerides. However, emulsions formulated with medium-chain triglycerides (MCT) and long-chain triglycerides (LCT) have much smaller droplet size on the order of 50 nm than emulsions with short-chain (C4) triglycerides. The addition of short-chain triglycerides resulted in droplet sizes around 800 nm, and the emulsions formed were very unstable. The droplet size, polydispersity index, zeta potential, and emulsion stability for all of these systems will be described as a function of oil phase composition.

Introduction

Spontaneous emulsification, or self-emulsification, is a very attractive production method in many areas including agriculture *(1, 2)*, the cosmetics industry *(3, 4)*, and pharmaceuticals *(5, 6)*. The method is simple and can produce stable nanoscale emulsions with great solubilization properties for the delivery of active ingredients in a variety of applications.

Spontaneous emulsification occurs when the oil phase is introduced to the water phase, and a fine emulsion is produced after gentle agitation or even without it *(7)*. Many parameters can

[3] This is an Accepted Manuscript of an article published by Taylor & Francis in Journal of Dispersion Science and Technology on 12/02/2017, available online: https://doi.org/10.1080/01932691.2017.1281141

affect the production of self-emulsifying emulsions including the nature of the oil phase, the choice of surfactants and their concentration, the presence of co-surfactants, and the ratio between all components *(8-10)*. Here, the focus will be on the impact of oil composition on formation of spontaneous emulsions. A number of studies demonstrate that relatively more polar oils such as long- and medium-chain triglycerides are better candidates for the low energy production methods than nonpolar oils (n-alkanes) *(10-12)*. At the same time, some applications, such as crop oil concentrates in agriculture *(13)*, personal-care products *(14)*, and animal vaccine adjuvants *(15)*, requires the presence of different oils/or excipients including nonpolar n-alkanes (mineral or paraffin oil) to improve the efficacy of the final formulation.

The impact of the addition of different proportions of triglycerides to the oil phase on the ability of paraffin oil to produce emulsions by spontaneous emulsification is investigated here. Although several groups have reported the addition of long- and medium-chain triglycerides to essential oils and oils with high solubility in water improves the stability and decreases the droplet size of those emulsions at particular triglyceride contents *(16-18)*. No report exists, to the best of our knowledge, on how the triglycerides impact the formation and stability of nonpolar paraffin oil emulsions. In addition, the impact of the triglycerides with different chain lengths on droplet size, polydispersity, and stability of nonpolar paraffin oil emulsions is compared in this study. These observations will be useful for formulation scientists in many fields, where the mixture of different types of oils including nonpolar mineral oils is employed in emulsion oil phase.

The nonionic surfactant, Tween 85, was employed as the emulsifier for this system as it has been shown to be a good choice for self-emulsifying formulations *(8)*. Glycerol was selected as a co-surfactant. It has been demonstrated that polyhydroxy alcohols, such as ethylene glycol and glycerol, can effectively reduce droplet size of the emulsions when paired with nonionic surfactants in emulsion production *(19-21)*.

Materials and methods

Materials

The oil phase of these emulsions was comprised of paraffin oil (a mixture of n-alkanes C_nH_{2n+2}, where n=16-24) obtained from Sigma-Aldrich (St. Louis, MO, USA) and one of three triglycerides. Soybean oil purchased from a local grocery store was used as a source of long-chain triglycerides (LCT). Soybean oil is essentially composed of triglycerides with polyunsaturated linoleic acid (C-18:2), α-linolenic acid (C-18:3), and monounsaturated oleic acid (C-18:1) being the major constituents (22). Medium-chain triglycerides (MCT) were supplied by Swanson Health Products (Fargo, ND, USA). According to the manufacturer, these triglycerides are composed of 50–65% caprylic acid (C-8:0) and 30-45% capric acid (C-10:0). Tributyrin (98%, C-4:0) was used as a source of short-chain triglycerides (SCT) (Fisher Scientific, Fair Lawn, NJ, USA). The nonionic surfactant, polyoxyethylenesorbitan trioleate (Tween 85), was purchased from MP Biomedicals (Solon, OH, USA). Glycerol (Fisher Scientific, Fair Lawn, NJ, USA) was used as a co-surfactant. All reagents were used as received. Nanopure deionized water was prepared using Barnstead NANOpure Infinity water system (Thermo Fisher Scientific, Marietta, OH, USA).

Emulsion preparation

The emulsions were prepared in two steps. First, oils and surfactants were mixed together. Paraffin oil and triglycerides were blended in different mass ratios (from 0 to 100 wt.% triglycerides) to produce homogenous oil mixtures. The fixed amounts of nonionic surfactant, Tween 85, and co-surfactant, glycerol, were added to the oil mixtures prior emulsification with water. The final concentration of components in all blends was 50 wt.% oil phase, 25 wt.% surfactant, and 25 wt.% co-surfactant. In the second step, the oil/surfactant mixture was slowly (within 10 sec.) added to deionized water in a mass ratio of 1:2 upon stirring on a magnetic mixer

(350 rpm) at room temperature (20°C) to produce the final emulsion. All samples were stirred for 20 min.

Emulsion characterization

Droplet size analysis

The droplet size of the emulsions was measured with a Zetasizer Nano ZS 90 instrument (Malvern Instruments, Westborough, MA) by dynamic light scattering (DLS). Immediately before measurement, the samples were diluted by factor of 100 with deionized water to avoid multiple scattering effects. A 633 nm He-Ne laser was employed at a scattering angle of 173 degrees to measure the hydrodynamic diameter of emulsion droplets. The polydispersity index (PDI) was also collected for each sample. A PDI value less than 0.2 indicates a narrow size distribution of emulsion droplets, while a value of 0.7 and higher indicates a very broad size distribution (23). Each measurement was performed in triplicate on two different samples of the same composition at constant temperature (25°C) to ensure reproducibility of results. The results are reported as a mean ± standard error of the mean (SEM).

Zeta potential measurements

Zeta potential measurements were performed with a Zetasizer Nano ZS 90 instrument (Malvern Instruments, Westborough, MA) using a disposable folded capillary cell. Before measurement, samples were diluted by a factor of 100 with deionized water. The electric field was applied to the cell to determine the electrophoretic mobility of the particles. The calculation of zeta potential through Henry's equation then was performed. Each sample was measured three times. Two different samples with the same composition were studied to insure reproducibility of results. The results are reported as a mean value ± SEM.

pH measurements

The pH of the emulsions was measured with a VWR SympHony digital pH meter SB21 (VWR International, Radnor, PN, USA). Before use, the instrument was calibrated by a three-point method according to manufacturer's manual.

Long term stability of emulsions

To evaluate long term shelf stability of emulsions in this study, samples were kept at two different temperatures, 4°C and 20°C, and visually inspected after one month. The samples were considered to pass this visual test if they did not demonstrate any signs of creaming, sedimentation, and/or phase separation (oiling off). Some samples showed a color change during the storage, but it was not considered as a criterion for the failing the visual test. The droplet size of emulsions that have passed the visual test was measured with DLS at the end of the test. Each sample was measured three times and the results are reported as a mean ± standard deviation (S.D.).

Results

The effect of addition of triglycerides on droplet size of paraffin oil emulsions

The effect of different proportions of triglycerides and paraffin oil in the oil phase on the droplet diameters of the emulsions is shown in Figure 2.1. An emulsion prepared with pure paraffin oil had a mean droplet diameter of 2090.0±480.0 nm. When the long-chain triglycerides were added to oil phase, the mean droplet diameter decreased steeply reaching a minimum of 53.0±1.0 nm at 15 wt.% soybean oil. With further addition of soybean oil, the droplet size of the emulsions increased slowly reaching 139.0±12.0 nm at 100 wt.% soybean oil. A similar result was observed when medium-chain triglycerides were added to paraffin oil before emulsion production. A minimum droplet diameter of 51.0±1.0 nm was obtained when the oil phase was comprised of 15 wt.% MCT oil. Increasing the MCT oil in the oil phase led to increasing the droplet size, culminating in a diameter of 141.0±7.0 nm at 100 wt.% MCT oil. The addition of short-chain

triglycerides produced a very different result. The smallest droplets were 818.0±55.0 nm in diameter, which was obtained at a concentration of 25 wt.% tributyrin. At 100 wt.% tributyrin, the emulsion had a mean droplet diameter of 3880.0±720.0 nm.

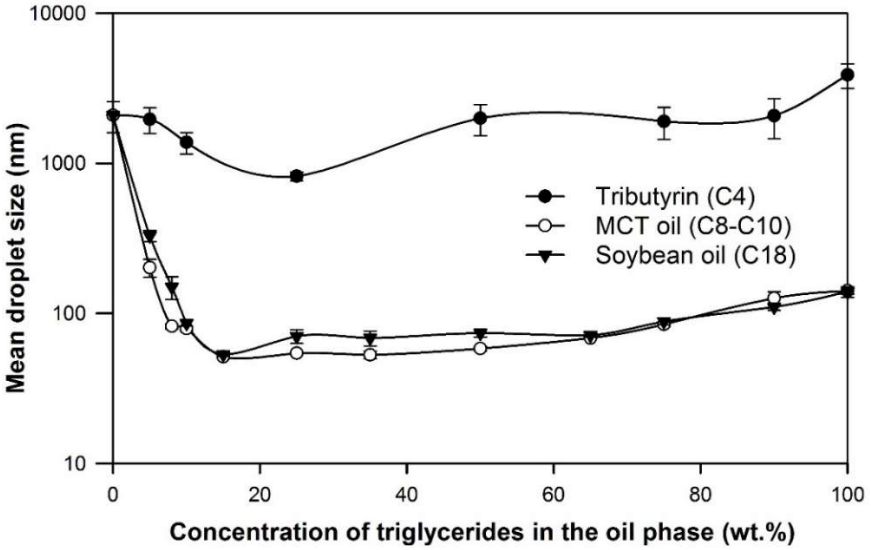

Figure 2.1 Effect of different proportions of triglycerides and paraffin oil in the oil phase on the droplet size of emulsions.
Data plotted as a mean ± standard error of mean (SEM).

The addition of medium-chain and long-chain triglycerides to the oil phase before emulsification contributed to narrowing the droplet size distribution, as indicated by a decreased polydispersity index. The steep reduction in the PDI from 1 to 0.2 was observed when the LCT or MCT content was increased from 0 to 15 wt.%. It remained approximately this value up to 100 wt.% triglycerides (Fig. 2.2). Short-chain triglycerides did not impact polydispersity of paraffin oil emulsions; it stayed at essentially 1 throughout the entire concentration range.

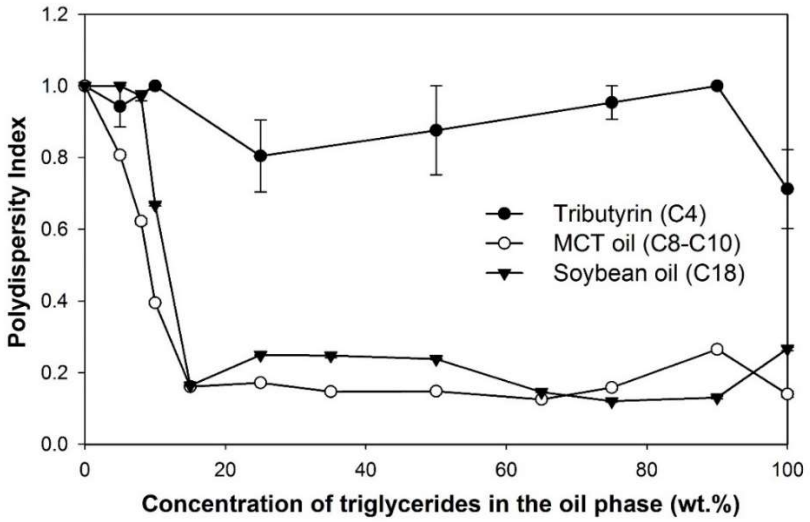

Figure 2.2 Effect of different proportions of triglycerides and paraffin oil in the oil phase on polydispersity index of emulsions
Data plotted as a mean ± SEM.

Zeta potential and pH of emulsions with triglycerides/paraffin oil

Figure 2.3 demonstrates that the addition of triglycerides to a paraffin oil before emulsification impacts the value of zeta potential of emulsions. A sudden increase in zeta-potential value is observed when the concentration of LCT and MCT in the oil phase changes from 15 to 20 wt.%. A pure paraffin oil emulsion had a zeta-potential of -38.0±1.0 mV. This value remains essentially the same with LCT and MCT up to 15 wt.% triglycerides. The zeta potential increases to ≈ -25 mV when the amount of LCT or MCT reaches 20 wt.%. Remarkably, it does not change significantly after the LCT and MCT is increased up to 100 wt.% (Fig. 2.3a-b).

The behavior with SCT addition is very different (Fig. 2.3c). At small concentrations of tributyrin in the oil phase, no significant change is observed in zeta potential; it remains around -38 mV up to 10% of SCT in oil phase. With addition of tributyrin, the zeta potential decreases down to -41.2±0.3 mV before increasing slowly with increasing concentration of triglycerides in the oil phase of emulsions, reaching a value of -23.0±0.2 mV at 100 wt.% triglycerides.

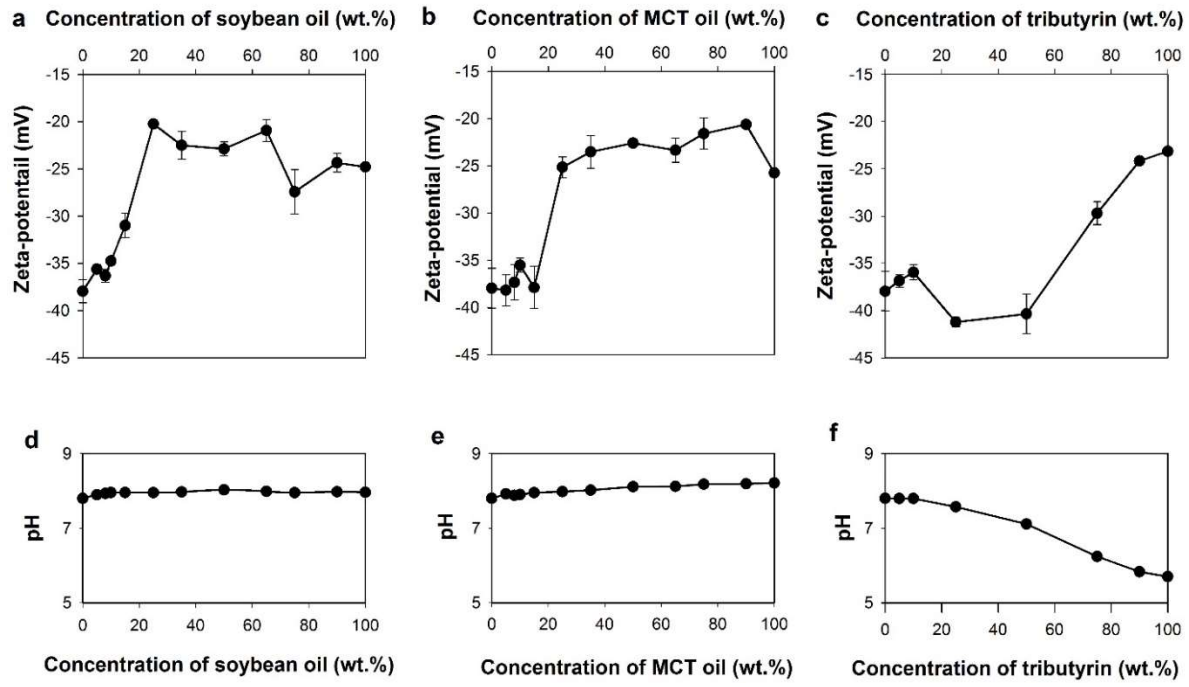

Figure 2.3 Effect of different proportions of long-chain (a, d), medium-chain (b, e), short-chain triglycerides (c, f) and paraffin oil on zeta potential and pH of resulting emulsions.

Data of zeta potential represented as a mean ± SEM.

To confirm that these trends in zeta potential are not a consequence of changes in pH within the system, the pH was measured for each composition (Fig 2.3d-f). In the case of long- and medium-chain triglycerides, the pH essentially remains constant. Emulsions with pure paraffin oil had a pH of 7.8 while the emulsions with pure soybean oil and pure MCT oil emulsion had pH values of 7.9 and 8.2, respectively. The addition of SCT indeed impacts the pH of these emulsions (Fig. 2.3f). The pH slowly decreases with increasing tributyrin concentration in the oil mixture reaching 5.7 at 100 wt. % tributyrin.

Emulsion stability and droplet size evolution over time at different storage conditions

Emulsions prepared with tributyrin and paraffin oil were very unstable. Emulsions prepared with pure paraffin oil demonstrated creaming immediately after preparation. Creaming, oiling off, and sedimentation in tributyrin/paraffin oil emulsions also had been noticed shortly after

preparation. A thin creaming layer was also observed in emulsions prepared with 5 to 10 wt.% MCT and LCT emulsions after just a few hours of preparation. Emulsion samples with 15 to 100 wt.% long- and medium-chain triglycerides did not cream, or phase separate after one month of storage at 4°C (not shown) and 20°C. However, the color change from yellowish translucent to white turbid was noticed in MCT/paraffin oil emulsions starting from 35 wt.% of MCT and from 15 wt.% in LCT/paraffin oil emulsions. Interestingly, two samples of MCT/paraffin oil emulsions (15 wt.% and 25 wt.%) preserved their color and visual appearance after one month at 20°C.

Figure 2.4 shows the emulsion droplet diameters after one-month storage at 4°C and 20°C. Mean droplet size did not change significantly in samples stored at 4ºC for both systems, MCT/paraffin oil and LCT/paraffin oil. Although at 20°C, the significant droplet growth was observed in all samples except 15 wt. % and 25 wt. % MCT oil emulsions.

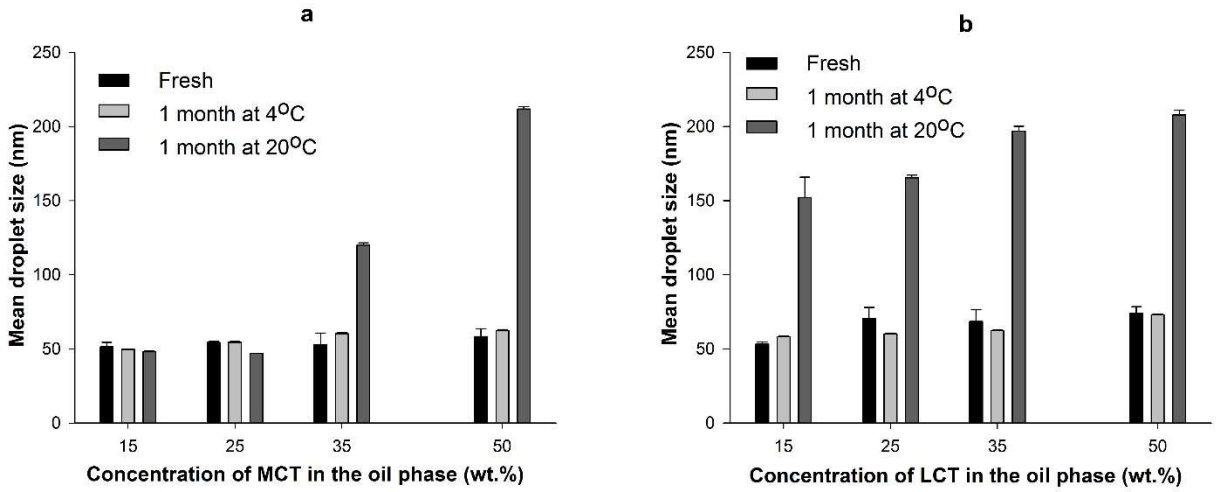

Figure 2.4 Change of emulsion droplet size after one-month storage at different conditions: (a) MCT/paraffin oil emulsions; (b) LCT/paraffin oil emulsions.
Data represented as a mean ± standard deviation.

Discussion

Numerous studies indicate that the addition of medium- and long-chain triglycerides reduces the droplet size and improves emulsion stability size by inhibiting the Ostwald ripening

process *(16, 17, 24)*. Ostwald ripening instability is associated with a growth of particle size due to difference in solubility of small droplets and big droplets and the deposition of molecules from small droplets into bigger droplets resulting in disappearance of small droplets and enlargement of big droplets over time. The rate of Oswald ripening is dependent on molar volume of the oils, with higher molar volume oils lowering the rate of ripening *(25)*. As a result, medium- and long-chain triglycerides, having a larger molar volume than n-alkane oils, can act as Oswald ripening inhibitors. Results of our study agree with these observations. Addition of LCT and MCT to paraffin oil indeed decreases droplet size and improves the stability of these emulsions. While SCT did not achieve the same result as they have a lower value of molar volume of the oil and therefore poor Ostwald ripening inhibitory properties. Although the question remains why, when the content of triglycerides in the oil phase exceeds 15 wt.%, the droplet diameter increases slowly from 51.0±1.0 nm to 141.0±7.0 nm in case of addition of MCT oil and from 53.0±1.0 nm to 139.0±12.0 nm in case of LCT. This phenomenon has been observed in other studies when the emulsions with mixed oils were produced via a high-pressure homogenizing method *(24, 26)*. For instance, the droplet size of emulsions in which an oil phase was comprised of an orange oil and corn oil (LCT) exhibited the similar behavior as a function of corn oil concentration. A steep decrease of the emulsion droplet size when the oil phase contained 0-20% corn oil and a gradual droplet diameter enlargement when the concentration of corn oil was raised from 20 to 100% were observed. The researchers attributed it to the higher viscosity of the corn oil and higher interfacial tension of the corn oil-water interface in comparison with orange oil *(24)*. In our systems, both LCT and MCT have lower viscosity and interfacial tension than paraffin oil. Therefore, the particle size increase with increased triglyceride content cannot be attributed to these factors.

It has been demonstrated that lower polydispersity of colloidal systems signifies their higher stability attributed to the lower ripening rate *(27, 28)*. The addition of medium- and long-

chain triglycerides to paraffin oil reduces the polydispersity of emulsion droplets as demonstrated in Figure 2.2. This and the fact that MCT and LCT contributes to droplet size reduction makes them superior to short-chain triglycerides in formation of stable emulsions.

Zeta potential is often used to predict colloidal stability of emulsions, and it is dependent on pH, ionic strength, and chemistry of the surface and dispersant. Therefore, it is not a surprise that by changing the composition of oil phase of the emulsions would lead to changes in the zeta-potential. However, the behavior of the zeta-potential as a function of triglycerides content still raises some questions. Marinova *(29)* and other research groups *(30)* have explained the nature of negative charge on the n-alkanes oil droplets stabilized with nonionic surfactants due to the adsorption of hydroxyl ions. According to this theory, the oxygen atoms of the interfacial water molecules are specifically oriented towards the hydrophobic nonpolar phase creating the negative potential at the interface. In this study, the pure paraffin oil emulsion stabilized with nonionic surfactant also had a negative zeta potential (-38 mv), and therefore, agreed with this theory. At small concentrations of triglycerides (up to 15 wt.%), the triglycerides did not produce any significant change in the system. Yet for the concentrations of MCT and LCT in excess of 25 wt.%, the zeta potential jumped to -25 mV and remained at this value as additional triglycerides were incorporated into the oil phase. It appears a particular amount of triglycerides is needed to affect the surface charge of emulsion droplets. One possible explanation can be the orientation of triglyceride molecules within the oil droplets. The more polar hydrophilic heads of triglycerides appear to reside at the water-oil interface, while hydrophobic fatty acid tails dwell inside the droplet. With this orientation, triglycerides can exhibit surfactant-like behavior which, in its turn, may affect the adsorption of hydroxyl ions responsible for negative charging. Although this theory does not explain why the further increases in the triglyceride content do not reduce the negative charging even more. The addition of short-chain triglycerides reduces zeta potential eventually as

well, but, in this case, a higher concentration of triglycerides (up to 90 wt.%) is needed to achieve the same result as with MCT and LCT. Clearly, more experiments have to be performed to explain zeta potential behavior. Molecular dynamic simulations could shed additional light on the interfacial organization of molecules in mixed oil – water systems as well.

The long-term shelf stability at different temperatures is one of most important properties of emulsions for the most application areas. The experiments with stability at different temperatures demonstrate that the incorporation of MCT in the oil phase is more effective than LCT. Although, both systems had very similar results initially, two formulations with 15 wt.% and 25 wt.% MCT preserved their droplet size after one-month storage at 20°C, while none of the LCT formulations demonstrated similar results. These observations contradict the Oswald ripening inhibition theory *(25)*, according to which long-chain triglycerides, having a larger molar volume and lower solubility in water than medium-chain triglycerides, should be superior in the suppression of Ostwald ripening rate.

Conclusions

Spontaneous emulsification of paraffin oil emulsions was improved by addition of triglycerides with long- and medium-chain lengths to the oil phase of emulsion before emulsification. It was found that medium-chain triglycerides are better candidates for decreasing the droplet size of emulsions, narrowing droplet size distribution, and improving emulsion stability over time. The addition of short-chain triglycerides did not prolong the shelf stability of emulsions, and only a small decrease in droplet size was observed. Emulsion droplet size and distribution can be decreased dramatically by the addition of LCT to paraffin oil, but the overall stability of emulsions formed was worse than in case of MCT/paraffin oil emulsions. The system zeta potential was found to be sensitive to a particular concentration of triglycerides, with LCT and MCT, 25

wt% was enough to decrease negative charging of droplets; in the case of SCT, 90 wt% triglycerides had to be employed to achieve the same zeta potential value. Additional experiments must be performed to explain "plateau effect" of zeta potential at concentrations of 25 – 100 wt.% MCT and LCT.

References

1. Lee, G. W. J.; Tadros, T. F. Formation and stability of emulsions produced by dilution of emulsifiable concentrates. Part I. An investigation of the dispersion on dilution of emulsifiable concentrates containing cationic and non-ionic surfactants. *Colloids and Surfaces* **1982***, 5*, 105-115.

2. Wang, L.; Li, X.; Zhang, G.; Dong, J.; Eastoe, J. Oil-in-water nanoemulsions for pesticide formulations. *J. Colloid Interface Sci.* **2007***, 314*, 230-235.

3. Boonme, P. Applications of microemulsions in cosmetics. *J Cosmet Dermatol* **2007***, 6*, 223-228.

4. Kim, E. J.; Kong, B. J.; Kwon, S. S.; Jang, H. N.; Park, S. N. Preparation and characterization of W/O microemulsion for removal of oily make-up cosmetics. *Int. J. Cosmetic Sci.* **2014***, 36*, 606-612.

5. Shah, R. R.; Dodd, S.; Schaefer, M.; Ugozzoli, M.; Singh, M.; Otten, G. R.; Amiji, M. M.; O'hagan, D. T.; Brito, L. A. The Development of Self-Emulsifying Oil-in-Water Emulsion Adjuvant and an Evaluation of the Impact of Droplet Size on Performance. *J. Pharm. Sci.* **2015***, 104*, 1352-1361.

6. Lo, J.; Chen, B.; Lee, T.; Han, J.; Li, J. Self-emulsifying O/W formulations of paclitaxel prepared from mixed nonionic surfactants. *J. Pharm. Sci.* **2010***, 99*, 2320-2332.

7. Solans, C.; Morales, D.; Homs, M. Spontaneous emulsification. *Curr. Opin. Colloid Interface Sci.* **2016***, 22*, 88-93.

8. Pouton, C. W. Formulation of self- emulsifying drug delivery systems. *Adv. Drug Deliv. Rev.* **1997***, 25*, 47-58.

9. Bouchemal, K.; Briançon, S.; Perrier, E.; Fessi, H. Nano-emulsion formulation using spontaneous emulsification: solvent, oil and surfactant optimisation. *Int. J. Pharm.* **2004***, 280*, 241-251.

10. Komaiko, J.; McClements, D. J. Low-energy formation of edible nanoemulsions by spontaneous emulsification: Factors influencing particle size. *J. Food Eng.* **2015***, 146*, 122-128.

11. Lo, I.; Florence, A. T.; Treguier, J.; Seiller, M.; Puisieux, F. The influence of surfactant HLB and the nature of the oil phase on the phase diagrams of nonionic surfactant-oil-water systems. *J. Colloid Interface Sci.* **1977***, 59*, 319-327.

12. Ostertag, F.; Weiss, J.; McClements, D. J. Low-energy formation of edible nanoemulsions: Factors influencing droplet size produced by emulsion phase inversion. *J. Colloid Interface Sci.* **2012***, 388*, 95-102.

13. Tu, M.; Randall, J. M. In *Adjuvants;* Tu, M., Hurd, C. and Randall, J. M., Eds.; Weed Control Methods Handbook:Tools and Techniques for Use in Natural Areas; The Global Invasive Species Team: 2001; .

14. Morrison, D. S.; Schmidt, J.; Paulli, R. The scope of mineral oil in personal care products and its role in cosmetic formulation. *J. Appl. Cosmetol.* **1996***, 14*, 111-118.

15. Jansen, T.; Hofmans, M. P. M.; Theelen, M. J. G.; Manders, F.; Schijns, V. E. J. C. Structure- and oil type-based efficacy of emulsion adjuvants. *Vaccine* **2006***, 24*, 5400-5405.

16. Liang, R.; Xu, S.; Shoemaker, C. F.; Li, Y.; Zhong, F.; Huang, Q. Physical and Antimicrobial Properties of Peppermint Oil Nanoemulsions. *J. Agric. Food Chem.* **2012***, 60*, 7548-7555.

17. Chang, Y.; McLandsborough, L.; McClements, D. J. Physical Properties and Antimicrobial Efficacy of Thyme Oil Nanoemulsions: Influence of Ripening Inhibitors. *J. Agric. Food Chem.* **2012***, 60*, 12056-12063.

18. Gulotta, A.; Saberi, A. H.; Nicoli, M. C.; Mcclements, D. J. Nanoemulsion- based delivery systems for polyunsaturated (ω- 3) oils: formation using a spontaneous emulsification method. *J. Agric. Food Chem.* **2014***, 62*, 1720.

19. Chanana, G. D.; Sheth, B. B. Particle size reduction of emulsions by formulation design. I: Effect of polyhydroxy alcohols. *J Parenter Sci Technol* **1993***, 47*, 130.

20. Krishna, G.; Sheth, B. B. A novel self emulsifying parenteral drug delivery system. *PDA J. Pharm. Sci. Technol.* **1999***, 53*, 168.

21. Saberi, A. H.; Fang, Y.; Mcclements, D. J. Effect of glycerol on formation, stability, and properties of vitamin-E enriched nanoemulsions produced using spontaneous emulsification. *J. Colloid Interface Sci.* **2013***, 411*, 105-113.

22. Ivanov, D. S.; Levic, J. D.; Sredanovic, S. A. Fatty Acid Composition Of Various Soybean Products. *Food and Feed Research* **2010***, 37(2)*, 65-70.

23. Malvern Instruments Ltd. Dynamic light scattering - common terms defined. http://www.malvern.com/en/support/resource-center/Whitepapers/WP111214DLSTermsDefined.aspx (accessed 11/1, 2016).

24. McClements, J. D.; Henson, L.; Popplewell, L. M.; Decker, E. A.; Jun Choi, S. Inhibition of Ostwald Ripening in Model Beverage Emulsions by Addition of Poorly Water Soluble Triglyceride Oils. *J. Food Sci.* **2012***, 77*, C33-C38.

25. Wooster, T. J.; Golding, M.; Sanguansri, P. Impact of Oil Type on Nanoemulsion Formation and Ostwald Ripening Stability. *Langmuir* **2008***, 24*, 12758-12765.

26. Ziani, K.; Chang, Y.; Mclandsborough, L.; Mcclements, D. J. Influence of surfactant charge on antimicrobial efficacy of surfactant- stabilized thyme oil nanoemulsions. *J. Agric. Food Chem.* **2011***, 59*, 6247.

27. Djerdjev, A. M.; Beattie, J. K. Enhancement of Ostwald ripening by depletion flocculation. *Langmuir* **2008***, 24*, 7711.

28. Solè, I.; Solans, C.; Maestro, A.; González, C.; Gutiérrez, J. M. Study of nano-emulsion formation by dilution of microemulsions. *J. Colloid Interface Sci.* **2012***, 376*, 133-139.

29. Marinova, K. G.; Alargova, R. G.; Denkov, N. D.; Velev, O. D.; Petsev, D. N.; Ivanov, I. B.; Borwankar, R. P. Charging of Oil-Water Interfaces Due to Spontaneous Adsorption of Hydroxyl Ions. *Langmuir* **1996***, 12*, 2045-2051.

30. Stachurski, J.; Michałek, M. The Effect of the ζ Potential on the Stability of a Non- Polar Oil-in- Water Emulsion. *J. Colloid Interface Sci.* **1996***, 184*, 433-436.

Chapter 3 - Box-Behnken Design of Emulsions Produced by Spontaneous Emulsification

Abstract

Emulsions produced by spontaneous emulsification are dependent on many formulation parameters. A detailed understanding of the relationship between these parameters and their effect on responses are very important in the design of optimal formulations. The influence of several formulation variables and the interactions between them on the formation and stability of self-emulsified emulsions were studied using response surface methodology. A four-factor, three-level Box-Behnken design was employed to determine optimal design space and which parameters have the largest effect. The gels producing emulsions were comprised of oil (mixtures of light mineral oil and MCT oil), two surfactants (sucrose palmitate and Tween 60), and glycerol. After addition to the saline solution (water phase) and gentle agitation, emulsions with nanoscale droplet sizes formed. Four critical parameters for emulsion formation were identified: the sucrose palmitate-to-glycerol ratio, Tween 60-to-oil phase ratio, glycerol-to-oil ratio, and, finally, the gel-to-water phase ratio. Effects of these factors on droplet size, polydispersity, zeta potential, and stability of emulsions were described quantitatively with polynomial equations. The Tween 60-to-oil ratio followed by the oil-to-glycerol ratio were the most significant parameters in determining the droplet size and polydispersity of emulsions. The oil-to-glycerol ratio has also impacted stability of the emulsions. Interestingly, less negative zeta potential values correlated with emulsions having higher stability; less stable emulsions were formed as the zeta potential became more negative. The response surface methodology permitted to establish the important interconnections between formulation variables and qualities of final emulsions. In addition, the optimal design space was defined.

Introduction

Spontaneous emulsification or self-emulsification occurs when an oil phase is added to a water phase and an emulsion is formed with or without gentle agitation *(1)*. Self-emulsifying emulsions have earned a lot of attention in various applications including pharmaceutical drug delivery systems *(2, 3)*, agricultural pesticides *(4)*, cosmetics *(5)*, and oil recovery *(6)*. Simplicity of preparation, nanoscale droplet size, extended solubilization capacities, and prolonged shelf stability are qualities that make self-emulsifying emulsions very attractive for these areas. However, emulsions formulated by spontaneous emulsification are sensitive to many parameters such as the nature of oil, the choice and concentration of surfactants, the choice and presence of co-solvents/co-surfactants, and the proportions between all components. Generally, determination of optimal formulation space has proceeded by exploring the composition field one-factor-at-a-time, which demands a lot of sample handling and does not consider the important relationships between different independent parameters and the final response they produce. Recently, response surface methodology (RSM) *(7)* has gained in popularity among formulation scientists *(8-10)*. The RSM allows for optimizing formulations by employing a sequence of designed experiments and determining simultaneous effects of several variables on the response of interest. This methodology helps to minimize the number of treatment combinations and provides very essential information about complex interconnections between process variables and responses by using second-degree polynomials. In the present study, a Box-Behnken design (BBD) was used to study the effect of several formulation variables on physical characteristics of self-emulsifying emulsions for application as components in animal vaccines.

Introduced in 1960 by G. E. P. Box and D. Behnken, a BBD is a quadratic experimental design for RSM *(11)*. This design is particularly convenient for four or fewer factors, or

independent variables, requiring fewer sample combinations than a conventional central composite design. The BBD does not use the extreme points in treatment combinations; it employs central points and requires three levels for each impacting factor.

First, the gels were formulated that produce emulsions after spontaneous emulsification with a water phase. The gels were comprised of components suitable for application in animal vaccines. The oil component of the gels was a mixture of light mineral oil and medium chain triglycerides (MCT). Mineral oil has been commonly used in emulsion-based animal vaccines and elicits stronger immune responses in comparison with vegetable oil-based vaccines *(12, 13)*. In addition, a previous investigation has demonstrated that the combination of nonpolar mineral oil and medium chain triglycerides helps to achieve stable emulsions with nanoscale droplets *(14)*. Tween 60 was incorporated into the oil phase and served as a surfactant. Next, the glycerol was added to the oil phase to form gels. The biocompatibility of glycerol allows it to be used in cosmetics and pharmaceutical formulations as a co-solvent and/or co-surfactant. Furthermore, several studies have shown the beneficial effect of glycerol presence on the formation of self-emulsified emulsions including significant droplet size reduction and improved stability *(15, 16)*. However, the phase separation between polar glycerol and a nonpolar oil phase in self-emulsified formulations creates a challenge in the design of stable oil-glycerol mixtures requiring the application of additional surfactants or stabilizers. To achieve stable oil-glycerol gels, a biocompatible surfactant, sucrose palmitate, was dissolved in glycerol prior to its addition to the oil phase.

The formulation and optimization of self-emulsified emulsions formed from the oil-glycerol gels with respect to droplet size, polydispersity, zeta potential and stability are reported herein. These parameters are not only important indicators of the physical stability of these colloidal systems, but also have a great impact on the efficacy of the emulsions as delivery agents

in vaccines *(17)*. Four formulation parameters (sucrose palmitate-to-glycerol ratio, Tween 60-to-oil phase ratio, glycerol-to-oil ratio, and gel-to-water phase ratio) were determined in the preliminary studies to be important for formation of stable emulsions. Their impact on the emulsion physical characteristics mentioned above was studied quantitatively with a Box-Behnken designed experiment, and empirical models were developed to describe the system behavior.

Materials and methods

Materials

Light mineral oil (Drakeol®5) was obtained from Calumet Penreco LLC (USA). Medium Chain Triglycerides (MCT oil) were purchased from Jedwards International Inc. (USA). According to the manufacturer, it is comprised of triglycerides with 57.8% caprylic acid (C8:0) and 42.1% capric acid (C10:0). Sucrose palmitate (Hydrophilic-lipophilic balance (HLB) =16) was obtained from Sisterna B.V. (the Netherlands). Polyoxyethylene sorbitan monostearate (Tween 60, HLB=14.9), glycerol (99+% pure), and phosphate buffered saline (PBS, 100 ml tablets) were purchased from Fisher Scientific (USA). PBS tablets were diluted in nanopure deionized water (1 tablet per 100 ml of water) to obtain 1X PBS solution. All other reagents were used as received.

Preparation of oil-glycerol gels and emulsions

Oil-glycerol gels were prepared by mixing the oil phase with the glycerol phase. First, sucrose palmitate was dissolved in glycerol (85% water solution) to produce the glycerol phase. Then Tween 60 was mixed with an oil mixture comprised of 60 wt.% MCT oil and 40 wt.% mineral oil, resulting in a homogeneous oil phase. Both the glycerol and oil phases were heated to 75°C separately. After that, oil was added slowly (drop-by-drop) to the glycerol phase by using a magnetic stirrer at 1000 rpm. Finally, the oil-glycerol gel was obtained by stirring for an additional 2 min and then cooled.

To prepare the emulsion, the gel was warmed up to 37°C and added to PBS, followed by gentle mixing with a magnetic stirrer for 20 min at 350 rpm at room temperature.

Dynamic light scattering of the emulsion samples

The droplet size, polydispersity, and zeta potential of the emulsions were measured employing a Zetasizer Nano ZS 90 dynamic light scattering (DLS) instrument (Malvern Instruments, USA) with a 633 nm He-Ne laser at a scattering angle of 173 degrees. Each sample was diluted by at least a factor of 100 with PBS in the case of droplet size analysis and with 0.001M NaCl solution in the case of zeta potential measurements to prevent multiple scattering effects. Each sample was measured three times. Results are represented as a mean of three measurements.

Stability assessment

To investigate impact of different proportions of ingredients on emulsion shelf stability, all emulsions were stored in the dark at room temperature (~20°C). Visual tests were performed after 1 hour, 10 hours, 100 hours, and 1000 hours of storage. The samples were considered to pass the visual test if they did not cream or have phase separation.

Transmission electron microscopy

Emulsions were visualized with a transmission electron microscope (TEM) housed in the Nanotechnology Innovation Center of Kansas State (NICKS) (Kansas State University, Manhattan, KS, USA). Before imaging, samples were diluted by a factor of 20 and stained with uranyl acetate. Approximately 5µl of sample was placed on a 200 mesh formvar-carbon coated, copper grid (Electron Microscopy Sciences, USA) and vacuum-dried. The emulsion droplets were visualized with a Tecnai G2 Spirit BioTWIN electron microscope (FEI, USA) equipped with a GATAN digital image capturing system at a magnification of 23,000 and an acceleration voltage of 80 kV.

Experimental design

A four-factor, three-level Box-Behnken design was constructed to generate the response surface using the statistical software tool Minitab 17 (Minitab Inc., USA). The design consisted of 27 treatment combinations, 3 of which were replicates of the central point; the remaining 24 were midpoints of the edges of formulation space. The design was performed in 3 blocks, and all combinations were run in a random order. The non-linear quadratic model generated by the design represents the quantitative effect of formulation variables (X_1 - sucrose palmitate-to-glycerol ratio, X_2 - Tween 60-to-oil phase ratio, X_3 - oil phase-to- glycerol phase ratio, X_4 - oil-glycerol gel-to-aqueous phase ratio) on the responses (Y):

$$Y = a_0 + a_1X_1 + a_2X_2 + a_3X_3 + a_4X_4 + a_5X_1X_2 + a_6X_1X_3 + a_7X_1X_4 + a_8X_2X_3 + a_9X_3X_4 + a_{10}X_1^2 + a_{11}X_2^2 + a_{12}X_3^2 + a_{13}X_4^2 \quad (3.1)$$

where a_n – empirical regression coefficients, X_n – formulation variables, and Y - measured responses. Table 3.1 provides the list of all formulation variables and responses. Low, midpoint, and high levels of each formulation variables were determined from preliminary experiments.

Table 3.1 Independent process parameters and design responses.

Process variables	**Low level (-1)**	**Midpoint (0)**	**High level (1)**
X_1: sucrose palmitate-to-glycerol ratio (wt. /wt.)	0.06	0.09	0.11
X_2: Tween 60-to-oil phase ratio (wt. /wt.)	0.54	0.88	1.22
X_3: oil phase-to-glycerol phase ratio (wt. /wt.)	0.25	0.46	0.67
X_4: gel-to-water phase ratio (wt. /wt.)	0.50	1.25	2.00
Responses			
Y_1: droplet size, nm			
Y_2: zeta potential, mV			
Y_3: polydispersity (PDI)			
Y_4: stability at 20°C, hrs.			

HLB calculation

Hydrophilic-lipophilic balance (HLB) was calculated for all 27 experimental combinations using the following equation *(18)*:

$$HLB_m = x_{SP} * HLB_{SP} + x_T * HLB_T \quad (3.2)$$

where x_{SP} – weight fraction of sucrose palmitate in the mixture; x_T – weight fraction of Tween 60 in the mixture; HLB_{SP} – HLB of sucrose palmitate; HLB_T – HLB of Tween 60; HLB_m – HLB of the surfactant mixture.

Results

Visual appearance of the gels and emulsions and their corresponding TEM analysis

Figure 3.1 demonstrates the visual appearance of prepared gels and emulsions. At room temperature, gels were opaque and pale yellow in color with a semi-solid texture. When warmed to 37°C, gels became fluid and transparent. After gentle mixing with PBS, self-emulsified gels produced bluish translucent or opaque-white emulsions (Fig 3.1). Not all oil-glycerol gels were stable, as can be seen from Figure 3.1. Four formulations (#5, 6, 12, 22) had separation of glycerol from the oil-glycerol mixture (shown with black arrows in Fig. 3-1). In addition, several emulsions started to cream after 100 hours of storage (indicated with white arrows in Fig. 3.1) or had precipitation.

Figure 3.2a demonstrates a transparent and slightly yellow appearance of emulsion #1 in Table 3.2. This emulsion sample was a subject of TEM analysis, which showed the droplets to be round and to have diameters less than 200 nm (Fig. 3.2b). According to DLS analysis, this emulsion had droplets ranging from 15 to 140 nm in diameter with a small portion of droplets greater than 3000 nm (Fig. 3.2c).

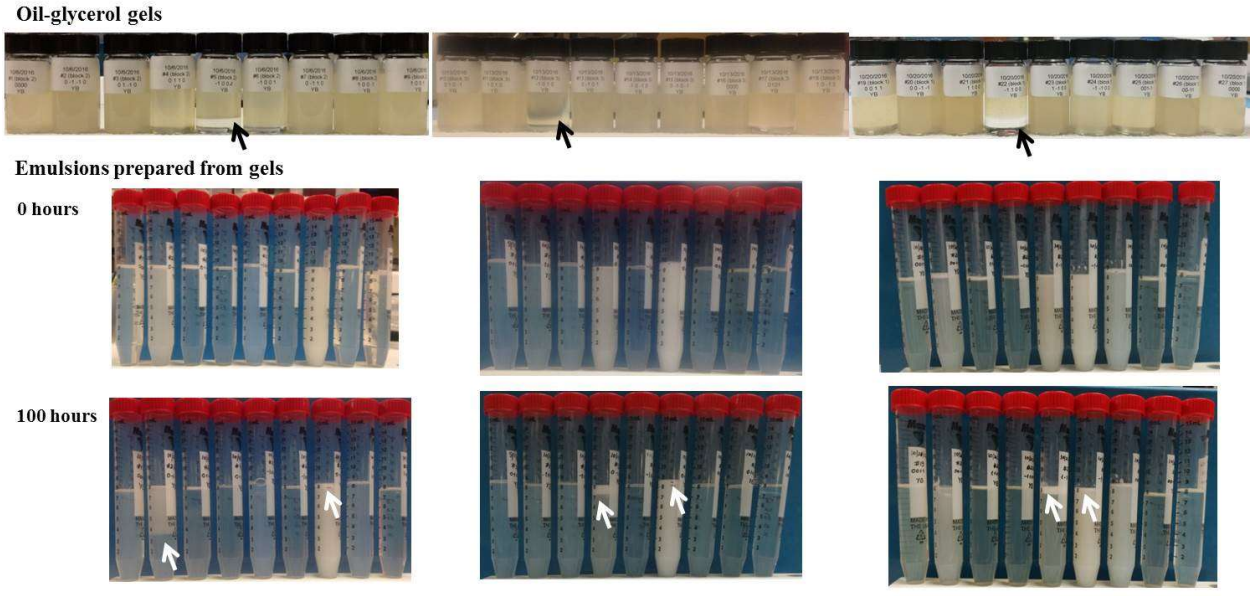

Figure 3.1 Visual appearance of oil-glycerol gels and emulsions prepared from the gels.

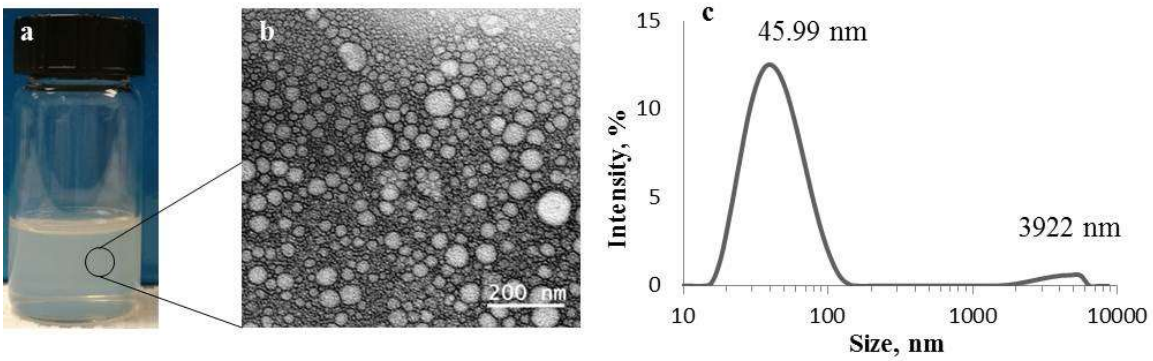

Figure 3.2 Visual appearance (a), TEM micrograph (b), and DLS droplet size distribution (c) of the emulsion made from self-emulsified gel (Sample #1).

DLS data and regression coefficients

Table 3.2 contains the design matrix, droplet size, zeta potential, polydispersity, and stability data for 27 emulsion samples. The smallest mean droplet size (24.86 nm) was observed in formulation #18 while sample #7 had the largest mean droplet size of 132.60 nm. In addition, these samples had the smallest and largest PDI, respectively. The lowest zeta potential was

observed in sample #2 (-26.9 mV) and the highest was in sample #17 (-8.66 mV). Four samples were stable for less than an hour, while twelve samples were stable for at least 1000 hours at room temperature. The rest demonstrated intermediate stability between 10 and 100 hours.

Table 3.2 Design matrix and collected response data.

Run order	Block	X_1	X_2	X_3	X_4	Y_1	Y_2	Y_3	Y_4	HLB_m
1	2	0	0	0	0	40.76	-13.07	0.205	1000	15.198
2	2	0	-1	-1	0	49.71	-26.90	0.373	1	15.425
3	2	0	1	-1	0	25.13	-22.63	0.248	10	15.305
4	2	0	1	1	0	29.13	-13.00	0.053	100	15.096
5	2	-1	0	0	-1	37.53	-10.90	0.071	1000	15.140
6	2	-1	0	0	1	34.74	-9.53	0.047	1000	15.140
7	2	0	-1	1	0	132.60	-21.73	0.447	1	15.180
8	2	1	0	0	-1	35.56	-12.90	0.107	1000	15.249
9	2	1	0	0	1	39.15	-9.50	0.217	100	15.249
10	3	0	1	0	-1	43.34	-9.70	0.223	1000	15.165
11	3	1	0	1	0	44.01	-14.70	0.211	1000	15.166
12	3	-1	0	1	0	44.27	-11.60	0.129	1000	15.077
13	3	0	-1	0	1	118.30	-20.87	0.992	1	15.265
14	3	-1	0	-1	0	31.19	-11.90	0.141	1000	15.273
15	3	0	-1	0	-1	122.77	-22.37	0.261	10	15.265
16	3	0	0	0	0	51.02	-11.10	0.342	1000	15.198
17	3	0	1	0	1	27.61	-8.66	0.041	100	15.165
18	3	1	0	-1	0	24.86	-17.00	0.068	100	15.407
19	1	0	0	1	1	47.58	-13.03	0.229	1000	15.123
20	1	0	0	-1	-1	59.59	-15.7	0.524	100	15.347
21	1	1	1	0	0	25.33	-16.27	0.060	100	15.212
22	1	-1	1	0	0	27.66	-17.43	0.060	100	15.111
23	1	1	-1	0	0	115.77	-22.73	0.869	1	15.321
24	1	-1	-1	0	0	108.97	-18.37	0.380	10	15.198
25	1	0	0	1	-1	67.29	-12.53	0.244	1000	15.123
26	1	0	0	-1	1	25.95	-11.63	0.044	100	15.347
27	1	0	0	0	0	34.16	-10.60	0.075	1000	15.198

X_1 –sucrose palmitate-to-glycerol phase ratio; X_2 –Tween 60-to-oil phase ratio; X_3 –oil phase-to-glycerol phase ratio; X_4 – gel-to-water phase ratio; Y_1 - mean droplet size, nm; Y_2 – zeta potential, mV
Y_3 – polydispersity index; Y_4 – visual stability (after 1 hr., 10 hrs., 100 hrs., 1000 hrs.)

According to Table 3.2, HLB of the surfactant mixture (HLB_m) was approximately 15 in all emulsion samples, with the highest equal to 15.425 in sample #2 and lowest equal to 15.077 in sample #12.

The data from Table 3.2 were used to obtain regression coefficients with Minitab software for quadratic polynomials (Table 3.3). Each coefficient estimated change in the mean response corresponding to the unit change in the independent variable while all other variables were held constant. A regression coefficient with a p-value less than 0.05 indicated a statistically significant relationship between the formulation variable and the response. Thus, Tween 60-to-oil phase ratio (X_2) and oil-to-glycerol phase ratio (X_3) had the largest effect on the mean droplet size of emulsions. The Tween 60-to-oil phase ratio had an antagonistic effect on droplet size; a higher proportion of Tween 60 in the oil phase lowered emulsion droplet size. Decreasing the ratio of the oil phase to the glycerol phase increased the droplet size of emulsions. Interestingly, the amount of the second emulsifier, sucrose palmitate, did not affect the diameter of emulsion droplets significantly. The Tween 60-to-oil phase ratio also affected both zeta potential and polydispersity of emulsions. The stability of emulsions was most dependent on the oil phase-to-glycerol phase ratio (X_3) and the squared Tween 60-to-oil phase ratio (X_2).

Only the regression coefficients with statistically significant effects on outcomes (Table 3.3) were included in the polynomial equations to quantify the relationship between responses and formulation parameters.

$$Y_1 = 41.98 - 39.16X_2 + 12.37X_3 - 19.72X_2X_3 - 27.38X_2^2 \quad (3.3)$$

$$Y_2 = 0.207 - 0.220X_2 - 0.228X_2X_4 + 0.146X_2^2 \quad (3.4)$$

$$Y_3 = -11.59 + 3.78X_2 - 6.31X_2^2 - 2.77X_3^2 \quad (3.5)$$

$$Y_4 = 1{,}000 + 232.2X_3 - 731X_2^2 \quad (3.6)$$

In addition, the most accurate correlation (R^2=0.9341) was between predicted and measured droplet size; the least accurate correlation (R^2=0.7915) was observed for prediction of the polydispersity index (Table 3.3).

Table 3.3 Regression coefficients obtained for each response.

	Y_1 – Size (nm)		Y_2 – Zeta potential (mV)		Y_3 - Polydispersity		Y_4 – Stability (hrs.)	
	Coefficient	P-value*	Coefficient	P-value*	Coefficient	P-value*	Coefficient	P-value*
Constant	**41.98**	**0.000**	**-11.59**	**0.000**	**0.207**	**0.044**	**1000**	**0.000**
X_1	0.03	0.994	-1.114	0.173	0.0587	0.228	-150.7	0.094
X_2	**-39.16**	**0.000**	**3.772**	**0.000**	**-0.2198**	**0.000**	115.5	0.188
X_3	**12.37**	**0.006**	1.597	0.060	-0.007	0.882	**232.2**	**0.016**
X_4	-6.06	0.128	0.907	0.261	0.0114	0.809	-150.6	0.094
X_1*X_1	-4.78	0.407	-0.330	0.783	-0.0604	0.401	-109	0.398
X_2*X_2	**27.38**	**0.000**	**-6.310**	**0.000**	**0.1455**	**0.058**	**-731**	**0.000**
X_3*X_3	-3.25	0.570	**-2.770**	**0.034**	-0.0164	0.817	-233	0.085
X_4*X_4	6.52	0.264	1.610	0.188	0.0196	0.782	-108	0.400
X_1*X_2	-2.28	0.728	1.380	0.320	-0.1225	0.152	3	0.986
X_1*X_3	1.52	0.817	0.500	0.714	0.0386	0.639	225	0.142
X_1*X_4	1.5	0.808	0.510	0.710	0.0335	0.683	-225	0.143
X_2*X_3	**-19.72**	**0.010**	1.12	0.418	-0.0674	0.416	22	0.879
X_2*X_4	-2.82	0.669	-0.11	0.933	**-0.2283**	**0.015**	-223	0.146
X_3*X_4	3.48	0.598	-1.14	0.408	0.1163	0.172	0	1.000
R^2	**0.9341**		**0.8691**		**0.7915**		**0.8351**	

***p-value < 0.05 indicates coefficients with the largest effect presented in bold numbers**

X_1 –sucrose palmitate-to-glycerol phase ratio; X_2 –Tween 60-to-oil phase ratio; X_3 –oil phase-to-glycerol phase ratio; X_4 –gel-to-water phase ratio.

R^2 - coefficient of determination indicating how close the model fits data.

The effect of formulation variables on the physical characteristics of emulsions

Table 3.3 shows that two independent variables, the Tween 60-to-oil phase ratio (X_2) and oil phase-to-glycerol phase ratio (X_3), had the most significant effect on all responses. The relationship between these two variables and their impact on all responses were demonstrated using contour plots (Fig. 3.3). Impact of the Tween 60-to-oil phase ratio on droplet size of emulsions and on polydispersity (PDI) was similar (Fig. 3.3a, b). At high Tween 60-to-oil phase ratios, the emulsions exhibited the smallest droplets (40 nm and less) and less than 0.2 PDI (Fig. 3.3a, b). However, emulsions had bigger droplets (>60 nm) and higher polydispersity (>0.3) at low Tween 60-to-oil phase ratios.

In addition, at low Tween 60-to-oil phase ratios, the oil phase-to-glycerol phase ratio impacted droplet size of emulsions. Thus, emulsions had smaller droplets (<80 nm) at low oil content, while considerably bigger mean sizes (>120 nm) were observed at higher oil contents. Moreover, emulsions having bimodal size distributions were present in regions with low Tween 60-to-oil phase ratios (filled markers on Fig. 3.3a). Remarkably, formulations with stabilities higher than 800 hrs. were achieved at medium Tween 60-to-oil phase ratios and high oil-to-glycerol ratios (Fig. 3.3d). In addition, when Figures 3.3c and 3.3d were compared side-by-side, emulsions with zeta potential values higher than -14 mV were stable longer than emulsions with a surface charge less than -20 mV. However, if precipitation was not considered as emulsion instability, the appearance of the stability contour became similar to the mean droplet size contour with more stable emulsions observed at high Tween 60-to-oil phase ratios (Fig. 3.3e).

Response optimization

The composition of emulsions was optimized to achieve minimum and maximum mean droplet size by using Equation 3.3. For example, it was estimated that to formulate the emulsion with the smallest possible mean droplet size the following ratios of components should be used: sucrose palmitate to glycerol ratio equal to 0.06, Tween 60 to oil - 1.22, the oil phase to glycerol phase - 0.67, and gel to water phase – 1.65 (Table 3.4). The model predicted average droplet size to be 13.7 nm with 15.9 standard error fit (SE fit) (Table 3.4). To validate the predicted outcome, three replicates of the above formulation were prepared according to the technique described in the Methods section followed by DLS and visual observation to measure the actual responses (Table 3.4). Thus, the observed mean droplet size in all three repeated measurements was around 30 nm. All had comparable size distributions with droplets ranging from 15.7 nm to 68.0 nm (Fig. 3.4a).

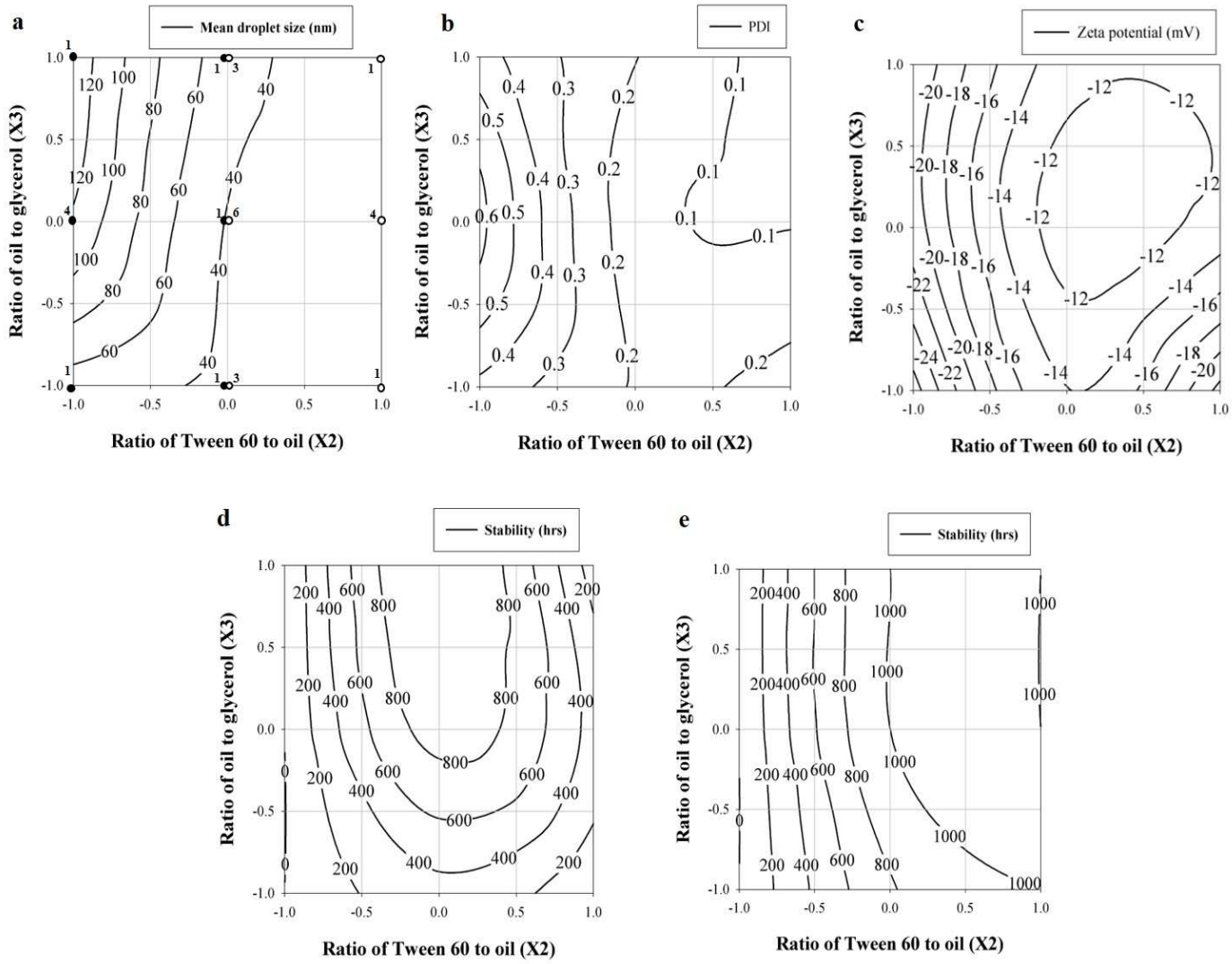

Figure 3.3 Contour plots showing the effect of Tween 60-to-oil ratio (X_2) and oil-to-glycerol ratio (X_3) on the droplet size (a), polydispersity (b), zeta potential (c), and stability (d, e) of self-emulsified emulsions. Filled and blank marks with numbers next to the mark show how many samples with this composition have bimodal and single size distributions, respectively.

For an optimized emulsion with maximal mean droplet size, the model predicted an outcome of 145.6 nm. While observed average droplet sizes were 86.3 nm, 120.0 nm, and 82.4 nm in each of the three replicates, the DLS size distributions in two samples were bimodal (Fig. 3.4b). For example, bimodality was detected in the second repeat with a larger particle population at sizes ranging from 68 to 712 nm and a peak at 190 nm. A smaller number of droplets were within a smaller range sizes from 21 to 58 nm with a peak at 37.8 nm. Similarly, the bimodal size distribution was in the third repeat where approximately equal populations of droplets were within a smaller size range (21-91 nm) with a maximum at 50.7 nm, and within a larger size range (106-712 nm) with a peak at 164 nm (Fig. 3.4b). In addition, all three replications of this emulsion were only stable for 1 hour.

Table 3.4 Optimization of emulsion mean droplet size and stability.

Composition	Response	Goal	Predicted response			Observed response***
			Fit	SE fit*	95% CI**	
$X_1 = 0.06$ $X_2 = 1.22$ $X_3 = 0.67$ $X_4 = 1.65$	Size	Minimize	13.7 nm	15.9	(-21.1, 48.4)	31.3 ± 0.3 nm 30.7 ± 0.2 nm 35.8 ± 0.2 nm
$X_1 = 0.10$ $X_2 = 0.54$ $X_3 = 0.67$ $X_4 = 2.00$	Size	Maximize	145.6 nm	16.1	(110.4, 180.8)	86.3 ± 0.9 nm 120.0 ± 1.7 nm 82.4 ± 0.9 nm
$X_1 = 0.11$ $X_2 = 0.97$ $X_3 = 0.67$ $X_4 = 0.50$	Stability	Maximize	1277 hrs. (-11.0 mV)	330	(558, 1996)	10 hrs. (-9.7±1.4 mV) 1000 hrs. (-12.3±4.4 mV) 1 hr. (-14.5±0.6 mV)

X_1 –sucrose palmitate-to-glycerol phase ratio; X_2 –Tween 60-to-oil phase ratio; X_3 –oil phase-to-glycerol phase ratio; X_4 –gel-to-water phase ratio.

*Standard error of the fit estimates the variation in the estimated mean response for the specified variable settings; **95% confidence interval; *** Droplet size data collected from three DLS measurements of each replicate and represented as a mean ± standard deviation (SD).

Likewise, the model validation and response optimization were performed with respect to emulsion stability (Equation 3.6). The emulsion was formulated with a predicted maximum

stability of 1277 hours (Table 3.4). Three replications of the same formulation had similar droplet size distribution and zeta potential values (Fig. 3.4c, Table 3.4). However, two out of three were stable less than predicted having precipitation after 1 hour and 10 hours of storage, respectively, none of the samples had creaming or phase separation after 1000 hours of storage (photograph insertion in Fig. 3.4c).

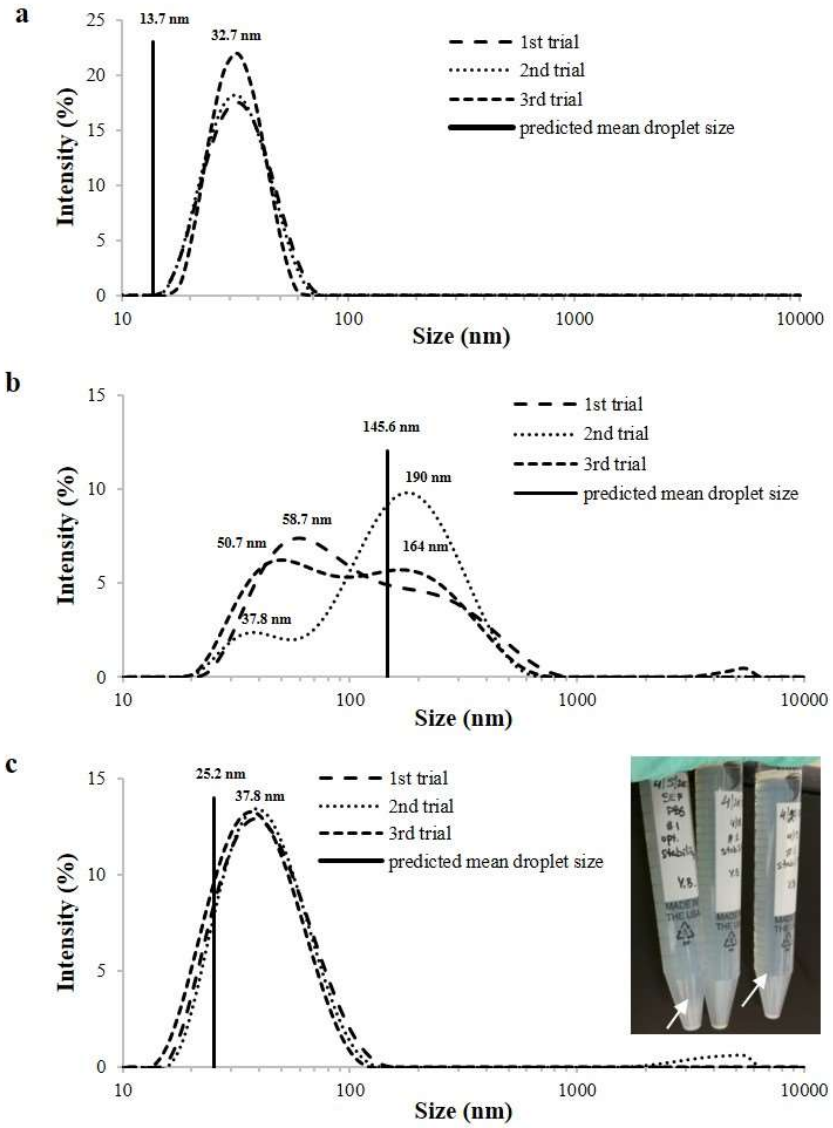

Figure 3.4 DLS size distribution of optimized emulsion replicates with minimal mean droplet size (a); maximum mean droplet size (b), and maximum stability (c). Photograph insertion depicts emulsion appearance after 1000-hour storage at room temperature and has white arrows indicating the level of precepitation.

In addition, emulsions were optimized to have three following outcomes: minimum average droplet size with maximum stability, mean droplet size of 70 nm and maximum stability, and maximum average droplet size with maximum stability (Table 3.5). Emulsions were formulated according to the compositions indicated in Table 3.5. In the sample with minimum mean droplet size and maximum stability, the observed responses of 29.31 nm average droplet diameter and 1000 hrs. stability were in agreement with the predicted values, 24.90 nm and 1000 hrs., respectively (Table 3.5, Fig. 3.5).

Table 3.5 Response optimization with respect to two dependent parameters: size and stability.

Response	Criteria	Composition	Predicted response			Observed response***
			Fit	SE fit*	95% CI**	
Size	Minimize	X_1=0.11 X_2=1.06	24.90 nm	11.7	(-0.6, 50.3)	29.31 ± 0.09 nm
Stability	Maximize	X_3=0.67 X_4=0.97	1000 hrs.	260	(433, 1567)	1000 hrs.
Size	70 nm	X_1=0.09 X_2=0.8	70.01 nm	7.30	(54.10, 85.92)	52.32 ± 0.48 nm
Stability	Maximize	X_3=0.56 X_4=0.5	999 hrs.	163	(644, 1353)	100 hrs.
Size	Maximize	X_1=0.11 X_2=0.71	91.60 nm	14.9	(59.1, 124.1)	62.18 ± 0.76 nm
Stability	Maximize	X_3=0.67 X_4=0.5	866 hrs.	333	(141, 1592)	100 hrs.

X_1 –sucrose palmitate-to-glycerol phase ratio; X_2 –Tween 60-to-oil phase ratio; X_3 –oil phase-to-glycerol phase ratio; X_4 –gel-to-water phase ratio.

*Standard error of the fit estimates the variation in the estimated mean response for the specified variable settings; **95% confidence interval; *** Droplet size data collected from three DLS measurements and represented as a mean ± SD

The observed responses for the two other desired outcomes were different from the predicted values. For example, the emulsion designed to have maximum average droplet size and maximum stability had predicted values 91.60 nm for droplet size and 866 hours for stability, while the measured responses were 62.18 nm (droplets ranging from 18.2 to 459.0 nm) and less than 100 hours, respectively (Table 3.5, Fig. 3.5).

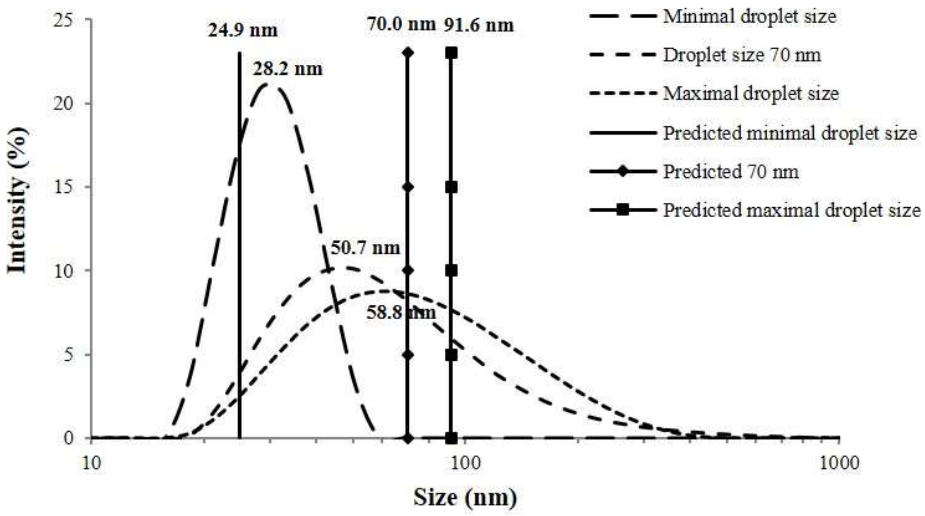

Figure 3.5 DLS droplet size distributions in optimized emulsions with maximal stability and three desired mean droplet sizes.

Discussion

Many formulation parameters impact the formation of emulsions produced by spontaneous emulsification. In this project, response surface methodology was employed to study the effect of four composition ratios on formation of emulsions with the goal to optimize these emulsions for application in animal vaccines. DLS and visual observation were used to collect response data for 27 treatment combinations.

Most of the prepared self-emulsified gels were stable and homogenous in appearance (Fig. 3.1). However, a few samples showed separation of glycerol from the oil phase. The low sucrose palmitate formulation affected the stability of the gels. Nevertheless, stable emulsions were still formed by these gels (Fig. 3.1) indicating that the sucrose palmitate concentration played a larger role in the stability of the oil-glycerol gels than it did in the stability of the final emulsions.

TEM confirmed that DLS data regarding droplet size distributions. Both methods provided similar data for emulsion size distribution (Fig. 3.2) signifying that DLS was an appropriate choice for measuring emulsion droplet size.

As different oils require a specific HLB value for successful emulsification *(18)*, HLB of the surfactant mixtures was calculated for all 27 treatment combinations. The oil composition stayed constant in all mixtures while the proportions of the surfactants changed. However, the HLB value was estimated to be similar (~15) in all mixtures indicating that it did not affect the formulation properties of the emulsions (Table 3.2).

The mean droplet size of the emulsions was largely dependent on the Tween 60-to-oil phase ratio. Thus, at high Tween 60-to-oil ratios, emulsion samples had droplets smaller than 40 nm and size distributions with a single peak (Fig. 3.3a). Moreover, polydispersity was also lower in samples with a high Tween 60-to-oil phase ratio (Fig. 3.3b). This observation agrees with a general understanding that high surfactant contents decrease droplet size of emulsions and provide more uniform droplets by reducing the surface tension between phases.

In the region with low Tween 60-to-oil phase ratio, the oil phase-to-glycerol phase ratio also affected the mean droplet size (Fig. 3.3a). At high oil to glycerol ratios, the emulsion produced from gels had larger droplets in comparison with region where ratios of oil to glycerol were lower. This indicates that the amount of the glycerol had an impact on the diameters of the emulsion droplets produced. Indeed, it has been proposed that glycerol reduces the droplet size of emulsions by lowering interfacial tension between oil and aqueous phases and affects the solubility and adsorption properties of the surfactants *(19)*. Similarly, in this study, the increase in content of glycerol provided a reduction in average droplet size of emulsions from 120 to 60 nm.

The effects of Tween 60-to-oil and oil phase-to-glycerol phase ratios on zeta potential and stability of emulsions were different. The less negative zeta potential values were observed in formulation at medium levels of both ratios. The emulsions were stable longer in the region with medium Tween 60-to-oil ratio and medium or high oil-to-glycerol ratio as well, coinciding with less negative zeta potential values (Fig 3.3c, d). It is generally presumed that emulsions are more

stable with high zeta potential (negative or positive) due to stronger electrostatic repulsion forces between droplets *(20)*. In this study, more stable emulsions had zeta potential values higher than -14 mV, while samples with zeta potentials lower than -20 mV were less stable. Although zeta potential can be a good indicator of emulsion stability, it has been suggested that the differences in values should be at least 10 mV to observe the correlation between these two parameters *(21)*. Thus, Roland has reported that there was no correlation between the stability of emulsions and zeta potential in a range of -43.1 to -50.2 mV *(22)*. However, in this study, one sample having zeta potential -26.9 mV was stable for 1 hour (#2), while another sample with the surface charge -9.7 mV was stable for at least 1000 hours (#10). In addition, according to Table 3.2, both samples had comparable average droplet size, 49.71 and 43.34 nm, respectively, indicating that it was not a variation in the droplet size that impacted the observed stability difference. However, the #10 emulsion contained a higher amount of Tween 60 than the #2 emulsion, suggesting that the steric repulsion provided by the nonionic surfactant was a key factor in stabilizing the #10 sample but not in the #2 emulsion where the amount of the surfactant was low.

Several emulsions had precipitation after the storage. The nature of the precipitation was not determined in this study and shall be investigated in the future. Nevertheless, when the precipitation was not considered as a type of emulsion visual instability, the appearance of the stability contour plot had changed (Fig. 3.3e). In this case, emulsions were more stable (no creaming) in areas with a high Tween 60 content, coinciding with small mean droplet size and low polydispersity regions (Fig. 3.3a, b, e).

Polynomial equations describing relationships between formulation parameters and responses were used to optimize emulsions and create samples with predicted outcomes. The model predicted a minimal average droplet size for emulsion to be 13.7 nm with a 95% confidence interval (CI) between -21.1 and 48.4 nm. The observed average droplet size was ~30 nm with very

similar size distributions in each of the three repeats of the formulation falling into a 95% CI estimated by the model (Fig. 3.4a, Table 3.4).

The predicted maximal average droplet size of optimized emulsion was different from that which was observed. While the model predicted a mean droplet size of 145.6 nm, the measured responses in three replicates were 86.3, 120.0, 82.4 nm, respectively. However, the DLS provided bimodal droplet size distributions of the measured samples (Fig. 3.4b). Additionally, the optimized emulsion contained a low Tween 60 to oil ratio and the bimodality had already been observed in this formulation region (Fig. 3.3a). Presumably, both bimodal size distribution and the fact that all three emulsion repeats were stable for less than 1 hour contributed to the differences between predicted and estimated mean droplet size.

Predicted and observed values for the maximal stability of the optimized emulsion were not in agreement. Although all repeats had very similar droplet size distributions and zeta potentials, two out of three had a small amount of precipitation after 1 hour and 10 hours of storage, respectively (Fig. 3.4b). As with precipitation that was observed in the original experimental combinations, the nature of the precipitation was not determined in the optimized emulsions. The aim of future work shall be to establish its connection to the emulsion instability or to the impurities in emulsion components.

Furthermore, when two responses (size and stability) were optimized simultaneously, a good correlation was observed for predicted and measured mean droplet sizes. However, predicted and observed stabilities of the emulsions disagreed (Table 3.5).

Considering the observations above and the fact that the R^2 values were 0.9341 and 0.8351 for droplet size and stability data, respectively, it was found that the polynomial equation developed provided close predictions for the average droplet size. However, some improvements are needed with respect to the impact of formulation parameters on the stability of the emulsions.

Therefore, it has been proposed for future research to investigate what additional parameters need to be included in the experimental design to improve the model describing emulsion stability.

Conclusions

This study used response surface methodology to study the impact of four formulation parameters (sucrose palmitate-to-glycerol ratio, Tween 60-to-oil phase ratio, glycerol-to-oil ratio, and gel-to-water phase ratio) on the physical characteristics of emulsions produced by spontaneous emulsification from oil-glycerol gels. Gels formed emulsions with nanometer droplet sizes. Two parameters, Tween 60-to-oil phase ratio and glycerol-to-oil ratio, had the largest effect on average diameter and polydispersity of droplets. Remarkably, sucrose palmitate contents did not influence the droplet size, PDI, zeta potential or stability of emulsions significantly; it only affected the formation of stable oil-glycerol gels. In addition, the correlation between zeta potential values and stability of the emulsions did not follow the prior understanding suggesting that more stable emulsions formed in the region where zeta potential was less negative.

Polynomial equations were developed to describe the relationships between formulation variables of the emulsions and the outcome. These were employed to design emulsions with predicted responses. Although the model demonstrated a close prediction for the mean droplet size of emulsions, apparently, additional parameters need to be added to improve the reliability of the model optimizing emulsion stability.

References

1. Solans, C.; Morales, D.; Homs, M. Spontaneous emulsification. *Curr. Opin. Colloid Interface Sci.* **2016***, 22*, 88-93.

2. Charman, S.; Charman, W.; Rogge, M.; Wilson, T.; Dutko, F.; Pouton, C. Self- Emulsifying Drug Delivery Systems: Formulation and Biopharmaceutic Evaluation of an Investigational Lipophilic Compound. *Pharm. Res.* **1992***, 9*, 87-93.

3. Gursoy, N. R.; Benita, S. Self-emulsifying drug delivery systems (SEDDS) for improved oral delivery of lipophilic drugs. *Biomedicine & Pharmacotherapy* **2004***, 58*, 173-182.

4. Wang, L.; Li, X.; Zhang, G.; Dong, J.; Eastoe, J. Oil-in-water nanoemulsions for pesticide formulations. *J. Colloid Interface Sci.* **2007***, 314*, 230-235.

5. Boonme, P. Applications of microemulsions in cosmetics. *J Cosmet Dermatol* **2007***, 6*, 223-228.

6. Shenglong, S.; Yefei, W.; Lushan, W.; Yanxin, J.; Tao, W.; Jing, W. Potential of Spontaneous Emulsification Flooding for Enhancing Oil Recovery in High Temperature and High Salinity Oil Reservoir. *J. Dispersion Sci. Technol.* **2014**.

7. Myers, R. H. *Response surface methodology;* Boston, Allyn and Bacon: Boston, 1971; .

8. Zidan, A. S.; Sammour, O. A.; Hammad, M. A.; Megrab, N. A.; Habib, M. J.; Khan, M. A. Quality by design: Understanding the formulation variables of a cyclosporine A self-nanoemulsified drug delivery systems by Box– Behnken design and desirability function. *Int. J. Pharm.* **2007***, 332*, 55-63.

9. Zhu, S.; Hong, M.; Liu, C.; Pei, Y. Application of Box- Behnken design in understanding the quality of genistein self- nanoemulsified drug delivery systems and optimizing its formulation. *Pharm. Dev. Technol.* **2009***, 14*, 642.

10. Hao, J.; Fang, X.; Zhou, Y.; Wang, J.; Guo, F.; Li, F.; Peng, X. Development and optimization of solid lipid nanoparticle formulation for ophthalmic delivery of chloramphenicol using a Box-Behnken design. *Int J Nanomedicine* **2011***, 6*, 683-692.

11. Box, G. E. P.; Behnken, D. W. Some new three level designs for the study of quantitative variables. *Technometrics* **1960***, 2*, 455-475.

12. Stone, H. D. Newcastle Disease Oil Emulsion Vaccines Prepared with Animal, Vegetable, and Synthetic Oils. *Avian Dis.* **1997***, 41*, 591-597.

13. Jansen, T.; Hofmans, M. P. M.; Theelen, M. J. G.; Manders, F.; Schijns, V. E. J. C. Structure-and oil type-based efficacy of emulsion adjuvants. *Vaccine* **2006***, 24*, 5400-5405.

14. Burakova, Y.; Shi, J.; Schlup, J. R. Impact of oil composition on formation and stability of emulsions produced by spontaneous emulsification. *J. Dispersion Sci. Technol.* **2017***, 38*, 1749-1754.

15. Krishna, G.; Sheth, B. B. A novel self emulsifying parenteral drug delivery system. *PDA J. Pharm. Sci. Technol.* **1999***, 53*, 168.

16. Saberi, A. H.; Fang, Y.; Mcclements, D. J. Effect of glycerol on formation, stability, and properties of vitamin-E enriched nanoemulsions produced using spontaneous emulsification. *J. Colloid Interface Sci.* **2013***, 411*, 105-113.

17. Floyd, A. G. Top ten considerations in the development of parenteral emulsions. *Pharm. Sci. Technol. Today* **1999***, 2*, 134-143.

18. Pasquali, R. C.; Taurozzi, M. P.; Bregni, C. Some considerations about the hydrophilic–lipophilic balance system. *Int J Pharm* **2008***, 356*, 44-51.

19. Magdassi, S.; Frank, S. Formation of oil-in- glycerol/ water emulsions. *J. Dispersion Sci. Technol.* **1986***, 7*, 599-612.

20. Sharma, S.; Shukla, P.; Misra, A.; Mishra, P. R. In *Chapter 8 - Interfacial and colloidal properties of emulsified systems: Pharmaceutical and biological perspective;* Ohshima, H., Makino, K., Eds.; Colloid and Interface Science in Pharmaceutical Research and Development; Elsevier: Amsterdam, 2014; pp 149-172.

21. Lu, G. W.; Gao, P. In *CHAPTER 3 - Emulsions and Microemulsions for Topical and Transdermal Drug Delivery;* Kulkarni, V. S., Ed.; Handbook of Non-Invasive Drug Delivery Systems; William Andrew Publishing: Boston, 2010; pp 59-94.

22. Roland, I.; Piel, G.; Delattre, L.; Evrard, B. Systematic characterization of oil-in-water emulsions for formulation design. *International Journal of Pharmaceutics* **2003***, 263*, 85-94.

Chapter 4 - Food-Grade Saponin Extract as an Emulsifier and Immunostimulant in Emulsion-Based Subunit Vaccine for Pigs

Abstract

Subunit vaccines consisting of highly purified antigens require the presence of adjuvants to create effective and long-lasting protective immunity. Advances on adjuvant research include designing combination adjuvants which incorporate two or more adjuvants to enhance vaccine efficacy. Previously, an oil-in-water emulsion adjuvant (OW-14) composed of mineral oil and an inexpensive gum Arabic emulsifier has been reported demonstrating enhanced and robust immune responses when used as an adjuvant in swine subunit vaccines. This study presents modified version of OW-14 prepared with food-grade *Quillaja* saponin extract (OWq). In new OWq emulsion, saponins served as an emulsifier for stabilization of emulsion droplets and as an immunoactive compound. The use of saponins allowed to reduce the required amount of emulsifier in the original OW-14. However, emulsion stabilized with saponin extract demonstrated extended physical stability even at elevated temperature (37°C). The two-dose vaccination with a classical swine fever virus (CSFV) glycoprotein E2-based vaccine formulated with OWq produced higher levels of E2-specific IgG and virus neutralizing antibodies in pigs in contrast with animals that received the vaccine adjuvanted with oil only. In addition, new OWq adjuvant was safe to use in the vaccination of pigs.

Introduction

The effectiveness of subunit vaccines relies on immunostimulatory adjuvants to induce potent and long-lasting antigen-specific immune responses. Early adjuvants, like aluminum salts and emulsions, are still the primary choice in vaccine formulations for livestock species because of their safety, simple formulation, and low cost *(1, 2)*. However, the efficacy of these conventional

adjuvants in induction of antibody responses warrants further improvements. Combination of aluminum salts or emulsions with immunostimulant substances is currently considered to be a promising approach in boosting of the vaccine performance *(3, 4)*. Combination of the adjuvants with different modes of action presents potential on both enhanced and tailored immune responses for long-lasting protection against the disease. Co-administration of two or more adjuvants in one vaccine has also been explored in veterinary medicine *(2)*. The combination of different immunostimulant substances, such as saponins, with emulsions and aluminum salts in vaccines for livestock has been actively studied by several research groups *(5-7)*. For instance, the addition of saponin extract Quil A® to commercial emulsion-based vaccine was reported to improve humoral immune responses in pigs vaccinated for foot-and-mouth disease *(7).* In this present study, we utilized saponin extract, not only as immunostimulatory compound, but also as emulsifier to stabilize the emulsion adjuvant.

Saponins are naturally occurring triterpene glucoside compounds (Fig. 4.1) that are commonly used in vaccine research studies against both animal and human pathogens *(8)*. *Quillaja saponaria* Molina tree is a main source of saponins for vaccine adjuvants, although there are reports of immunostimulant activity of saponins obtained from other plants *(9)* and semisynthetic saponins *(10)*. Commercial saponin-based adjuvants isolated from *Q. saponaria* tree such as Quil-A (Brenntag Biosector A/S, Denmark) and QS-21 (Desert King, USA) are very potent in inducing high antigen-specific immune responses of both T-helper 1 (Th1) and T-helper 2 (Th2) origins *(11)*. Studies show that the carbohydrate groups of the saponins molecule interact with receptors on antigen-presenting cells (APCs) and promote antigen phagocytosis and secretion of cytokines by APCs while acyl chain domain assist in delivery of exogenous antigens into APCs and facilitates Th1 immunity *(12)*. Aldehyde group on the triterpene domain promotes co-stimulation

of T-cell surface receptors (Fig. 4.1) *(13)*. However, the commercial application of these saponins extracts in animal vaccines is hindered by their high costs.

The food-grade *Q. saponin* extracts are also used as emulsifiers to produce flavored and vitamin beverages. Saponin molecule contains both hydrophobic and hydrophilic domains making it good candidate for stabilization of oil-in-water emulsions (Fig.4.1) *(14, 15)*.

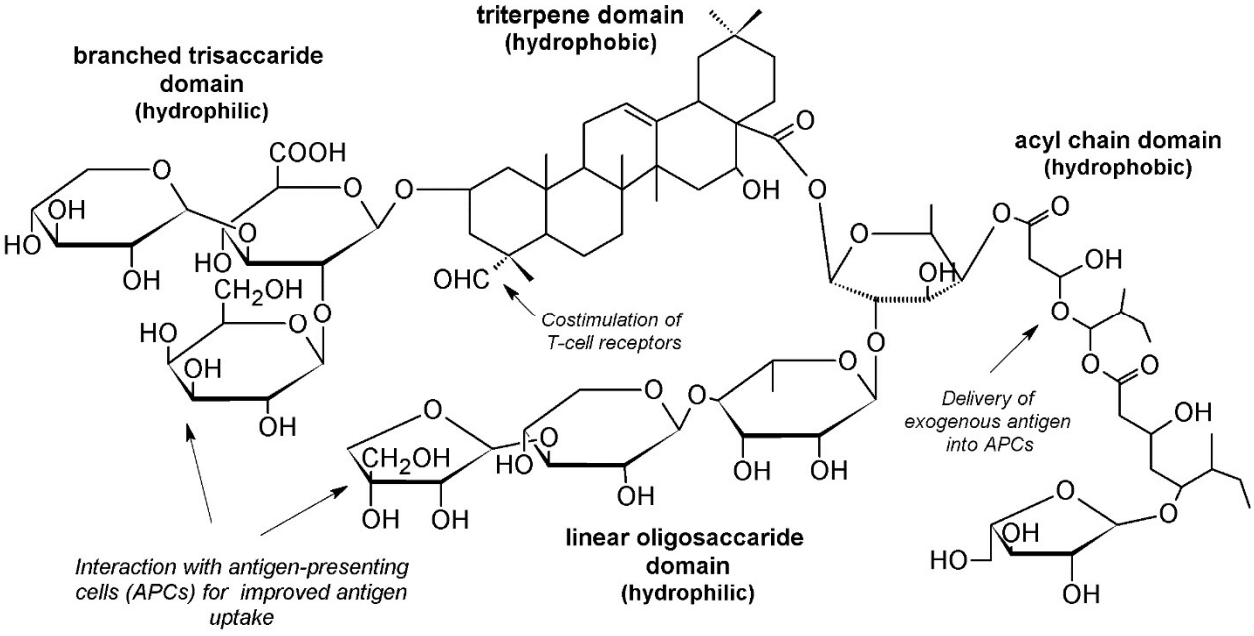

Figure 4.1 General structure of the saponin molecule adapted from Yang, et al *(14).*

A low-cost emulsion OW-14 adjuvant composed of light mineral oil and food-grade gum Arabic emulsifier has been reported previously demonstrating high level of antigen-specific antibody responses in vaccines for swine influenza (SI), *Mycoplasma hyopneumoniae*, and classical swine fever (CSF) *(16, 17)*. In the present study, a variation of the OW-14 emulsion adjuvant formulated with the food-grade saponins extract, Sapnov LS^{TM} (Naturex, USA), in the subunit vaccine for CSF were tested.

The CSF is caused by CSF virus, which is a small, enveloped RNA virus in the genus *Pestivirus* of the family *Flaviviridae (18)*. The disease is responsible for economic losses in the

swine industry in many countries. Subunit vaccines based on envelope glycoprotein E2 of classical swine fever virus (CSFV) have been shown to induce high level antigen-specific immune responses and clinical protection of pigs from CSFV challenge *(17, 19)*.

The safety and efficacy of food-grade saponin extract as the emulsifier and immunostimulant in emulsion-based adjuvant co-administered with E2 antigen were investigated. Sapnov LS^{TM} is a water extract of *Q. saponaria* with saponin content around 65% on the dry basis according to manufacturer. This cost-effective non-ionic surfactant is used for production of flavored and colored emulsions such as beverage concentrates and alcoholic drinks. To the best of our knowledge, this is the first report on application of food-grade saponin extract in emulsion-based vaccines for livestock. In addition, an experimental oil-based adjuvant (OBA) that produces an emulsion after low-energy mixing with aqueous solution of E2 antigen was tested in comparison with a saponins-based emulsion vaccine.

Materials and Methods

Materials

Light mineral oils, Drakeol 5 and Drakeol 6, were purchased from Calumet Panreco (Karns City, PA, USA). Ticamulsion A-2010 emulsifier (gum Arabic) was obtained from Tic Gums (White Marsh, MD, USA). *Quillaja* water extract Sapnov^{TM} (65% saponins content) was provided by Naturex Inc., (Chicago, IL, USA). Polymeric surfactants Atlas G-5002L and Atlox 4916 were obtained from Croda Inc. (New Castle, DE, USA). Medium chain triglyceride oil (MCT oil) was purchased from Jedwards International Inc. (Braintree, MA, USA).

Formulation of adjuvants and vaccines

Emulsion adjuvant with saponin extract (OWq) was prepared by dissolving Ticamulsion A-2010 (5% w/v) in nano-pure water and stirred overnight with a magnetic bar. *Quillaja* extract Sapnov emulsifier (0.5% v/v) was added to the Ticamulsion solution and inverted several times to

ensure complete mixing of both emulsifiers in water. Mineral oil Drakeol 5 (15% v/v) was added to the solution with emulsifiers. The coarse emulsion was mixed with high shear lab mixer (L5MA, Silverson Inc., East Longmeadow, MA, USA) at 10,000 rpm for 15 min and then passed through a microfluidizer M110P (Microfluidics, Westwood, MA, USA) for five times at 10,000 psi. OWq was stored at 4°C until use.

Insect cell-expressed CSFV E2 protein was prepared as described previously *(17)*. Subunit vaccine was formulated by mixing of 2 vol. of E2 protein solution dissolved in phosphate-buffered saline (PBS) and 1 vol. of OWq emulsion adjuvant using a vortex mixer for several seconds.

Oil-based adjuvant (OBA) was prepared by dissolving two non-ionic block copolymer surfactants, Atlas G-5002L and Atlox 4916, in a 7:1 by weight ratio mixture of MCT oil and Drakeol 6 mineral oil, respectively. Oils and surfactants were mixed together in an 80:20 by weight ratio to produce a clear yellow mixture. To prepare emulsion-based subunit vaccine, OBA was slowly added to the solution of E2 protein in PBS in a 1:1 ratio of the adjuvant to aqueous phase and stirred using a magnetic stirrer for 30 min at room temperature.

The final concentration of the antigenic E2 protein in all vaccine formulations was 50 µg per dose.

Physical characteristics and stability study of adjuvants

Freshly prepared emulsions were analyzed using dynamic light scattering (DLS) with a Malvern Zetasizer Nano ZS 90 (Malvern Instruments, Westborough, MA, USA) to determine droplet size, polydispersity, and zeta potential. The OWq emulsion adjuvant was analyzed as prepared. OBA was mixed with PBS in a 1:1 weight ratio using a magnetic stirrer to obtain emulsion for DLS analysis and storage stability assessment.

Approximately 5 µl of each emulsion sample was diluted in 1 ml of deionized water to achieve a translucent solution and perform the measurements. All samples were measured 3 times

at room temperature. Results are presented as a mean of 3 measurements ± the standard deviation (SD). The pH values of the emulsions were measured using a VWR SympHony digital pH meter SB21 (VWR International, Radnor, PA, USA), calibrated according to the manufacturer's manual. To assess the shelf stability, samples were stored at 4°C, room temperature (RT), and 37°C and then analyzed again for droplet size and pH after 6 months of storage. Emulsions were also observed visually for the presence of creaming, phase separation, and color change.

Pig immunization

The animal study was conducted in accordance with Institutional Animal Care and Use Committee (IACUC). Animals were housed at the Large Animal Research Center (LARC) facility, Kansas State University. Conventional Large White-Duroc crossbread weaned specific-pathogen free piglets (3 weeks of age) were randomly divided into two vaccine groups (n=6 for each group) and 1 negative control group (n=2). Pigs were immunized intramuscularly with 2 ml each of subunit vaccines. First group received E2 protein adjuvanted with OWq (E2+OWq). Second vaccine group was immunized with E2 and oil-based adjuvant (E2+OBA). Three out of the 6 animals in each vaccine group received a second dose of the subunit vaccines 14 days after the first immunization (two-dose pigs). The negative control group received 2 ml intramuscularly of PBS. Blood samples were collected on days 0, 7, 14, 21, and 28 of the experiment. Sera was separated from the blood and stored at -20ºC until further use in assays. Pig weights were measured weekly. Pig health was monitored daily including vaccine injection site reactions. Animals were humanely euthanized and disposed of at the end of the experiment (day 28).

Antibody responses

The E2-specific IgG, IgG1 and IgG2 antibody titers were determined in pig sera by enzyme-linked immunosorbent assay (ELISA) as described previously *(17, 20)*. Briefly, the 96-well flat-bottom microtiter plates (Corning®) were coated overnight with 62.5 ng/ml of purified

E2 followed by washing with ELISA wash buffer (0.05% Tween 20 in PBS) and blocked with ELISA blocking buffer (2% Fetal Bovine Serum in PBS) for 1 hour at 37°C. Diluted sera were added to plates and incubated for 1 hour at RT, followed by washing 3 times with ELISA wash buffer. Goat anti-swine IgG conjugated with horseradish peroxidase (HRP) (#sc-2914, Santa Cruz Biotechnology, USA, dilution 1/1,000), mouse anti-swine IgG1 (#MCA635GA, Bio-Rad Antibodies, USA, dilution 1/300) or mouse anti-swine IgG2 (#MCA636GA, Bio-Rad Antibodies, USA, dilution 1/300) in ELISA blocking buffer were added in wells at 100 µl/well as secondary antibodies and incubated 1 hour at RT followed by washing 3 times with ELISA wash buffer. HRP-conjugated goat anti-mouse IgG (H+L) (#115-035-003, Jackson ImmunoResearch, USA, dilution 1/1,000) was added to wells at 100 µl/well in case of IgG1 and IgG2 titers analysis and incubated 1 hour at RT followed by washing 3 times with washing buffer. 3,3,5,5-tetramethylbenzidine (TMB) stabilized chromogen (Novex) was used to develop the ELISA plates following by 2N sulfuric acid to stop the reaction. Relative antibody concentration was determined with an optical spectrophotometer using a SpectraMAX microplate reader at 450 nm and was analyzed with Softmax® Pro 6.4 Software (Molecular Devices, USA).

Anti-CSFV neutralization assay of pig serum

The anti-CSFV neutralizing antibody levels were measured using indirect fluorescent antibody assay (IFA) in pig serum collected on day 21 after the first dose of subunit vaccines or PBS as described elsewhere *(20)*. Neutralizing titers in serum samples were calculated as the reciprocal of the highest dilution that caused neutralization of the virus in 50% of the wells.

Statistical analysis

Data from pig experiments were reported as the mean values ± standard error of measurement (SEM). The differences between treatment groups were analyzed by one-way

analysis of variance (ANOVA) using SigmaPlot 11.0 software (Systat Software Inc., USA). Differences were considered statistically significant when $p < 0.05$.

Results

Designed adjuvants preserved their physical characteristics after prolonged storage at different temperatures

According to DLS measurements, freshly prepared OWq emulsion adjuvant had a nanoscale size of droplets with a mean value of approximately 200 nm and relatively low polydispersity, while emulsion prepared with OBA had droplets around 320 nm with the higher difference in droplet sizes (Table 4.1). All formulations had pH values around 7 (Table 4-1). The OWq emulsion had a relatively narrow size distribution ranging from 91 to 531 nm, while an emulsion prepared from oil-based adjuvant had droplets with diameters from 106 nm up to 3090 nm (Fig. 4.2A). In addition, a saponins-based emulsion had lower zeta potential value (-51.7 mV) than an emulsion prepared with OBA (-25.0 mV) (Table 4.1).

Table 4.1 Physical characteristics of fresh emulsion adjuvants and after 180-day storage at different temperatures.

Emulsion		Mean droplet size ± SD, nm	Polydispersity ± SD	Zeta potential ± SD, mV	pH
OWq	Fresh	203.40 ± 1.83	0.115 ± 0.008	-51.7 ± 0.2	7.1
	180 days at 4°C	272.50 ± 4.86	0.117 ± 0.025	-53.2 ± 0.7	6.2
	at RT	266.57 ± 5.73	0.054 ± 0.035	-58.0 ± 3.1	7.1
	at 37°C	277.80 ± 4.98	0.142 ± 0.022	-56.0 ± 3.9	6.3
OBA in PBS	Fresh	327.40 ± 4.59	0.270 ± 0.004	-25.0 ± 3.7	7.3
	180 days at 4°C	310.37 ± 2.29	0.193 ± 0.005	-12.4 ± 0.2	7.2
	at RT	217.97 ± 1.85	0.147 ± 0.010	-6.8 ± 0.4	7.2
	at 37°C	367.37 ± 0.51	0.242 ± 0.012	-11.5 ± 0.2	7.2

RT, room temperature; SD, standard deviation

After six months of storage at different temperatures, the OWq emulsion adjuvant did not undergo any significant changes in the mean size of emulsion droplets, polydispersity, zeta

potential, and pH (Table 4.1). DLS analysis detected a small shift in the emulsion size distribution towards larger droplets for all OWq samples (4°C, RT, and 37°C) (Fig. 4.2B). Thus, after 6-month storage at 37°C, the size of the OWq emulsion droplets ranged from 106 to 955 nm. However, no creaming, phase separation, and color changes were noticed in the appearance of the OWq emulsion after extended storage even at 37°C (Fig. 4.2B, photograph insertion). The mean droplet size of an emulsion prepared with OBA did not change after storage at 4°C and 37°C. However, a decrease from 320 nm to 217 nm was detected in samples stored at RT (Table 4.1). Visual observations did not detect any changes in the appearance of all OBA emulsion samples (data not shown).

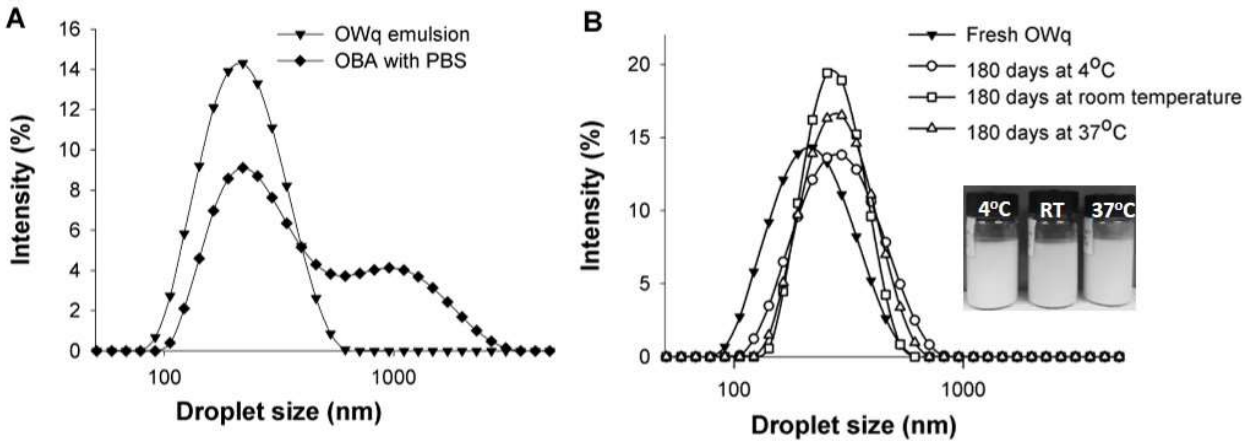

Figure 4.2 Size distribution of emulsion-based adjuvants obtained with dynamic light scattering (DLS).

A) Freshly prepared OWq emulsion had droplets within 90 – 600 nm size range, while oil-based adjuvant (OBA) mixed with PBS produced emulsion with droplets between 100 and 3,000 nm. B) After 180-day storage at different temperatures, the slight shift of size distributions towards bigger droplets were detected in OWq emulsion, however, no creaming or phase separation were observed in visual appearance of emulsion samples (photograph insertion).

Subunit vaccine with saponins-based emulsion did not produce health issues in animals and induced high antibody responses

After vaccination with E2 subunit vaccines, all pigs grew consistently; and, no difference in weight gain was observed between the animals that received one dose and two doses of the

subunit vaccines and negative control group injected with PBS (Fig.3A). The presence of small (1-2 cm) subcutaneous bumps was observed at the injection sites in the E2 + OWq vaccinated pig groups. By day 28 of study, they decreased in size and mostly disappeared. The negative control group and the E2 + OBA vaccinated pig group did not have any pathological changes at injection sites (data not shown). No issues were observed in pig health, and all animals survived by the end of the study.

Pigs that received the boost vaccine on day 14 of the study had increased E2-specific IgG levels on day 21 and 28 of the experiment (Fig. 4.3B). The animals immunized with E2 + OWq had statistically significant higher IgG titers in comparison with the vaccine group that received E2 with OBA ($p = 0.009$) and control group (Fig. 4.3C). As expected, a two-dose immunization schedule provided significantly higher IgG titers than one-dose in both vaccine groups on day 21 of the study (Fig 4.3C). The IgG1 and IgG2 antibody titers were also higher in E2 + OWq group in comparison with E2 + OBA vaccine group, although it should be noted that there was no statistically significant difference between the two groups ($p = 0.08$ and 0.12 for IgG1 and IgG2 titer analysis, respectively) (Fig. 4.3D).

Table 4.2 represents the results of anti-CSFV neutralization assay performed with pig serum collected on day 21 of the study. The highest neutralizing antibody titers were detected in pigs immunized with two doses of E2 subunit vaccine adjuvanted with OWq emulsion. Very low or no detectable titers were detected in all other pigs including animals inoculated with PBS instead of the subunit vaccine (Table 4.2).

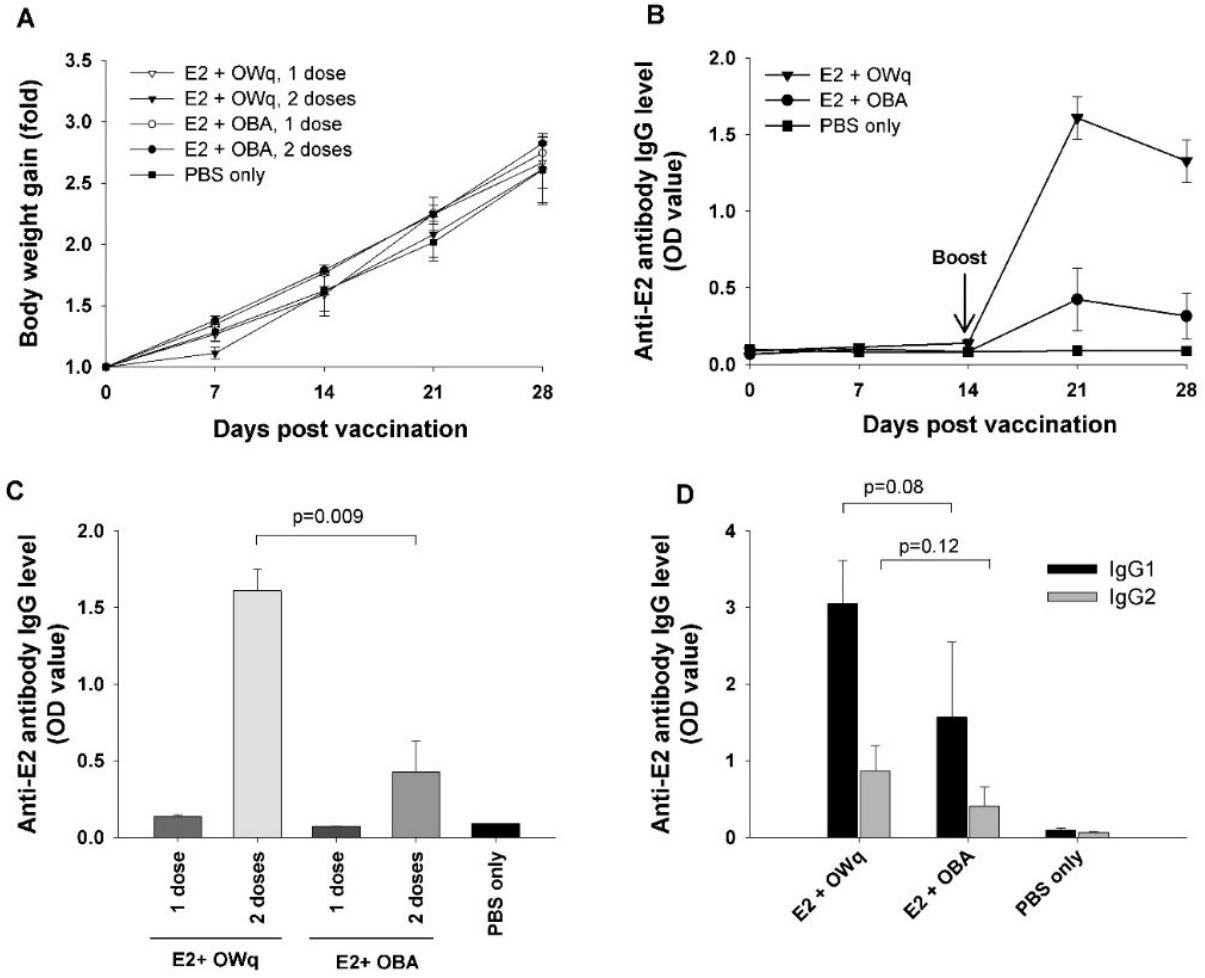

Figure 4.3 Safety and immunological effect of OWq and OBA injected with E2 antigenic protein.

Table 4.2 Anti-CSFV-neutralizing antibody titers (ND_{50}) in pigs on day 21 of the study.

Treatment group	Pig #	Day 21
E2 + OWq, 1 dose	178	<5
	181	5
	185	5
E2 + OWq, 2 doses	186	640
	188	960
	195	480
E2 + OBA, 1 dose	177	<5
	180	<5
	187	<5
E2 + OBA, 2 doses	189	480
	190	20
	193	40
PBS only	184	<5
	191	<5

Discussion

Emulsions are cost-effective vaccine adjuvants, and their combination with saponins is a promising way to increase the efficacy of veterinary vaccines. Saponins are very effective immunostimulants and have been studied in vaccine formulations for the past decades *(2)*. However, saponins' high toxicity due to their detergent properties presents the main drawback in their wide application in human and animal vaccines *(11)*. There are commercially available purified saponins extracts (Quil-A, QS-21); however, their high cost precludes their application as adjuvants in mass livestock immunization.

Safety, efficacy, and physical and chemical stability of the vaccine adjuvants are the key factors in designing novel vaccine formulations. In addition, the cost of materials and production are of paramount importance in developing of livestock vaccines *(21)*. In this study, a mineral oil-

based emulsion with a food-grade inexpensive saponins extract (OWq) and oil-based adjuvant that produces an emulsion after gentle mixing with an aqueous phase were tested for safety and immunological activity in swine vaccination.

In OWq, the saponins extract served as an emulsifier for stabilization of emulsion droplets and as an immunostimulant in the subunit vaccine. Thus, the addition of saponins extract to original formulation (OW-14) *(16)* allowed reducing the amount of Ticamulsion A-2010 emulsifier from 7.5% w/v to 5% w/v without affecting the shelf stability of adjuvant. Moreover, OWq emulsion adjuvant demonstrated good physical stability after 180 days of storage at all tested temperatures. Mean droplet size remained less than 300 nm with low polydispersity among the droplets (Table 4.1, Fig. 4.2B). The slight drop in pH values in samples stored at 4°C and 37°C was detected after 180 days. However, no physical changes in emulsion samples, such as creaming or phase separation, were observed. Physical stability is very important for livestock vaccines, especially in developing countries where refrigeration during transportation and storage of the vaccines are not always available or cost-effective.

The droplet diameters, polydispersity and zeta potential of prepared emulsions are important factors in predicting the physical stability of the emulsions. Freshly prepared OWq emulsion had nanosize droplets in a range from 91 to 531 nm and low zeta potential (-51.7 mV), which provides electrostatic repulsion between the droplets and prevents their fast flocculation and coalescence. The vaccine can be easily prepared at the site by simple hand mixing or gentle agitation of OWq with an antigenic solution. It can be readily administered through a standard syringe with 20-gauge needle.

The OBA mixed with PBS by a low-energy mixing method produced an emulsion with high polydispersity, mean droplet size around 320 nm, and zeta potential around -25 mV. No significant changes in mean droplet size were detected after 180-day storage. However, a decrease

in zeta potential value indicates lower colloidal stability over time in comparison with OWq emulsion.

The safety and immunological activity of designed adjuvants were tested in swine vaccination with E2 antigen. Pigs immunized with experimental adjuvants in subunit CSFV E2 vaccines did not experience any health issues and gained the weight on the same level as negative control pigs during the entire study (Fig 4.3A). Small subcutaneous bumps were observed at the injection sites of the OWq vaccine group, although they decreased in size significantly or disappeared towards the end of the experiment. These findings suggest that food-grade saponins extract can be safely utilized in veterinary vaccine formulations. Moreover, the group immunized with two doses of E2 subunit protein adjuvanted with OWq emulsion had higher E2-specific IgG levels (Fig. 4.3B-D) and anti-CSFV neutralizing antibody titers (Table 4-2) in comparison with vaccine group that received E2 formulated with emulsion and without saponins or other immunostimulant compounds.

The reason E2 + OBA vaccine did not induce strong IgG antibody responses and high anti-CSFV neutralizing titers can be attributed to the composition and physical characteristics of the adjuvant. OBA predominantly consisted of plant-derived MCT oil with small portion of mineral oil, while vaccines based on mineral oil generally produce more irritation at the injection sites and induce higher immune responses than vaccines with plant-derived oils *(22)*. In addition, the mean droplet size of emulsion fabricated from OBA was 327.40 nm. However, it has been demonstrated that particles less than 200 nm are processed more efficiently by the APCs *(23)*. Clearly, the changes in the composition of the OBA should be done to reduce the size of emulsion droplets and improve the emulsion stability and efficacy as a vaccine adjuvant.

Animals that were immunized twice with subunit vaccines have developed significantly higher IgG titers (Fig. 4-3C) and anti-CSFV neutralizing antibody titers (Table 4.2) in comparison

with pigs receiving the single vaccination. However, previous studies demonstrated that even one-dose vaccination with an emulsion-based subunit vaccine can protect the pigs from the challenge with CSF virus *(17, 20)*.

Previous findings have shown that saponins promote the production of IgG2 over IgG1 antibody subclass and favor Th1 and cytotoxic T-lymphocytes responses in contrast with conventional adjuvants such as aluminum salts and emulsions in murine models *(9, 11)*. These suggest that saponins adjuvants can be beneficial in vaccines against intracellular pathogens such as viruses. In the present study, IgG2 titer analysis of pig serum samples did not show statistically significant differences between saponins-based emulsion adjuvant and an emulsion without saponins (P=0.12) (Fig 4.3D). This can be attributed to several factors such as the difference between mice and swine immune responses to the saponins, heterogeneous composition of food-grade saponins extract or poor stability of the saponins resulting in stimulation of Th2 immunity rather than Th1. It has been demonstrated that various fractions of *Q. saponaria* extract have different immunological activity and can induce the production of different IgG antibody subclasses *(11)*. Another study showed that *Q. saponaria* extract are easily degraded during storage resulting in deacylation of the saponins molecules and the inability to promote a strong Th1 response and IgG2 production *(24)*. The exact fraction composition of the food-grade saponins extract used in this study is unknown and needed to be determined to verify these speculations. In addition, further investigation is required to confirm the level of protection of swine immunized with E2 protein and OWq saponins-based emulsion after the challenge with CSF virus.

Conclusion

Inexpensive food-grade saponin extract was employed to create emulsion-based adjuvant for swine subunit vaccine. Saponins served a dual purpose: stabilization of emulsion droplets and

stimulation of immune responses. The addition of saponin extract helped to reduce the amount of emulsifier in the original OW-14 adjuvant. This change in composition did not impact droplet size stability of the emulsion adjuvant. Thus, OWq can be stored at least 180 days at different temperatures without dramatic changes in droplet size, creaming, or phase separation. A saponin-based emulsion adjuvant was safe to use in swine immunization as no significant inflammations at the injection sites and consistent weight gain in animals were observed after co-administration with E2 antigenic protein. Two doses of CSF E2 subunit vaccine with OWq adjuvant demonstrated high total IgG and anti-CSFV neutralizing antibody titers in pigs in comparison with the emulsion vaccine prepared with oil-based adjuvant without saponins. This is the first demonstration that a cost-effective food-grade saponin extract can be incorporated in an emulsion-based adjuvant and safely used in livestock immunization promoting strong antibody responses.

References

1. Bowersock, T.L. and S. Martin, Vaccine delivery to animals. *Advanced Drug Delivery Reviews*, 1999. 38(2): p. 167-194.

2. Burakova, Y., et al., Adjuvants for Animal Vaccines. *Viral Immunol*, 2017. 31(1):11-22

3. Mutwiri, G., et al., Combination adjuvants: the next generation of adjuvants? *Expert Review of Vaccines*, 2011. 10(1): p. 95+.

4. Levast, B., et al., Vaccine Potentiation by Combination Adjuvants. *Vaccines*, 2014. 2(2).

5. Ren, J., et al., Enhanced immune responses in pigs by DNA vaccine coexpressing GP3 and GP5 of European type porcine reproductive and respiratory syndrome virus. *J Virol Methods*, 2014. 206: p. 27-37.

6. Çokçalışkan, C., et al., QS-21 enhances the early antibody response to oil adjuvant foot-and-mouth disease vaccine in cattle. *Clinical and Experimental Vaccine Research*, 2016. 5(2): p. 138-147.

7. Xiao, C., Z.I. Rajput, and S. Hu, Improvement of a commercial foot-and-mouth disease vaccine by supplement of Quil A. Vaccine, 2007. 25(25): p. 4795-4800.

8. Kensil, C.R., Saponins as vaccine adjuvants, in Crit. Rev. Ther. Drug Carr. Syst.1996. p. 1-55.

9. Silveira, F., et al., Quillaja brasiliensis saponins are less toxic than Quil A and have similar properties when used as an adjuvant for a viral antigen preparation. Vaccine, 2011. 29(49): p. 9177-9182.

10. Fernández-Tejada, A., D.S. Tan, and D.Y. Gin, Development of Improved Vaccine Adjuvants Based on the Saponin Natural Product QS-21 through Chemical Synthesis. Accounts of chemical research, 2016. 49(9): p. 1741.

11. Kensil, C.R., et al., Separation and characterization of saponins with adjuvant activity from Quillaja saponaria Molina cortex. Journal of Immunology, 1991. 146(2): p. 431-437.

12. Marciani, D.J., Vaccine adjuvants: role and mechanisms of action in vaccine immunogenicity. Drug Discovery Today, 2003. 8(20): p. 934-943.

13. Soltysik, S., et al., Structure/function studies of QS-21 adjuvant: assessment of triterpene aldehyde and glucuronic acid roles in adjuvant function. Vaccine, 1995. 13(15): p. 1403-1410.

14. Yang, Y., et al., Formation and stability of emulsions using a natural small molecule surfactant: Quillaja saponin (Q-Naturale (R)). Food Hydrocolloids, 2013. 30(2): p. 589-596.

15. Zhang, J., L. Bing, and G.A. Reineccius, Formation, optical property and stability of orange oil nanoemulsions stabilized by Quallija saponins. LWT - Food Science and Technology, 2015. 64(2): p. 1063-1070.

16. Galliher-Beckley, A., et al., Characterization of a novel oil-in-water emulsion adjuvant for swine influenza virus and Mycoplasma hyopneumoniae vaccines. Vaccine, 2015. 33(25): p. 2903-8.

17. Madera, R., et al., Pigs immunized with a novel E2 subunit vaccine are protected from subgenotype heterologous classical swine fever virus challenge. BMC Vet Res, 2016. 12(1): p. 197.

18. Moennig, V., Introduction to classical swine fever: virus, disease and control policy. Veterinary Microbiology, 2000. 73(2): p. 93-102.

19. Lin, G.-J., et al., Yeast expressed classical swine fever E2 subunit vaccine candidate provides complete protection against lethal challenge infection and prevents horizontal virus transmission. Vaccine, 2012. 30(13): p. 2336-2341.

20. Madera, R., et al., Toward the development of a one-dose classical swine fever subunit vaccine: antigen titration, immunity onset, and duration of immunity. J Vet Sci. 2018 31;19(3):393-405

21. Knight-Jones, T.J.D., et al., Veterinary and human vaccine evaluation methods. Proceedings of the Royal Society B: Biological Sciences, 2014. 281(1784): p. 20132839.

22. Jansen, T., et al., Structure- and oil type-based efficacy of emulsion adjuvants. Vaccine, 2006. 24(26): p. 5400-5405.

23. Kanchan, V.; Panda, A. K. Interactions of antigen-loaded polylactide particles with macrophages and their correlation with the immune response. Biomaterials 2007, 28, 5344-5357

24. Marciani, D.J., et al., Altered immunomodulating and toxicological properties of degraded Quillaja saponaria Molina saponins. International Immunopharmacology, 2001, 1(4): 813-818.

Chapter 5 - Multiple Emulsions via an One-Step Low-Energy Method I: Formulation and Characteristics

Abstract

Water-in-oil-in-water (multiple) emulsions are attractive delivery vehicles in animal vaccines. However, formulating emulsions with multiple structure, nanoscale droplet size, and prolonged physical stability is a very challenging task. This study presents novel oil mixtures that produce multiple nanoscale emulsions after one-step gentle mixing of an aqueous phase with the application of phase inversion composition. Different types of mineral oils and mixture of mineral and plant-based oils were investigated in preparation of emulsions with uniform nanosized droplets. In addition, the impact of five emulsification parameters on droplet diameters and polydispersity of emulsions was studied. The emulsions were characterized with dynamic light scattering (DLS) and transmission electron microscopy (TEM) to examine average droplet size, polydispersity, zeta potential, and emulsion structure. The oil mixtures containing more viscous oil formed emulsions with narrower size distributions. Moreover, multiple droplets less than 200 nm in size were detected in TEM images of the emulsions. Physical characteristics of samples were preserved after prolonged storage even at elevated temperatures. Two oil mixtures were proposed for further immunological studies as vaccine adjuvants for animals.

Introduction

Emulsion-based vaccines are a popular choice in veterinary medicine offering inexpensive and effective ways to induce immune responses to antigens and provide protection against pathogens *(1)*. Currently, several animal vaccines based on water-in-oil and oil-in-water emulsion adjuvants can be found on the market *(2)*. However, vaccines formulated with multiple (water-in-oil-in-water) emulsions are not so common. It has been suggested that water-in-oil-in-water

(w/o/w) emulsions contain the antigen in both the external and internal water phases providing immediate and prolonged stimulation of the immune system by both fast and slow release of antigen upon breakdown *(3)*. In addition, Huang and co-workers have demonstrated that w/o/w formulations are more fluid and, therefore, easier to inject and less toxic in contrast to w/o emulsions *(4)*. However, the formulation of stable multiple emulsions is a more complex process than production of oil-in-water or water-in-oil emulsions. Furthermore, multiple emulsions tend to have large, nonuniform droplets and are prone to fast break down and creaming *(5)*.

Generally, creation of w/o/w emulsions requires a two-step approach *(6)*. First, the primary w/o emulsion is formed with the help of a lipophilic surfactant (hydrophile–lipophile balance (HLB) <6) and high-speed homogenization. Then, the w/o emulsion is re-dispersed in water containing a hydrophilic surfactant with HLB>8 under low-speed homogenization to obtain a w/o/w emulsion *(6)*. One-step production of multiple emulsions has been also explored and involves either phase inversion procedures *(7-9)* or application of microfluidic devices *(10, 11)*. While very uniform microscale droplets are obtained with microfluidics, low throughput hinders its commercial application. Phase-inversion procedures are a low-energy method to make emulsions which utilize the changes in temperature or volume fraction of one of the phases *(12)*. Thus, phase inversion composition (PIC) involves the gradual addition of the water phase to oil inverting a w/o emulsion into an o/w emulsion with intermediate formation of w/o/w droplets. *(13)*. However, the selection of the suitable surfactants, the physical stability, and big droplet size are among the key challenges in the production of multiple emulsions by this method *(8)*. In addition, low-energy emulsification generally requires the high concentration of surfactants to produce stable emulsions, which can constrain their application in vaccinations.

In the present study, the PIC method was used to formulate multiple emulsions from homogeneous mixtures of oils and surfactants. Three types of light mineral oil were studied to

determine the most effective in the formation of emulsions with narrow nanoscale size distribution. In addition, a mixture that contained a combination of mineral and medium-chain triglyceride (MCT) oils and a reduced concentration of emulsifiers was also studied. Previous investigation has demonstrated that two polymeric emulsifiers (Compound A and Compound B; for more information, please contact jshi@ksu.edu), can be incorporated into the oil-based vaccine adjuvant without causing toxic side effects in pig immunization (Chapter 4). Nevertheless, the designed adjuvant did not induce strong antibody responses in pigs even after a two-dose co-administration with antigen suggesting that the composition needs to be changed (Chapter 4). In this study, the content of the mineral oil in the mixtures was increased to promote higher inflammation at the injection sites and, therefore, stronger antibody responses. Furthermore, polyoxyethylenesorbitan trioleate (Tween 85) was used instead of Atlas G-5002L as it demonstrated higher solubility in mineral oils in preliminary studies. Tween 85, surfactant suitable for production of o/w emulsions, has also been commonly used in pharmaceutical formulations as it shows lower cytotoxicity in comparison with other nonionic emulsifiers *(14, 15)*. Compound A is a nonionic polymeric surfactant with a molecular weight more than 50 kDa and an HLB of 6 that is composed of hydrophilic polyethylene glycol and hydrophobic polymerized fatty acids blocks. Due to its low HLB value, it is an appropriate choice for formation of w/o emulsions. The highly branched structure of Compound A provides improved steric stabilization between the droplets and is beneficial for the colloidal stability of emulsions with multiple structure *(16)*.

This information was redacted intentionally. Please contact jshi@vet.k-state.edu for additional details.

Emulsions were made by gradual dilution of the oil-surfactants mixtures with the aqueous phase and gentle agitation employing magnetic stirrer. The mean droplet size, zeta potential and polydispersity measurements were performed with dynamic light scattering (DLS). In addition, transmission electron microscopy (TEM) was used to confirm the size and multiple structure of the droplets. The stability of the emulsion samples at different temperatures and the impact of

different emulsification parameters on the droplet size were investigated and the results presented herein.

Materials and Methods

Materials

Three mineral oils (Peneteck, Drakeol® 5, Drakeol® 6) were obtained from Calumet Penreco LLC (Karns City, USA). Table 5.1 contains the physical characteristics of the oils provided by the manufacturer. Medium Chain Triglyceride (MCT) oil comprised of 57.8% caprylic acid (C8:0) and 42.1% capric acid (C10:0) was purchased from Jedwards International Inc. (Braintree, USA). A nonionic surfactant, Tween 85, was purchased from MP Biomedicals (Solon, USA). Polymeric surfactant, Compound A was purchased from a commercial supplier. This information was redacted intentionally. Please contact jshi@vet.k-state.edu for additional details. Phosphate buffered saline (PBS, 100 ml tablets) was purchased from Fisher Scientific (Fair Lawn, USA). PBS tablets were diluted in nano-pure deionized water (1 tablet per 100 ml of water) to obtain a 1X PBS solution. All other reagents were used as received.

Table 5.1 Physical characteristics of mineral oils used in this study.

Oil	Viscosity at 40°C, cSt	Specific gravity at 25°C
Peneteck	4.60	0.8290
Drakeol® 5	8.25	0.8395
Drakeol® 6	9.68	0.8351

Formulation of mixtures and emulsions

Four formulations were prepared by mixing different oils with surfactants using a magnetic bar for 5 hours at 500 rpm at room temperature (RT). The final concentrations of the mixture components were determined in the preliminary studies and presented in Table 5.2. Formulations were stored in the dark at RT until further use.

Emulsions were formed by dilution of the oil-surfactant mixtures with an aqueous phase (PBS). The PBS was added slowly to the mixtures in a 2:1 volume ratio while stirring with a magnetic bar at 500 rpm at room temperature. The emulsions were stirred for an additional 60 min.

Table 5.2 Composition of oil-surfactant mixtures.

Mixture	Component	%, w/w
#1	Peneteck oil Tween 85 Compound A	This information was redacted intentionally. Please contact jshi@vet.k-state.edu for additional details.
#2	Drakeol 5 oil Tween 85 Compound A	
#3	Drakeol 6 oil Tween 85 Compound A	
#4	Drakeol 5 oil MCT oil Tween 85 Compound A	

Physical characteristics of prepared emulsions

The droplet size, polydispersity, and zeta potential of the emulsions were determined with dynamic light scattering. A Zetasizer Nano ZS 90 (Malvern Instruments, Westborough, MA) with a 633 nm He-Ne laser at a scattering angle of 173° was used to make the measurements. Each sample was diluted by a factor of 100 with PBS for droplet size analysis and with a 0.001M NaCl solution for zeta potential measurements to prevent multiple scattering effects. Measurements were taken in triplicate and results were reported as the mean of three measurements.

The pH of the emulsion samples was measured using a VWR SympHony digital pH meter SB21 (VWR International, Radnor, PN, USA). Before the measurements, calibration of the instrument was performed according to instructions from the manufacturer.

Emulsions were imaged with transmission electron microscopy (TEM) using the FEI CM100 housed at the Biology Department at Kansas State University. The detailed imaging procedure of the samples can be found in Appendix A. Briefly, drop of the emulsion sample was placed onto a 200 mesh formvar-carbon grid (Electron Microscopy Sciences, Hatfield, USA) followed by negative staining with uranyl acetate and brief air-drying. Imaging was done at an accelerating voltage of 100 kV.

After storage at 4°C, room temperature, and 37°C, the emulsion samples were checked for the presence of creaming, sedimentation, and phase separation. In addition, physical characteristics of the emulsions were measured again after 1 and 3 months of storage.

Effect of emulsification parameters on the emulsion droplets

The impact of five emulsification parameters (time of mixing, initial temperature of components, speed of mixing, nature of aqueous phase, and amount of aqueous phase) on the droplet size and polydispersity of emulsions prepared from the #2 mixture were investigated (Table 5.3). The DLS was used to collect data for all experiments according to the procedure described in the previous section.

Time of mixing

The PBS (6 ml) was added to the oil-surfactant mixture (3 ml) followed by agitation with a magnetic stirrer (MultiMagstir Genie) for 5, 30, 60 or 120 minutes at 500 rpm at room temperature.

Table 5.3 Emulsification parameters used to study the effect on emulsion droplet size.

Emulsification parameters									
Time of mixing (min)	5	30	60	120					
Initial temperature of components (°C)	4	RT	40	50	70				
Speed of mixing (rpm)									
high shear lab mixer	700	1000	1200	2500	4000	5000	6000	8000	10000
magnetic stirrer	300	500	700	1000	1200				
Nature of aqueous phase	PBS	DI water							
Ratio of aqueous phase to the oil-surfactant mixture (vol./vol.)	1:1	2:1	3:1						

Values in bold indicate parameters that were held constant, while the other were varied
RT, room temperature
PSB, phosphate-buffered saline
DI water, deionized water

Initial temperature of components

The #2 mixture and PBS were cooled or heated to desired temperatures separately before emulsification. After that, emulsions were made by slow addition of PBS to the oil-surfactant mixture and were stirred at room temperature with a MultiMagstir Genie at 500 rpm at room temperature for 30 min. The investigated initial temperatures of components were 4°C, 20°C, 40°C, 50°C, and 70°C. Three replicates of each sample were prepared containing 6 ml of PBS and 3 ml of the #2 mixture.

Speed of mixing

Two types of mixers, a high shear lab mixer (L5M-A, Silverson) and a magnetic stirrer (MultiMagstir Genie) were used in this experiment. For the Silverson mixer, 10 ml of mixture #2 was poured into a beaker, the mixer was started, and PBS (20 ml) was added slowly within 10 seconds. The samples were agitated at 700, 1000, 1200, 2500, 4000, 5000, 6000, 8000, and 10000 rpm for 15 minutes. For the magnetic stirrer, 6 ml of PBS were slowly added to 3 ml of the oil-surfactant mixture followed by emulsification at 300, 500, 700, 1000, or 1200 rpm for 15 minutes

at room temperature. All samples were prepared in triplicate to confirm the reproducibility of the results.

Nature of aqueous phase

Two emulsion samples were prepared using PBS or deionized water as aqueous phases. The aqueous phase was poured into mixture #2 in a 2:1 volume ratio followed by emulsification with the MultiMagstir Genie for 30 min at 500 rpm and RT.

Amount of aqueous phase

The PBS was added to the #2 mixture in 1:1, 2:1, or 3:1 volume ratios followed by emulsification with the MultiMagstir Genie for 30 min at 500 rpm and RT.

Results

The effect of oil type on the droplet size distribution of emulsions obtained from the oil-surfactant mixtures

Figure 5.1 depicts the size distributions of emulsions prepared from oil-surfactant mixtures with different mineral oils. The oil with lowest viscosity (Peneteck, Table 5.1) formed emulsion with droplet sizes ranging from 37.8 nm to 255.0 nm. The mode in the size distribution was at 100.4 nm. Two other emulsion samples prepared with pure Drakeol 5 or Drakeol 6 oils had droplet diameters between 37.8 and 190 nm and 37.8 and 164.2 nm, respectively, with the modes in the droplet size distribution at ~80 nm (Fig. 5.1). An emulsion made from a mixture with a combination of Drakeol 5 and MCT oil had droplets ranging from 58.8 to 295.0 nm in diameter with the maximum in droplet size distribution at 122 nm. The #2 and #4 oil-surfactant mixtures were chosen for the further studies.

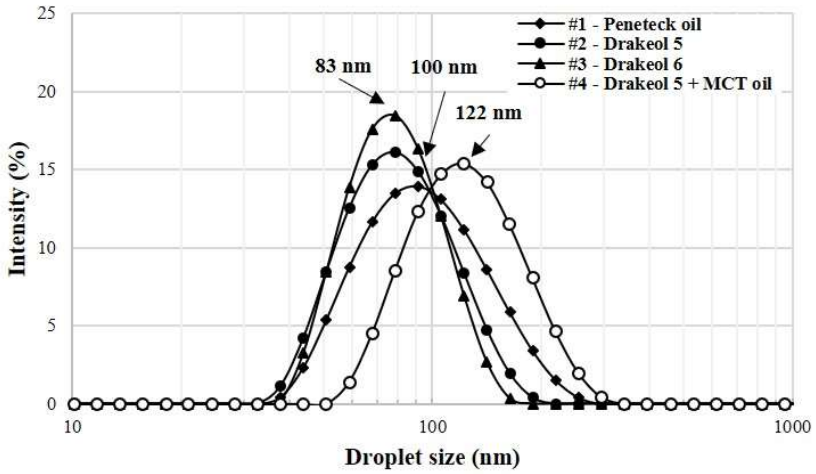

Figure 5.1 DLS size distribution of three emulsions prepared from mixtures with different mineral oils and combination of mineral and MCT oils.

Visual appearance of the mixtures and emulsions, TEM, and stability assessment

Figures 5.2a and 5.2b demonstrate the clear yellow appearance of two experimental oil-surfactant mixtures (#2 and #4) and the white emulsions made from them, respectively. Droplets with multiple structure (water-in-oil-in-water) were observed on TEM images of the #2 emulsion sample (Fig. 5.2c). White arrows indicate the presence of several smaller water droplets inside the bigger oil droplets. In addition, the size of the observed water-in-oil-in-water droplets was less than 200 nm (Fig. 5.2c).

The emulsion prepared from the #2 mixture preserved the mean droplet size, polydispersity, and zeta potential after three-month storage at 4°C, 20°C and 37°C (Table 5.4). On the contrary, the average droplet size of an emulsion made from the #4 mixture increased from 122.47 to 134.30 nm after storage at 4°C, and decreased to 94.61 nm after storage at 37°C (Table 5.4). The polydispersity index of the #4 emulsion sample dropped from 0.200 to 0.024 after 3 months at 37°C (Table 5.4). One-month storage at different temperatures did not affect the pH in either emulsions. No creaming, phase separation, or oiling off were observed in either sample after three months for all temperatures.

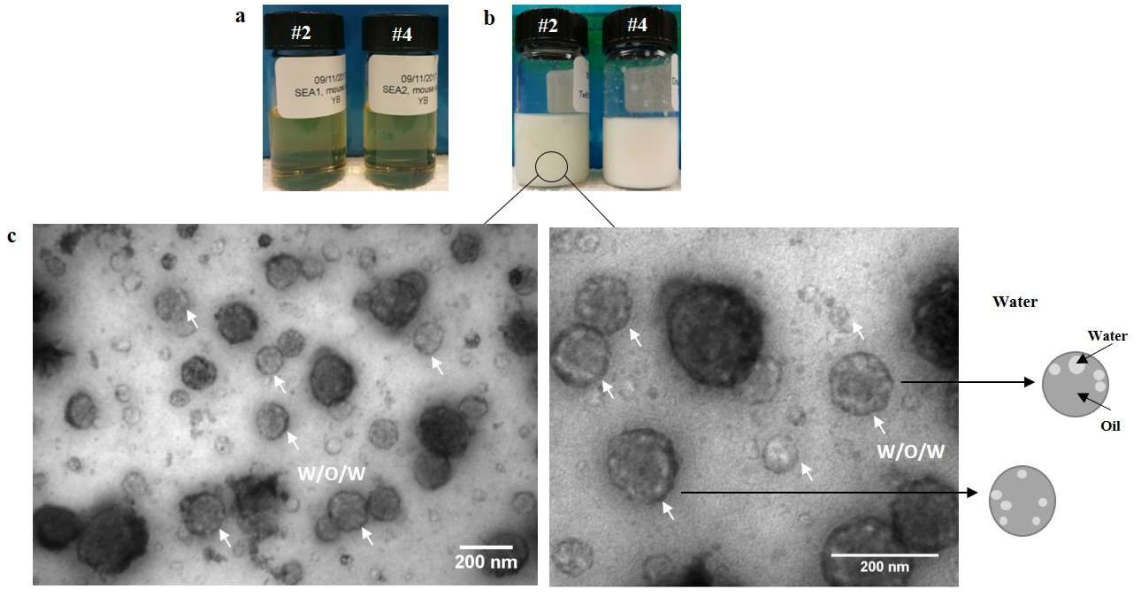

Figure 5.2 Visual appearance of #2 and #4 mixtures (a) and emulsions obtained after emulsification of the mixtures with phosphate-buffered saline as a water phase (b), TEM images of emulsion with multiple (W/O/W) structure prepared from #2 mixture (c).

White arrows indicated droplets with multiple structure. Graphical representation of the emulsion droplets depicts big oil droplets containing small internal water droplets while being dispersed in the external water phase.

Table 5.4 Physical characteristics of emulsions prepared from #2 and #4 mixtures.

Emulsion sample			Mean size, nm, ± S.D.	PDI ± S.D.	Zeta potential, mV, ± S.D.	**pH**
#2	Fresh		74.61 ± 0.81	0.049 ± 0.004	-23.67 ± 1.44	6.67
	1 month	4ºC	83.80 ± 0.81	0.177 ± 0.025	-24.00 ± 1.28	6.64
		RT	74.96 ± 0.59	0.047 ± 0.015	-23.10 ± 0.26	6.68
		37ºC	79.42 ± 0.29	0.044 ± 0.025	-25.40 ± 1.47	6.64
	3 months	4ºC	74.17 ± 0.78	0.055 ± 0.004	-20.77 ± 0.78	
		RT	77.88 ± 0.64	0.039 ± 0.007	-22.00 ± 0.10	
		37ºC	75.63 ± 0.54	0.052 ± 0.008	-20.87 ± 0.42	
#4	Fresh		122.47 ± 0.83	0.200 ± 0.008	-30.17 ± 0.55	6.78
	1 month	4ºC	120.30 ± 1.39	0.175 ± 0.015	-34.37 ± 0.81	6.74
		RT	121.07 ± 1.75	0.177 ± 0.011	-30.03 ± 0.72	6.72
		37ºC	93.36 ± 1.37	0.022 ± 0.024	-22.83 ± 1.10	6.74
	3 months	4ºC	134.30 ± 1.48	0.253 ± 0.011	-28.13 ± 0.65	
		RT	118.20 ± 0.36	0.168 ± 0.025	-25.80 ± 0.26	
		37ºC	94.61 ± 0.59	0.024 ± 0.006	-20.20 ± 0.10	

RT, room temperature

Impact of emulsification parameters on emulsion droplet size

The mean droplet size and polydispersity index of the emulsion made from the #2 mixture decreased gradually with increasing time of mixing (Fig. 5.3a). Thus, the smallest mean droplet size (79.2 nm) and PDI (0.097) were observed after emulsification for 120 min. The largest average droplet size and PDI (100.2 nm with 0.217, respectively) were detected after 5 min of stirring (Fig. 5.3a).

Figure 5.3b demonstrates the effect of the initial temperature of the mixture and PBS on the emulsion droplet size and polydispersity. If components were at 4°C before emulsification, the mean diameter of the droplets was 152 nm with a PDI equal to 0.3. On the contrary, the smallest average droplet size (77.5 nm) and polydispersity (0.08) were achieved when the temperature of components was 40°C before emulsification.

The impact of the speed of mixing on mean droplet size of emulsions is presented in Figure 5.3c. When a magnetic stirrer was used, the emulsion samples had mean droplet sizes less than 120 nm independent of emulsification mixing speed (300-1,200 rpm). However, when the high shear lab mixer was employed, the emulsion with the smallest mean droplet size (79 nm) was obtained at 10,000 rpm, while the emulsion mixed at 1,200 rpm had a mean droplet diameter of 135 nm (Fig. 5.3c).

Emulsions prepared with PBS and deionized water as aqueous phases had very similar droplet size distributions (Fig. 5.3d). On the contrary, when the amount of PBS was increased in the emulsion, the size distribution became wider (Fig. 5.3e). Thus, emulsions had droplets ranging from 37.8 to 190 nm when PBS and an oil-surfactant mixture were emulsified in 1:1 ratio, from 28.2 nm to 531 nm after emulsification in 2:1 ratio, and, finally, from 37.8 nm to 995 nm after emulsification in 3:1 ratio (Fig. 5.3e).

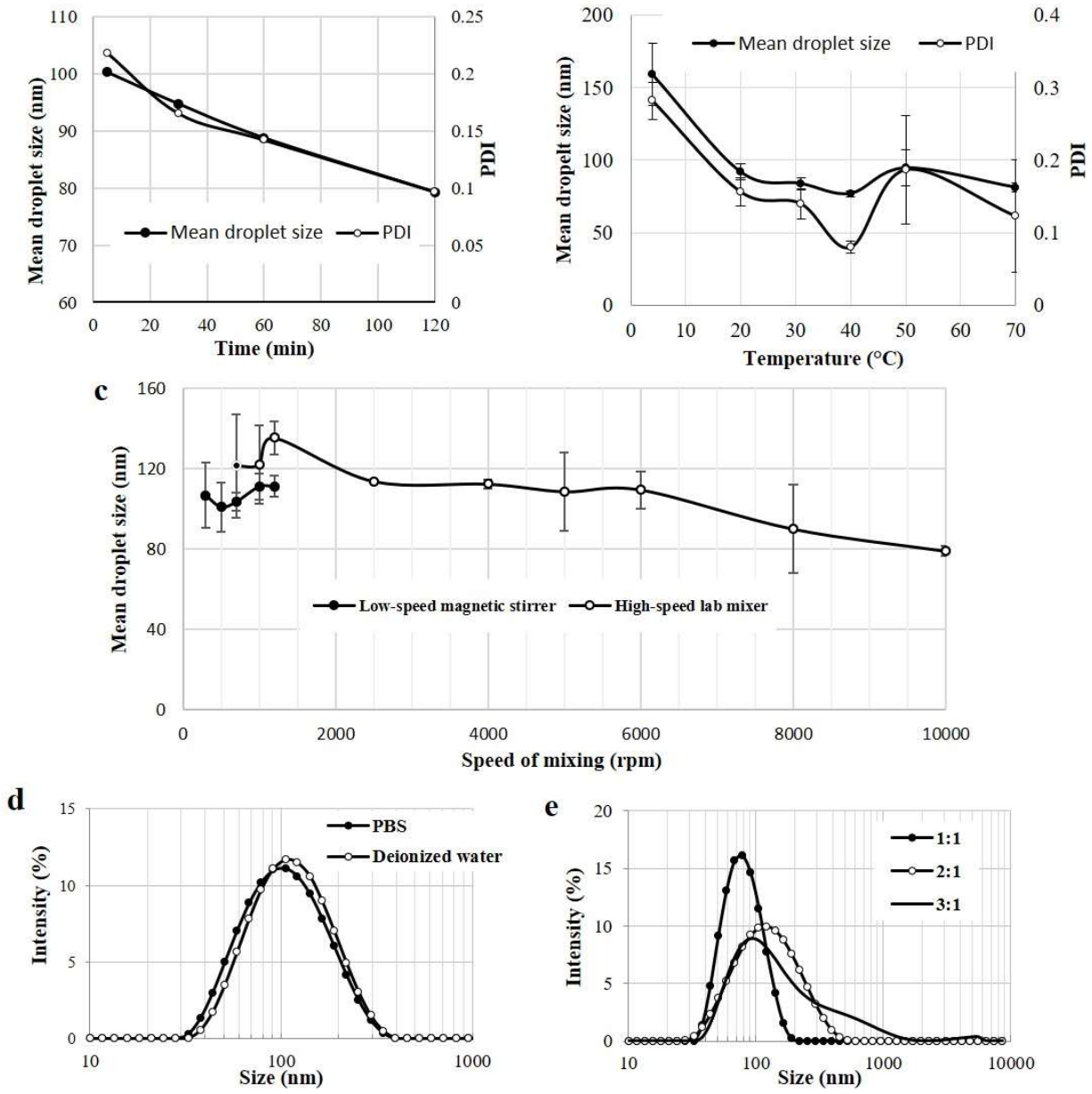

Figure 5.3 The effect of time of mixing (a), temperature of components (b) on mean droplet size (filled markers) and PDI (blank markers) of emulsions; the effect of speed of mixing on the mean droplet size of emulsions (c); the effect of nature of aqueous phase the effect of nature of aqueous phase (d) and amount of aqueous phase (e) on the droplet size distribution of emulsions.

Error bars represent the standard deviation between three DLS measurements of one sample.

Discussion

Vaccines based on emulsions are commonly used in animal immunizations for several reasons including low cost and efficacy in inducing protective immune responses *(2)*. Today only a few veterinary vaccine adjuvants that produce emulsion vaccines with multiple structure exist on the market. All of them are under the Montanide™ (Seppic, France) brand *(17-19)*. Due to the structure, w/o/w emulsions possess advantages when compared with conventional w/o or o/w emulsions. Multiple emulsions provide fast and slow releases of the antigenic molecules from the external and internal water phases, respectively. Therefore, there is a demand for cost-effective easy-to-prepare multiple emulsion-based vaccines for animal use. This study demonstrates oil-based mixtures for use as vaccine adjuvants that produce ready-to-go multiple emulsions after gentle mixing with PBS as a water phase.

The oil-surfactant mixtures containing more viscous oils (Drakeol 5 and Drakeol 6) formed emulsions with more uniform droplets in contrast with the mixture with Peneteck oil (Fig. 5.1). In addition, the reduced concentration of emulsifiers in the #4 mixture resulted in a wider size distribution of emulsion droplets in comparison with an emulsion formulated with pure Drakeol 5 oil (Fig. 5.1). As there was no significant difference between size distributions of emulsions prepared with Drakeol 5 and Drakeol 6 and the narrow size distribution is preferable to ensure better emulsion stability, the #2 mixture with pure Drakeol 5 will be selected for additional studies. In addition, the #4 mixture with a combination of Drakeol 5 and MCT oils will be studied further as an appropriate vaccine adjuvant candidate because of its lower emulsifier concentrations.

The mean droplet sizes of emulsions produced from experimental #2 and #4 mixtures were 74.61 nm and 122.47 nm, respectively (Table 5.4) making them promising candidates as delivery agents in antiviral vaccines. It has been shown that immune cells uptake and process more

efficiently particles in the nanoscale range, leading to cell-mediated immune responses *(20)* responsible for creating protection against viral diseases. In addition, emulsions with droplet size less than 200 nm can be sterilized by membrane filtration avoiding autoclaving, which is damaging for heat-sensitive formulations.

In general, emulsions which have smaller droplets and lower polydispersities are more stable. After a three-month storage at 37°C, the emulsion prepared from the #2 mixture preserved the mean droplet size, PDI, pH and zeta potential, indicating a good colloidal stability of this formulation (Table 5.3). This suggests that vaccines prepared with the #2 mixture as an adjuvant can be transported and stored at elevated temperatures without affecting its physical characteristics. However, the mean droplet size and PDI of the emulsion sample prepared from the #4 mixture significantly changed after storage at 37°C (Table 5.3). The reduction in the mean droplet size and PDI at elevated temperatures indicated instability caused by Ostwald ripening *(21)*. Presumably, the reduced concentration of surfactants in the #4 mixture in comparison with the #2 mixture (Table 5.2) led to the decreased physical stability of emulsion #4 over time.

TEM revealed a multiple structure of emulsion made from the #2 mixture (Fig. 5.2c, Appendix A). Only a few studies have reported nanoscale W/O/W emulsions. In these cases, the multiple emulsions were prepared either with the help of high-energy ultrasonic homogenization *(22)* or glass membranes *(23)*. Here, low-energy CPI was successfully employed to create stable emulsions with nanoscale w/o/w droplets.

The effect of different emulsification parameters on the droplet size and polydispersity of emulsions made from the #2 mixture was also investigated in this study (Table 5.4). Emulsions with minimum droplet size and PDI can be obtained after 120 min of mixing (Fig. 5.3a). Prolonged mixing appears to allow for better allocation of the surface-active molecules stabilizing oil-water interfaces *(24)*, leading to reduced mean droplet size and polydispersity with increasing time of

mixing (Fig. 5.3a). However, prolonged emulsification can be circumvented if the initial temperature of components is at 40°C (Fig. 5.3a, b). Both the mean droplet diameter and PDI of emulsions decreased with the initial temperature of the oil-surfactant mixture and PBS increased from 4°C to 40°C (Fig. 5.3b). Previously, moderately elevated temperatures had shown to promote faster dispersion of the oil droplets and improved solubility of the surfactant molecules in both phases providing smaller and more uniform droplets *(25)*. However, the subsequent increase of the initial components' temperature to 70°C did not produce smaller droplets and lower PDI in the emulsions (Fig. 5.3b). This can be explained by the decreased bulk viscosity and accelerated coalescence between the emulsion droplets at temperatures higher than 40°C.

Both the magnetic stirrer and high shear lab mixer produced emulsions with droplets having mean size less than 130 nm (Fig. 5.3c). Moreover, even very gentle mixing with a magnetic bar (300 rpm) was sufficient to obtain the average droplet diameter around 100 nm (Fig. 5.2c). As expected, for emulsification with a high shear lab mixer, the larger energy input led to smaller mean droplet sizes (Fig. 5.3c). These observations indicate that expensive high-energy mixing can be avoided in the production of the vaccines from oil-surfactant mixtures presented here.

Antigenic suspending fluid in the vaccines may contain saline. Therefore, the absence of the impact of electrolytes from PBS on droplet size distribution of the emulsion made from the #2 mixture in this study (Fig. 5.3d) confirms that the presence of saline will not affect the droplet size in the emulsion vaccine. In addition, emulsions made with saline solution and the #2 mixture had prolonged shelf stability (Table 5.3). Previously, it has been shown that the droplet size of emulsions stabilized with nonionic surfactants can be affected by electrolytes *(26)*. In this study, the highly branched structure of Compound A surfactant appears to provide additional steric stabilization between the emulsion droplets preserving their original size. This speculation agrees

This information was redacted intentionally. Please contact jshi@vet.k-state.edu for additional details.

with earlier findings that polymeric emulsifiers offer better stability of emulsions preventing instability associated with early coalescence of the droplets *(27)*.

As expected, the higher amount of aqueous phase in these emulsions led to wider droplet size distributions in comparison with the emulsion prepared with equal volumes of oil-surfactant mixture and water phase (Fig. 5.3e). Evidently, the reduced amount of surfactant molecules available in the larger aqueous volumes has resulted in formation of larger droplets. Nevertheless, even at a higher water content (2:1 vol. ratio), an experimental oil-surfactant mixture formed an emulsion with the majority of droplets around 100 nm in size.

In conclusion, the #2 mixture produced stable, nanoscale multiple emulsions after dilution with the aqueous phase. Four out of five emulsification parameters had a pronounced effect on the average droplet size and size distribution of the emulsions. The optimal production parameters were 40°C for initial temperature of the oil-surfactant mixture and aqueous phase, 30 min emulsification at 500 rpm employing low-energy magnetic stirrers, and a 1:1 volume ratio between oil and aqueous phases were the optimal production parameters. These parameters have been recommended for use in the preparation of vaccines in further immunological and safety studies.

Conclusions

Oil-surfactant mixtures producing multiple nanoscale emulsions after low-energy agitation with aqueous phase were formulated in this study. The mixtures with more viscous oils produced emulsions with narrower droplet size distributions. Two formulations were chosen for stability studies with emulsions made from a mixture with pure mineral oil was stable at least three months at different temperatures, preserving the initial physical characteristics. The time of emulsification, initial temperature of components, speed of mixing and amount of the aqueous phase had an impact on mean droplet size and polydispersity of emulsions, while the nature of aqueous phase did not

affect the size distribution of emulsion droplets. Proposed next steps include immunological and safety studies of the mixtures as vaccine adjuvants in animal immunizations.

References

1. Cox, J. C.; Coulter, A. R. Adjuvants—a classification and review of their modes of action. *Vaccine* **1997***, 15*, 248-256.

2. Burakova, Y.; Madera, R.; Mcvey, S.; Schlup, J. R.; Shi, J. Adjuvants for Animal Vaccines. *Viral Immunol.* **2018***, 31*, 11.

3. Bozkir, A.; Hayta, G. Preparation and evaluation of multiple emulsions water-in-oil-in-water (w/o/w) as delivery system for influenza virus antigens. *J. Drug Target.* **2004***, 12*, 157-164.

4. Huang, M. H.; Huang, C. Y.; Lien, S. P.; Siao, S. Y.; Chou, A. H.; Chen, H. W.; Liu, S. J.; Leng, C. H.; Chong, P. Development of multi-phase emulsions based on bioresorbable polymers and oily adjuvant. *Pharm. Res.* **2009***, 26*, 1856-1862.

5. Azhar, Y. K.; Sushama Talegaonkar; Zeenat Iqbal; Farhan Jalees Ahmed and Roop,Krishan Khar Multiple Emulsions: An Overview. *Current Drug Delivery* **2006***, 3*, 429-443.

6. Mataumoto, S.; Kang, W. W. Formation and application of multiple emulsions. *J. Dispersion Sci. Technol.* **1989***, 10*, 455-482.

7. Márquez, A. L.; Palazolo, G. G.; Wagner, J. R. Water in oil (w/o) and double (w/o/w) emulsions prepared with spans: microstructure, stability, and rheology. *J. R. Colloid Polym Sci* **2007***, 285 (10)*, 1119-1128.

8. Morais, J. M.; Santos, O. D. H.; Nunes, J.; Zanatta, C. F.; Rocha-Filho, P. A. W/O/W Multiple Emulsions Obtained by One-Step Emulsification Method and Evaluation of the Involved Variables. *J. Dispersion Sci. Technol.* **2008***, 29*, 63-69.

9. Hong, L.; Sun, G.; Cai, J.; Ngai, T. One-Step Formation of W/O/W Multiple Emulsions Stabilized by Single Amphiphilic Block Copolymers. *Langmuir* **2012***, 28*, 2332-2336.

10. Utada, A. S.; Lorenceau, E.; Link, D. R.; Kaplan, P. D.; Stone, H. A.; Weitz, D. A. Monodisperse Double Emulsions Generated from a Microcapillary Device. *Science* **2005***, 308*, 537.

11. Hughes, E.; Maan, A. A.; Acquistapace, S.; Burbidge, A.; Johns, M. L.; Gunes, D. Z.; Clausen, P.; Syrbe, A.; Hugo, J.; Schroen, K.; Miralles, V.; Atkins, T.; Gray, R.; Homewood, P.; Zick, K. Microfluidic preparation and self diffusion PFG-NMR analysis of monodisperse water-in-oil-in-water double emulsions. *J Colloid Interface Sci* **2013***, 389*, 147-156.

12. Perazzo, A.; Preziosi, V.; Guido, S. Phase inversion emulsification: Current understanding and applications. *Advances in Colloid and Interface Science* **2015**, *222*, 581-599.

13. Perazzo, A.; Preziosi, V. In *Chapter 3 - Catastrophic Phase Inversion Techniques for Nanoemulsification;* Jafari, S. M., McClements, D. J., Eds.; Nanoemulsions; Academic Press: 2018; pp 53-76.

14. Yang, Y.; Wei, A.; Shen, S. The immunogenicity-enhancing effect of emulsion vaccine adjuvants is independent of the dispersion type and antigen release rate—a revisit of the role of the hydrophile–lipophile balance (HLB) value. *Vaccine* **2005**, *23*, 2665-2675.

15. Sigward, E.; Mignet, N.; Rat, P.; Dutot, M.; Muhamed, S.; Guigner, J.; Scherman, D.; Brossard, D.; Crauste-Manciet, S. Formulation and cytotoxicity evaluation of new self-emulsifying multiple W/O/W nanoemulsions. *Int J Nanomedicine* **2013**, *8*, 611-625.

16. Croda, I. Polymeric Surfactants. *https://www.crodacropcare.com/en-gb/discovery-zone/technologies/polymeric-surfactants* (accessed 7/30, 2018).

17. SEPPIC Montanide™ ISA - W/O/W. Ready-to-use adjuvants for water-in-oil-in-water emulsions. *https://www.seppic.com/montanide-isa-w-o-w* (accessed 05/16, 2018).

18. Barnett, P. V.; Pullen, L.; Williams, L.; Doel, T. R. International bank for foot-and-mouth disease vaccine: assessment of Montanide ISA 25 and ISA 206, two commercially available oil adjuvants. *Vaccine* **1996**, *14*, 1187-1198.

19. Hunter, P. The performance of southern African territories serotypes of foot and mouth disease antigen in oil-adjuvanted vaccines. *Rev. - Off. Int. Epizoot.* **1996**, *15*, 913.

20. Kanchan, V.; Panda, A. K. Interactions of antigen-loaded polylactide particles with macrophages and their correlation with the immune response. *Biomaterials* **2007**, *28*, 5344-5357.

21. Kulkarni, V. S.; Shaw, C. In *Preparation and Stability Testing;* Kulkarni, V. S., Shaw, C., Eds.; Essential Chemistry for Formulators of Semisolid and Liquid Dosages; Academic Press: Boston, 2016; Vol. 7, pp 99-135.

22. Hanson, J. A.; Chang, C. B.; Graves, S. M.; Li, Z.; Mason, T. G.; Deming, T. J. Nanoscale double emulsions stabilized by single-component block copolypeptides. *Nature* **2008**, *455*, 85.

23. Koga, K.; Takarada, N.; Takada, K. Nano-sized water-in-oil-in-water emulsion enhances intestinal absorption of calcein, a high solubility and low permeability compound. *European Journal of Pharmaceutics and Biopharmaceutics* **2010**, *74*, 223-232.

24. Omole, O.; Falode, O. A. Effects of Mixing Conditions, Oil Type and Aqueous Phase Composition on Some Crude Oil Emulsions. *Journal of Applied Sciences* **2005**, *5(5)*, 873-877.

25. Yuan, Y.; Zou, X.; Xiong, P. Effects of Temperature on the Emulsification in Surfactant-Water-Oil Systems. *Int. J. Mod. Phys. B* **2003***, 17(14)*, 2773-2780.

26. Mei, Z.; Xu, J.; Sun, D. O/W nano-emulsions with tunable PIT induced by inorganic salts. *Colloids and Surfaces A: Physicochemical and Engineering Aspects* **2011***, 375*, 102-108.

27. Benichou, A.; Aserin, A.; Garti, N. Double emulsions stabilized with hybrids of natural polymers for entrapment and slow release of active matters. *Adv. Colloid Interface Sci.* **2004***, 108*, 29-41.

Chapter 6 - Multiple Emulsions via an One-Step Low-Energy Method II: Immunological Studies

Abstract

Vaccines based on multiple emulsions are not very common despite the advantages they offer over conventional water-in-oil vaccine emulsions. A previous chapter described oil-surfactant mixtures that form nanosized, stable, and multiple emulsions after gentle mixing with a phosphate-buffered saline. In this study, two mixtures were tested in animals as potential vaccine adjuvants. In mouse studies, vaccines containing ovalbumin (OVA) as an antigen and experimental or conventional emulsion-producing adjuvants were compared. In addition, the efficacy and safety of novel adjuvants were tested in a subunit vaccine for pigs against Classical Swine Fever (CSF) virus. Enzyme-linked immunosorbent assays (ELISA) were performed to compare the antibody levels in sera collected from animals. The anti-OVA IgG titers were similar between mice immunized with OVA emulsified in experimental adjuvant and mice that were inoculated with OVA and the conventional Montanide^{TM} ISA 206 adjuvant; however, the emulsions formed by these adjuvants had very different droplet sizes. In contrast to the commercial emulsion-forming adjuvant, the experimental adjuvant produced emulsions with average droplet sizes that were less than 100 nm suitable for sterilization with membrane filtration. In addition, a subunit CSF vaccine formulated with novel adjuvant induced strong antigen-specific antibodies in pigs even when it was prepared with a lower adjuvant content. No health issues nor significant local reactions were observed in pigs after immunization with the experimental subunit vaccine.

Introduction

Adjuvants are vaccine components that help to induce an immune response against weak immunogenic antigens *(1)*. Water-in-oil (w/o) emulsions have been explored as adjuvants for

decades in both human and animal vaccines and have been determined to offer a cost-effective approach to enhancing the immune response. However, difficulties with injections and numerous local reactions limit the clinical use of w/o emulsions *(2)*. Multiple, water-in-oil-in-water (w/o/w), emulsions can be attractive alternatives for w/o emulsion vaccines, as they are less viscous and have a lower toxicity *(3, 4)*. Multiple emulsions are systems where small water droplets are within the bigger oil droplets and are subsequently dispersed within the continuous water phase. Due to this complex structure, multiple emulsions preserve the antigenic molecules in both water phases, providing a fast and prolonged release for continuous stimulation of the immune cells. Despite these benefits, the wide application of w/o/w emulsion vaccines is hampered primarily because of difficulties related to the stability and large non-uniform droplets.

The previous chapter presented novel oil-surfactant mixtures that produce nanoscale w/o/w emulsions after dilution and gentle mixing with phosphate-buffered saline (PBS). The obtained emulsions preserved mean droplet size, polydispersity, zeta potential, and pH after prolonged storage at different temperatures. As a result, two oil-surfactant mixtures (#2 and #4) were proposed for studying as potential vaccine adjuvants (SEA1 and SEA2) in animal immunizations (Table 1).

Here, the potency of emulsion vaccines formulated with SEA adjuvants in inducing antibody responses was tested in mice and pigs. In the first study, the ability of the experimental adjuvants to produce strong anti-OVA immunoglobulin G (IgG) antibody responses in vaccination of BALB/c mice was compared with conventional Montanide™ ISA 206 oily adjuvant (Seppic, France). According to the manufacturer's web site, Montanide™ ISA 206 contains mineral oil and produces double emulsions with droplet sizes around 1 μm after dilution with the water phase *(5)*. Thus, vaccines based on Montanide™ ISA 206 can easily be prepared by low-energy mixing of the pre-warmed adjuvant and antigen diluted in water. Moreover, a comparison study with w/o

and o/w emulsion vaccines has demonstrated the superiority of Montanide™ ISA 206 in inducing higher and more prolonged antibody responses *(6)*.

The current study with BALB/c mice was performed twice as, during the first trial, it came to our attention that the sample animals had been infected with Murine Norovirus (MNV) at the supplier's facility. Thus, the experiment was repeated with new mice to ensure that a MNV infection did not affect the antibody responses generated by animals after immunization with the vaccines.

Additional vaccine groups were included in the vaccination of CD-1 mice in the third mouse study. The combination of an experimental SEA1 adjuvant with saponin extract and vaccine with saponins only were investigated along with vaccines that contained SEA1 or Montanide™ ISA 206 adjuvants alone. The possibility to combine emulsions and food-grade saponins to improve the antibody responses against antigens in vaccines has been already explored in Chapter 3 of this thesis. Indeed, saponins are recognized as capable adjuvants for generating high antibody titers and promoting strong cell-mediated immunities *(7)*. In this study, the vaccine–adjuvant combination was prepared by simple dilution of VetSap® (purified veterinary saponin adjuvant) (Desert King International, USA) in the antigenic water phase prior to emulsification with an experimental oil-based adjuvant.

Finally, the efficacy of the experimental oil-based adjuvant was studied in subunit vaccines against Classical Swine Fever Virus (CSFV) for pigs. CSF is a contagious pig disease causing devastating damage in the swine industry worldwide. In contrast to modified live virus vaccines for CSF, vaccines based on subunit recombinant proteins offer safety and the ability to differentiate infected from vaccinated animals *(8)*. However, highly purified subunit proteins require co-administration with the adjuvants to be effective in inducing protective immune responses. Previously, a subunit vaccine containing CSFV E2 antigenic protein formulated in an oil-in-water

emulsion (KNB-E2), has shown high potency in the production of antibody responses and protection of pigs after a challenge with CSFV *(9, 10)*. Here, pigs were immunized with an insect-derived E2 (iE2) subunit protein emulsified in experimental SEA1 oil-based adjuvant in 1:1 and 2:1 volume ratios. The IgG antibody responses were compared between the experimental groups and the group that received the KNB-E2 vaccine. In addition, the weight of the pigs and the injection sites were monitored throughout the study to confirm the safety of the administered experimental adjuvant vaccine.

Methods

Preparation of the adjuvants and vaccines

All adjuvants and emulsion vaccines used for immunizations of the animals were prepared in sterile laboratory glassware. The SEA1 and SEA2 oil-based adjuvants were made with materials and, according to the procedures specified in Chapter 5, in the proportions shown in Table 6.1.

Table 6.1 Composition of experimental oil-based adjuvants.

Oil-surfactant mixture	Adjuvant name	Component	%, w/w
#2	SEA1	Drakeol 5 oil Tween 85 Compound A	This information was redacted intentionally. Please contact jshi@vet.k-state.edu for additional details.
#4	SEA2	Drakeol 5 oil MCT oil Tween 85 Compound A	

To confirm the ability of experimental and commercial adjuvants to form emulsions with nanoscale droplet size, three samples were prepared by emulsification of SEA1, SEA2, and

Montanide™ ISA 206 (Seppic, France) adjuvants in PBS. Prior to mixing, the adjuvants and PBS were heated to 37°C (or 31°C for Montanide™ ISA 206) in a water bath. PBS was added slowly to the adjuvants and followed by stirring with a magnetic bar at 500 rpm for 30 min for SEA adjuvants and at 350 rpm for 5 min for Montanide™ ISA 206. The volume ratio of PBS to adjuvant was 2:1 for SEA adjuvants and 1:1 for Montanide™ ISA 206. The emulsions were analyzed with a Zetasizer Nano ZS dynamic light scattering instrument (Malvern, USA) according to the procedure described in Chapter 5.

The main component of the chicken egg white, ovalbumin (EndoFit™ OVA, Invivogen, San Diego, USA), served as an antigen in the mouse studies and was diluted in sterile endotoxin-free PBS (1X, Gibco™, Fisher Scientific, USA) at 10 µg/dose. Insect-derived E2 (iE2) CSF subunit protein was prepared as described elsewhere *(9)*, diluted in sterile endotoxin-free PBS, and served as an antigen at 50 µg/dose in the pig study.

Emulsion-based vaccines were made by separately warming the experimental SEA adjuvants and antigen in PBS solution to 37°C using the water bath before emulsification. Next, the antigenic solution was poured slowly into the adjuvants in a 2:1 volume ratio (or 1:1 if stated) with subsequent stirring utilizing a magnetic mixer for 30 min at 500 rpm and at room temperature to form a multiple emulsion.

Vaccines with the conventional Montanide™ ISA 206 adjuvant were prepared according to the procedure recommended by the manufacturer *(5)*. Briefly, the adjuvant and antigenic PBS solution were warmed to 31°C in a water bath. The antigenic solution was added to the adjuvant at a 1:1 volume ratio and stirred at room temperature with a magnetic bar for 5 min at 350 rpm. The vaccines were kept at room temperature for 1 hour before immunization.

Vaccines containing VetSap® as an adjuvant were made by the dilution of the VetSap® stock solution in an endotoxin-free molecular biology grade water (Fisher Scientific, USA) and were followed by the addition of PBS to obtain 5 µg of saponins per dose for mice vaccination. Vaccines having a combination of SEA1 oil-based adjuvant and VetSap® were prepared by addition of VetSap® (5 µg/mouse) to the antigenic PBS solution prior to emulsification with the SEA1 adjuvant as described above. Pigs were immunized with subunit iE2 vaccines containing 100 or 300 µg of VetSap® per dose.

KNB-E2 subunit vaccine for immunization of pigs was produced as described elsewhere *(9)*.

Animal immunizations

All animal studies were conducted in accordance with Institutional Animal Care and Use Committee (IACUC) procedures. The IACUC reference numbers are 3961 and 3436.

BALB/c mice

In two consecutive BALB/c mouse experiments, female mice (Charles River Laboratories International) were randomly divided into 3 vaccine groups and 2 control groups (n=5 for each group). Two vaccine groups received emulsion-based vaccines prepared with OVA antigen and SEA1 and SEA2 experimental adjuvants (OVA-SEA1 and OVA-SEA2 groups) while a third group was immunized with vaccine containing Montanide™ ISA 206 commercial adjuvant (OVA+ISA206 group). Mice were immunized subcutaneously with 100 µl of the vaccine per animal on day 0. At the same time, two control groups received 100 µl of OVA in PBS or PBS only. Blood samples were collected from animals on days 0, 14, 21, and 28 in the first study and additionally on day 35 in the second BALB/c mouse study. Serum was separated from blood samples via centrifugation and stored at -20°C until further use.

CD-1 mice

A total of 30, 3-week-old male and female CD-1 mice (Comparative Medicine Group, Kansas State University, USA) were randomly divided into four vaccine groups and two control groups (n=5 in each group). Two groups received emulsion-based vaccines formulated with SEA1 (OVA+SEA1 group) or Montanide^{TM} ISA 206 (OVA+ISA206 group). A third group was immunized with a vaccine prepared with the VetSap® (OVA+VetSap) adjuvant. Finally, a fourth group received the vaccine with a combination of SEA1 and VetSap® adjuvants (OVA+ SEA1+VetSap). On day 0 of the study, mice received 100 µl of the vaccine subcutaneously while control groups were injected with 100 µl of OVA in PBS or PBS only. Blood was collected on days 0, 14, 21, 28, and 35, followed by separation of the serum via centrifugation. Serum samples were stored at -20°C until further analysis.

Pigs

Duroc × White Large 3-week old female piglets were randomly allocated into 5 vaccine groups (n=5) and 1 control group (n=2). Pigs were housed at the Large Animal Research Center facility (Kansas State University, Manhattan, USA) during the 35 days of the study. On day 0, all groups received 2 ml of the vaccine or sterile PBS (in the case of the control group) intramuscularly. The first vaccine group was immunized with the KNB-E2 subunit vaccine. The vaccines for the second group were prepared by emulsification of the iE2 subunit protein solution in PBS and SEA1 adjuvant in a 1:1 volume ratio (E2+SEA1(1:1) group). The third vaccine group was vaccinated with iE2 protein formulated with SEA1 in a 2:1 volume ratio (E2+SEA1 (2:1) group). The fourth and fifth groups were immunized with iE2 protein co-administered with 100 or 300 µg of VetSap®, respectively [E2+VetSap (100 µg) and E2 + VetSap (300 µg) groups]. Blood samples were taken on days 0, 7, 14, 21, and 35 of the study, with subsequent serum separation and storage at -20°C. The weight of the pigs was recorded weekly, while pig health and vaccine injection sites were monitored daily. Animals were humanely euthanized at day 28 of the study.

The veterinary pathologist examined the postmortem tissues and lymph nodes surrounding the injection sites for any pathological changes to the muscular tissues in pigs that received vaccines adjuvanted with experimental SEA1 and VetSap® adjuvants.

Enzyme-linked immunosorbent assay (ELISA)

An ELISA was performed to determine OVA- and E2-specific IgG antibody titers in mouse and swine serum, respectively. The 96-well flat-bottom Corning® microtiter ELISA plates were coated with 5 µg/ml of ovalbumin (Fisher Bioreagents, USA) or 128 ng/ml of purified E2 overnight. The next morning the plates were washed once with PBST (0.05% Tween 20 in PBS) and blocked with 2% Fetal Bovine Serum in PBS (blocking buffer) for 1 hour at 37°C. Different dilutions of the serum in the blocking buffer were added into the wells of the ELISA plates and incubated for 1 hour at room temperature (RT) and were subsequently washed 3 times with PBST. Goat anti-mouse IgG (H+L) conjugated with Horseradish Peroxidase (HRP) (#115-035-003, Jackson ImmunoResearch, USA, dilution 1/1,000) was added at 100 µl/well as detecting antibodies in the case of mouse studies. The HRP-conjugated goat anti-porcine IgG (Southern Biotech, USA, dilution 1/1,000) antibodies were used at 100 µl/well for detection of E2-specific antibodies in pig serum samples. After an one-hour incubation with detecting antibodies at RT, ELISA plates were washed 3 times with PBST, and 3,3,5,5-tetramethylbenzidine chromogen (Novex, USA) was added at 100 µl/well for color development. To stop the reaction, 2N sulfuric acid (Ricca Chemical Company, USA) was used at 100 µl/well.

Relative antibody concentrations were determined with a SpectraMAX optical spectrophotometer at 450 nm and were analyzed with Softmax® Pro 6.4 Software (Molecular Devices, USA).

Statistical analysis

Data from animal studies were reported as the mean values ± standard error (SE) from groups of five (or 2, in the case of the control group in the pig study) animals. The differences between treatment groups were analyzed by one-way analysis of variance (ANOVA) utilizing SigmaPlot 11.0 (Systat Software Inc., USA). Differences were considered statistically significant when $p < 0.05$.

Results

Appearance of the adjuvants and emulsions

The experimental adjuvants were homogenous, clear-yellow mixtures, while vaccine emulsions made from them were white (Fig. 6.1a, b). Figure 1c depicts the droplet size distributions of the emulsions prepared with SEA1, SEA2, and Montanide^{TM} ISA 206 adjuvants and PBS as a water phase. While experimental SEA adjuvants produced emulsions with relatively narrow size distribution (droplet diameters ranging from 43.8 to 140 nm and 58.8 to 295.0 nm for SEA1 and SEA2, respectively), the conventional adjuvant formed emulsions with droplets ranging from 78.8 to 5,000 nm (Fig. 6.1c).

IgG antibody titers in vaccinated mice

Figure 6.2 demonstrates the results of the ELISA of serum samples from two BALB/c mouse studies. In the first study, IgG levels gradually increased in all vaccine groups with the highest detected on day 28 of the study. No significant antibody titers were produced by the two control groups (Fig. 6.2a). On day 28, mice immunized with OVA + SEA1 and OVA + ISA206 vaccines had very similar IgG levels in the serum ($p=0.841$), while the group vaccinated with OVA + SEA2 had significantly lower titers of IgG antibodies ($p=0.021$) (Fig. 6.2b).

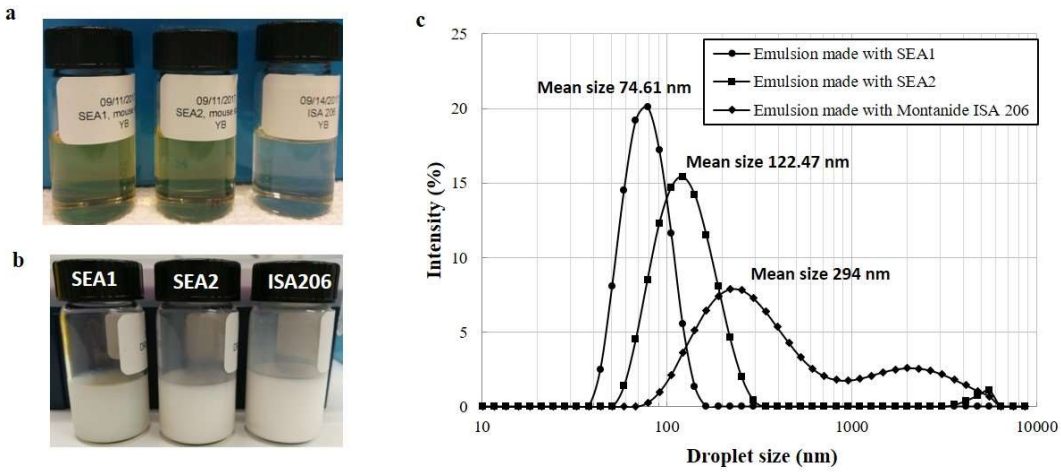

Figure 6.1 Appearance of experimental SEA and commercial MontanideTM ISA 206 (ISA206) adjuvants (a) and emulsions they formed after mixing with phosphate-buffered saline (b); droplet size distributions of these emulsions (c).

In the second BALB/c mouse experiment, IgG titers in mice immunized with OVA+SEA1, OVA+ SEA2, and OVA+ ISA206 progressively increased again after vaccination until day 35, in contrast to the groups inoculated with OVA only or PBS only (Fig. 6.2c). On day 35, the highest IgG antibody titers were observed in animals immunized with OVA+SEA2, while two other vaccine groups (OVA+SEA1 and OVA+ISA206) had comparable levels of IgG antibodies ($p=0.841$). However, there were no statistically significant differences ($p>0.05$) between OVA+SEA2 and OVA+ISA206 groups on day 35 of the experiment (Fig. 6.2d).

Figure 6.3 represents the ELISA results for the CD-1 mouse vaccination study. The gradual growth of IgG titers was observed from day 0 until day 35 of the study in all vaccine groups. In contrast, the control groups did not display signs of IgG titer growth (Fig. 6.3a). On day 35, antibody titers in all vaccine groups were higher in comparison with the group that received non-adjuvanted OVA ($p < 0.05$) (Fig. 6.3b). However, the lowest IgG titers among the vaccine groups were observed in mice immunized with OVA+VetSap. In fact, according to Fig. 6.3a, the IgG antibody levels in OVA+VetSap mice were lower in comparison with other vaccine groups

throughout the entire experiment. Animals vaccinated with OVA+SEA1 and OVA+SEA1+VetSap had higher antibody titers when compared with the OVA+VetSap group ($p < 0.05$), while no substantial differences were detected in IgG levels between OVA+SEA1 and OVA+SEA1+VetSap mice (Fig. 6.3b).

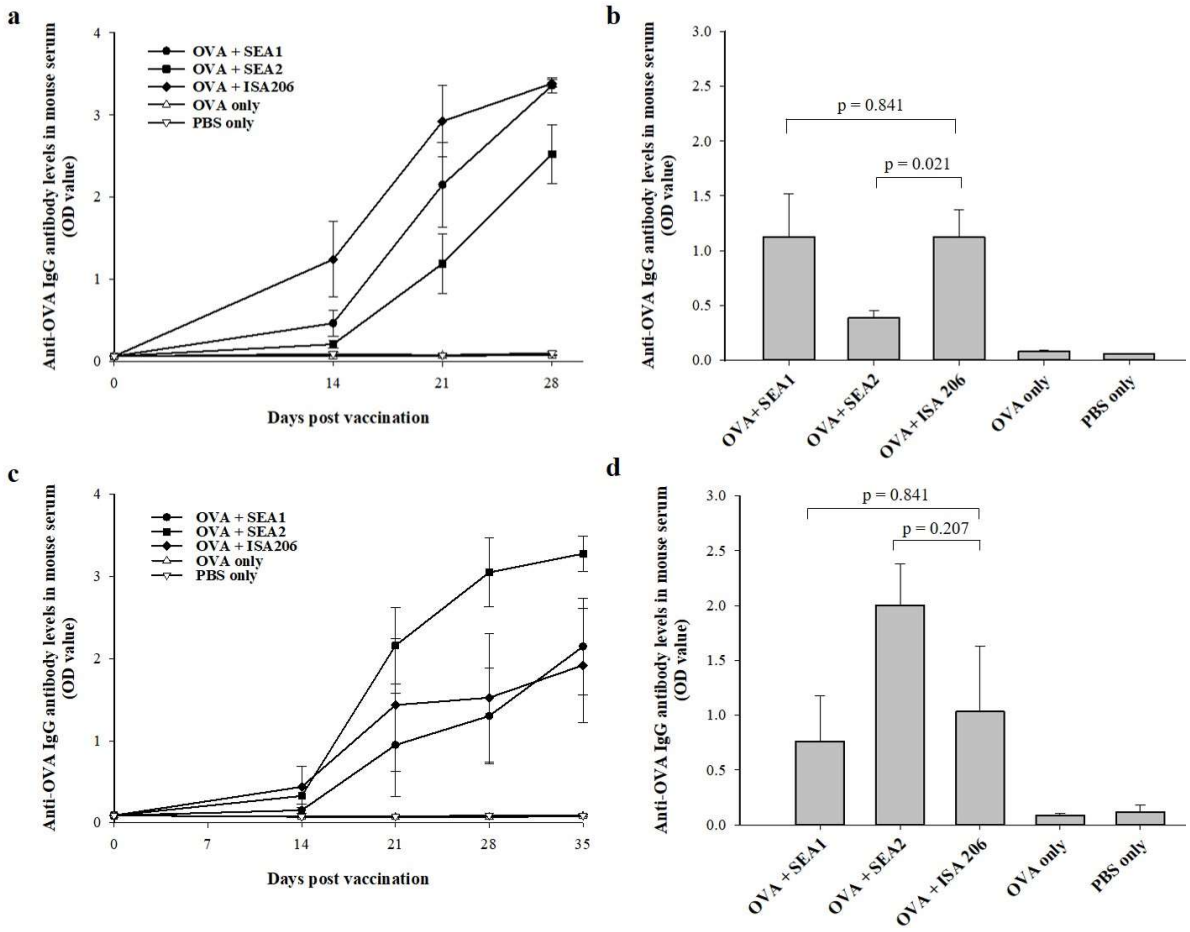

Figure 6.2 Anti-OVA IgG antibody titers detected in BALB/c mice vaccinated with OVA and different adjuvants from days 0 to 28 [dilution 1/5,000] (a) and on day 28 [dilution 1/50,000] (b) in the first study; from days 0 to 35 [dilution 1/5,000] (c) and on day 35 [dilution 1/50,000] (d) in the second study.

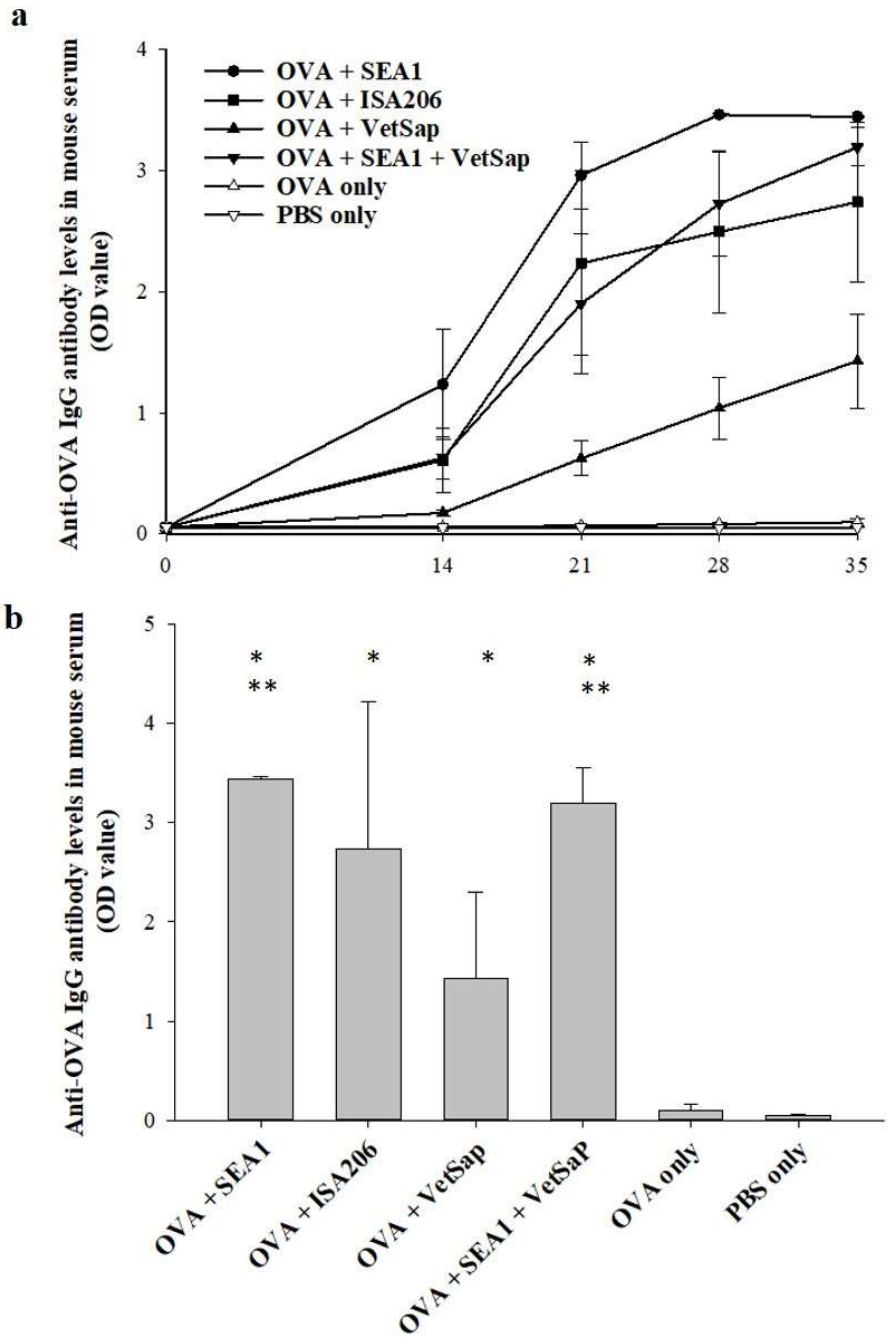

Figure 6.3 Anti-OVA IgG antibody levels detected in CD-1 mouse blood samples from day 0 post vaccination to day 35 [dilution 1/5,000] (a) and on day 35 [dilution 1/50,000] (b).

* - $p < 0.05$ compared to OVA only group, ** - $p < 0.05$ compared to OVA+VetSap group

Weight gain, serum antibody responses and vaccine reactions in pigs

The body weight of pigs immunized with adjuvanted iE2 subunit protein and pigs injected with PBS steadily increased starting from the day of vaccination to the end of the study (Fig. 6.4a). No difference in weight gain was observed between vaccinated and control animals (Fig. 6.4a). All pigs maintained good health during the study.

The ELISA of serum samples from day 28 revealed higher E2-specific IgG titers in pigs immunized with the KNB-E2 vaccine and iE2 emulsified in SEA1 (1:1) and SEA1 (2:1) in comparison with the PBS only group ($p < 0.05$); there were no statistical differences between these subunit vaccine groups (Fig. 6.4b). However, vaccination with iE2 adjuvanted with VetSap® (100 and 300 μg) did not elicit substantial levels of anti-E2 IgG antibodies ($p > 0.05$ in comparison with PBS only group) (Fig. 6.4b).

Daily monitoring of injection sites did not reveal any noticeable redness, swelling, or abnormal warmth after vaccinations in all pig groups. For most of the pigs analyzed, there were no significant changes detected by the pathologist during the postmortem analysis of incised tissues and lymph nodes surrounding the injection sites (Table 6.2). A few pigs had a darker than usual appearance of the lymph nodes closely located to the injection sites. However, these anomalies were noticed in all examined groups. In addition, one pig in the E2+SEA1 (1:1) vaccine group had a small necrotic area in the muscle at the vaccine injection site (Table 6.2). All pigs survived until the end of the study.

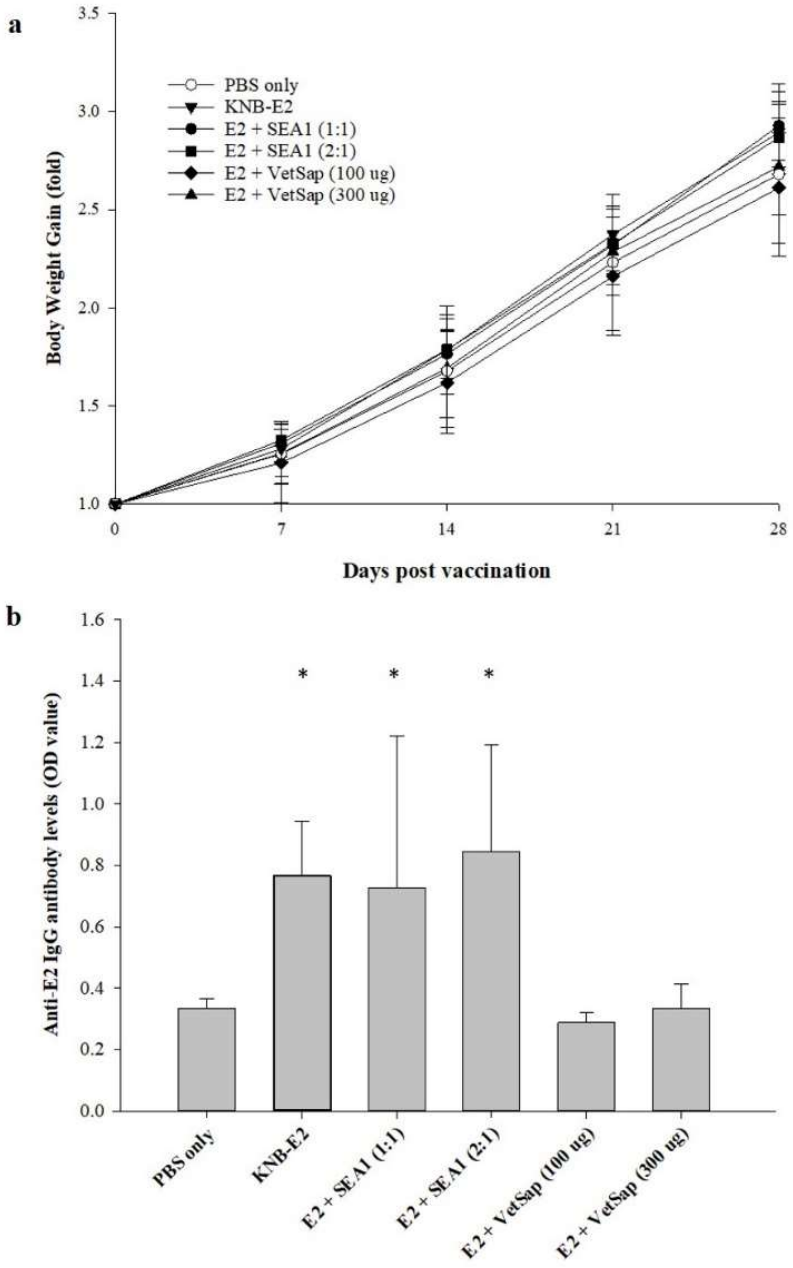

Figure 6.4 Changes in body weight gain of the pigs from day 0 until the end of the study (a) and anti-E2 IgG antibody levels in pig sera on day 28 of the study [dilution 1/500] (b).

* - $p < 0.05$ compared to PBS only group.

Table 6.2 Postmortem analysis of injection sites surrounding tissues and lymph nodes of pigs vaccinated with subunit CSFV E2 protein and different adjuvants.

Vaccine group	Pig #	Pathological changes at the injection sites
E2+SEA1 (1:1)	233	Small area of necrosis (~1.5 cm)
	235	NSC
	238	NSC
	245	NSC
	246	NSC
E2 + SEA1 (2:1)	230	NSC
	240	NSC
	242	NSC
	244	Grey-colored lymph node, not enlarged
	247	NSC
E2 + VetSap® (100 μg)	197	NSC
	229	NSC
	232	NSC
	234	Grey-colored lymph node, not enlarged
	239	Grey-colored lymph node, not enlarged
E2 + VetSap® (300 μg)	198	NSC
	241	Grey-colored lymph node, not enlarged
	248	NSC
	249	NSC
	250	NSC

NSC, no significant changes

Discussion

Immunization of animals with vaccines adjuvanted with emulsions has been done for decades. Conventional w/o emulsion vaccines are still the primary choice despite the numerous local, systemic, and allergic reactions associated with them *(2)*. Multiple emulsions have been shown to have a lower toxicity and better injectability in contrast to w/o formulations. However, the wide use of w/o/w emulsions is hampered by the challenges in designing stable formulations.

Therefore, only one company (Seppic, France) currently produces adjuvants that form multiple emulsion vaccines for animals *(5)*.

In the previous chapter, catastrophic phase inversion was explored for creating multiple emulsions with nanoscale droplet sizes from novel oil-surfactants mixtures and phosphate-buffered saline as a water phase. Two mixtures were proposed for immunological and safety studies as adjuvants in animal vaccination (Table 6.1). Two BALB/c and one CD-1 mouse studies were performed to test the potency of vaccines formulated with OVA antigen and experimental SEA adjuvants in inducing anti-OVA IgG antibodies in comparison with the vaccine prepared with OVA emulsified in commercial Montanide^{TM} ISA 206 adjuvant (Seppic, France). The results of all mouse studies indicated that vaccines with experimental SEA1 and commercial Montanide^{TM} ISA 206 adjuvants had comparable levels of anti-OVA IgG antibodies (Fig. 6.2b, 6.2d, 6.3b). Remarkably, the group immunized with the SEA2 adjuvanted vaccine had significantly lower IgG titers in the first mouse study ($p=0.021$), while, in the second study, the titer in this group was comparable with the two other vaccine groups ($p=0.207$).

Numerous researchers have tried to determine the optimal particle size for vaccine delivery vehicles producing strong immune responses *(11-14)*. However, these studies have delivered conflicting results as several experiments have shown no difference in immunological activities between small and large particulate adjuvants *(15, 16)*. Similarly, this study's experimental SEA1 and conventional Montanide^{TM} ISA 206 adjuvants produced emulsions with very different droplet size distributions (Fig. 6.1c) while the levels of IgG antibodies in the vaccinated mice were similar (Fig. 6.2b, 6.2d, 6.3b); this indicated that the size of emulsion droplets may not be the main factor affecting the IgG levels. It is recommended that the cell-mediated immune responses need to be compared in addition to antibody responses before the difference between potencies of experimental and conventional adjuvants can be fully established. Nevertheless, unlike with

commercial adjuvants, vaccines prepared with the experimental SEA1 adjuvant can be sterilized with 0.2 μm membrane filtration due to nanoscale size distribution (Fig. 6.1c).

Apparently, MNV infection in the first BALB/s mouse study did not interfere with the abilities of the animals to generate IgG antibodies. All vaccine groups progressively produced IgG antibodies after vaccination with OVA formulated with different adjuvants (Fig. 6.2a).

The combination of VetSap® saponin extract and SEA1 in the vaccine did not lead to stronger IgG antibody responses in CD-1 mice in comparison with the group immunized with a vaccine containing an emulsion only adjuvant (Fig. 6.3b). Thus, no synergistic effect for the combination of the two adjuvants was detected, as the antigen and emulsion only vaccine induced higher IgG titers in the mice than the vaccine with a combination of adjuvants (Fig. 6.3b). Furthermore, the mouse group that received OVA+VetSap had lower IgG titers when compared to the other vaccine groups throughout the study (Fig. 6.3a). In addition, the immunization of pigs with subunit E2 protein co-administered with VetSap® adjuvant did not produce a strong E2-specific antibody response, even when VetSap® was used at a higher content [300 μg per pig] (Fig. 6.4b). Supposedly, higher concentrations of VetSap® are required to achieve the desired improvement of the antibody responses in animals.

Considering the emulsion stability studies performed in Chapter 5 of this thesis and the results of mouse immunizations, the experimental SEA1 adjuvant advanced to the study with the large animals. Thus, subunit CSF E2 vaccine formulated with SEA1 was deemed safe to use, as pigs gained weight steadily after vaccination (Fig. 6.4a) and did not experience health issues. Moreover, the absence of both local vaccine site reactions and significant changes in the surrounding muscular tissues (Table 2) confirms the good safety profile of the experimental adjuvants. The potency of the KNB-E2 vaccine has already been proven in several earlier studies *(9, 10, 17)*. A comparison study of E2+SEA1 (1:1), E2+SEA1 (2:1) and KNB-E2 vaccines showed

similar anti-E2 IgG levels in these pig groups (Fig. 6.4b), signifying that the SEA1 adjuvant is a good candidate for enhancing antibody responses to poorly immunogenic subunit proteins even when used at lower content [group E2+SEA1 (2:1)]. In addition, the oil-in-water emulsion in the KNB-E2 vaccine required the high-pressure homogenizer for preparation and membrane filtration could not be applied due to the droplet size *(18)*. In contrast, the subunit vaccine prepared with SEA1 adjuvant was made with the help of inexpensive, low-energy gentle mixing and can be easily sterilized with a 0.2 μm membrane filter. Furthermore, SEA1 adjuvant contains cost-effective materials making it very attractive for the veterinary industry.

The next steps in this project will include testing the experimental SEA1 adjuvant in vaccination of animals with a subsequent viral challenge to establish its potency in creating humoral and cell-mediated protective immunities.

Conclusions

In this study, novel oil-based adjuvants that produced multiple emulsion vaccines after low-energy mixing with antigenic water phase were tested in mice and pigs on their ability to induce strong antibody responses. In mice, the levels of OVA-specific IgG titers were similar between vaccine groups immunized with OVA adjuvanted with experimental SEA1 and a commercial oil-based adjuvant proving that the novel adjuvant has equal potency. However, in contrast to the commercial adjuvant, SEA1-produced emulsion vaccines had a narrow nanoscale droplet size distribution suitable for sterilization with membrane filtration. In addition, the novel oil-based SEA1 adjuvant can be safely used in vaccination of pigs with subunit CSFV E2 antigenic protein and produced strong anti-E2 IgG titers on a level comparable with the conventional subunit vaccine even when utilized at a lower content. Additional experiments shall be performed to

confirm that the subunit vaccine formulated with SEA1 adjuvant will protect the pigs after challenge with CSF virus.

References

1. Reed, S. G.; Orr, M. T.; Fox, C. B. Key roles of adjuvants in modern vaccines. *Nat. Med.* **2013**, *19*, 1597-1608.

2. Stills, H. F. Adjuvants and Antibody Production: Dispelling the Myths Associated with Freund's Complete and Other Adjuvants. *ILAR Journal* **2005**, *46*, 280-293.

3. Huang, M.; Chou, A.; Lien, S.; Chen, H.; Huang, C.; Chen, W.; Chong, P.; Liu, S.; Leng, C. Formulation and immunological evaluation of novel vaccine delivery systems based on bioresorbable poly(ethylene glycol)-block-poly(lactide-co-e-caprolactone). *J. Biomed. Mater. Res. B Appl. Biomater.* **2009**, *90B*, 832-841.

4. Shakya, A. K.; Nandakumar, K. S. Applications of polymeric adjuvants in studying autoimmune responses and vaccination against infectious diseases. *J. R. Soc. Interface* **2012**, *10*, 20120536.

5. SEPPIC Montanide™ ISA - W/O/W. Ready-to-use adjuvants for water-in-oil-in-water emulsions. *https://www.seppic.com/montanide-isa-w-o-w* (accessed 05/16, 2018).

6. Hunter, P. The performance of southern African territories serotypes of foot and mouth disease antigen in oil-adjuvanted vaccines. *Rev. - Off. Int. Epizoot.* **1996**, *15*, 913.

7. Sun, H.; Xie, Y.; Ye, Y. Advances in saponin- based adjuvants. *Vaccine* **2009**, *27*, 1787-1796.

8. Blome, S.; Moß, C.; Reimann, I.; König, P.; Beer, M. Classical swine fever vaccines—State-of-the-art. *Vet. Microbiol.* **2017**, *206*, 10-20.

9. Madera, R.; Gong, W.; Wang, L.; Burakova, Y.; Lleellish, K.; Galliher-Beckley, A.; Nietfeld, J.; Henningson, J.; Jia, K.; Li, P.; Bai, J.; Schlup, J.; McVey, S.; Tu, C.; Shi, J. Pigs immunized with a novel E2 subunit vaccine are protected from subgenotype heterologous classical swine fever virus challenge.(Report). *BMC Vet. Res.* **2016**, *12:197*.

10. Madera, R. F.; Wang, L.; Gong, W.; Burakova, Y.; Buist, S.; Nietfeld, J.; Henningson, J.; Cino-Ozuna, A.; Tu, C.; Shi, J. Toward the development of a one-dose classical swine fever subunit vaccine: antigen titration, immunity onset, and duration of immunity. *J. Vet. Sci* **2018**, *19*, 393.

11. Kanchan, V.; Panda, A. K. Interactions of antigen-loaded polylactide particles with macrophages and their correlation with the immune response. *Biomaterials* **2007**, *28*, 5344-5357.

12. Manolova, V.; Flace, A.; Bauer, M.; Schwarz, K.; Saudan, P.; Bachmann, M. Nanoparticles target distinct dendritic cell populations according to their size. *Eur. J. Immunol.* **2008***, 38*, 1404-1413.

13. Joshi, V. B.; Geary, S. M.; Salem, A. K. Biodegradable Particles as Vaccine Delivery Systems: Size Matters. *The AAPS Journal* **2012***, 15*, 85-94.

14. Shah, R. R.; Dodd, S.; Schaefer, M.; Ugozzoli, M.; Singh, M.; Otten, G. R.; Amiji, M. M.; O'Hagan, D. T.; Brito, L. A. The Development of Self-Emulsifying Oil-in-Water Emulsion Adjuvant and an Evaluation of the Impact of Droplet Size on Performance. *J. Pharm. Sci.* **2015***, 104*, 1352-1361.

15. Wendorf, J.; Chesko, J.; Kazzaz, J.; Ugozzoli, M.; Vajdy, M.; O'Hagan, D.; Singh, M. A comparison of anionic nanoparticles and microparticles as vaccine delivery systems. *Hum. Vaccin.* **2008***, 4(1)*, 44-49.

16. Oyewumi, M. O.; Kumar, A.; Cui, Z. Nano-microparticles as immune adjuvants: correlating particle sizes and the resultant immune responses. *Expert Rev. Vaccines* **2010***, 9*, 1095.

17. Laughlin, R. C.; Madera, R.; Peres, Y.; Berquist, B. R.; Wang, L.; Buist, S.; Burakova, Y.; Palle, S.; Chung, C. J.; Rasmussen, M. V.; Martel, E.; Brake, D. A.; Neilan, J. G.; Lawhon, S. D.; Adams, L. G.; Shi, J.; Marcel, S. Plant- made E2 glycoprotein single- dose vaccine protects pigs against classical swine fever. *Plant Biotechnol. J.* **2018**.

18. Galliher-Beckley, A.; Pappan, L. K.; Madera, R.; Burakova, Y.; Waters, A.; Nickles, M.; Li, X.; Nietfeld, J.; Schlup, J. R.; Zhong, Q.; McVey, S.; Dritz, S. S.; Shi, J. Characterization of a novel oil-in-water emulsion adjuvant for swine influenza virus and Mycoplasma hyopneumoniae vaccines. *Vaccine* **2015***, 33*, 2903-2908.

Chapter 7 - Conclusion and Future Directions

The development of suitable and cost-effective adjuvants is a key factor for advancing vaccine technology. Emulsions are attractive adjuvants for veterinary vaccines as they can be formulated with inexpensive materials and are able to induce robust immune responses. However, the conventional production of emulsions commonly involves devices with high energy demands that affect the final price of the vaccines. This work focused on designing the adjuvant-producing emulsion vaccines via low-energy phase inversion and self-emulsification approaches. The goal was to create adjuvants containing inexpensive and readily available materials while also eliciting strong immune responses after co-administration with the antigens.

The role of oil composition in formation and stability of self-emulsified emulsions was investigated in Chapter 2. The comparison study between triglycerides with different chain length as a part of the oil phase revealed that medium-chain triglycerides (MCT) helped to form more stable emulsions with smaller droplet diameters. Zeta potential, an important characteristic of emulsion stability, has been found to be sensitive to a specific concentration of triglycerides when their amount was less than 25 wt.% and did not change when their concentration in the oil phase exceeded 25 wt. %. Therefore, additional experiments need to be performed to explain the behavior of zeta potential in self-emulsified emulsions with mixed triglyceride/mineral oil phase.

The Box-Behnken design (BBD) of response surface methodology was used in Chapter 3 to investigate the effect of multiple formulation variables (the ratio of sucrose palmitate to glycerol, the ratio of Tween 60 to oil phase, the ratio of glycerol to oil, and the ratio of oil/glycerol gel to water phase) on the physical characteristics of self-emulsified emulsions. The ratio of Tween 60 surfactant to the oil phase demonstrated the most pronounced impact on size, polydispersity, and zeta potential of emulsion droplets. In contrast, the stability of emulsions was mostly influenced

by the ratio of the oil phase to the glycerol phase. Additionally, BBD was used to create mathematical equations describing the relationship between formulation variables and responses. The equation describing the effect of formulation variables on the mean droplet size of emulsions predicted average droplet size comparable to the observed values. This can be used to optimize emulsions having the appropriate droplet size required for vaccines. For future steps, some adjustments need to be made to improve the reliability of the mathematical model defining the relationship between the formulation variables and emulsion stability.

Chapter 4 examined cost-effective saponin extract for formulation of oil-in-water emulsion-based adjuvants. Being substances with surfactant properties, saponins helped to preserve emulsion droplets for at least 180 days at different temperatures without creaming, phase separation, or significant change in size. In addition, the immunostimulatory activity of saponins help to produce strong IgG and neutralizing antibody titers in pigs when co-injected with subunit antigenic protein. This work demonstrated that inexpensive food-grade saponins can be safely used in swine immunization as the animals consistently increased in weight and there was no detection of significant inflammation at the injection sites.

Chapter 4 additionally studied the adjuvant containing mixture of oils and surfactants, as well as the approach for producing emulsions for pig vaccination via phase inversion composition (PIC). Although the approach for vaccines formulated with the adjuvant did not produce adverse reactions in animas, they also did not elicit high immune responses. This indicated that the composition of the adjuvant needs to be changed to promote stronger stimulation of the immune system.

To address this issue, new oil-surfactant mixtures were formulated containing a higher amount of mineral oil and a different surfactant. Their ability to form stable multiple emulsions via the PIC approach was examined in Chapter 5. The oil with higher viscosity formed the smallest

emulsion droplets. Furthermore, the time and speed of mixing, initial temperature of components, and amount of the aqueous phase demonstrated significant effects on the size distribution and polydispersity of emulsions. The nanometer size and multiple structures of the droplets were confirmed with dynamic light scattering and transmission electron microscopy. Emulsions preserved the droplet size, polydispersity, zeta potential and pH after 3-month storage at different temperatures. Thus, the low-energy phase inversion approach was successfully employed and yielded stable nanoscale emulsions. Emulsions with multiple structure were formed which is beneficial for delivering the antigenic molecules in vaccines. To confirm the potency of the developed formulations, two oil-surfactant mixtures containing mineral oil only (SEA1) and the mixture of mineral and MCT oils (SEA2) were proposed for further immunological studies in mice and swine models.

In Chapter 6, the results of testing the SEA1 and SEA2 potency in animal vaccination were presented. In both animal models, the levels of antigen-specific IgG antibodies were similar between the groups that received vaccines formulated with experimental SEA1 and conventional adjuvants, indicating that the novel adjuvant has equal effectiveness in inducing antibody responses. Moreover, vaccines with the novel adjuvant did not cause adverse reactions in animals and were produced via an energy-efficient approach without expensive equipment. Further studies shall be completed to confirm the efficacy of the vaccines with SEA1 adjuvant in protection of pigs after the viral challenge. Finally, the differences in the potency of the vaccines prepared with experimental and conventional adjuvants in inducing cell-mediated immune responses need to be determined in the future studies.

In conclusion, development of new adjuvants is an important step for advancing vaccine technology. The outcome of this research allows to implement new methods for designing emulsion-based adjuvants and developing new efficacious and inexpensive veterinary vaccines.

Appendix A - Transmission Electron Microscopy of Multiple Emulsions

Introduction

Transmission electron microscopy (TEM) is an essential tool for investigating the morphology, size, and size distribution characterization of nanoscale emulsions *(1)*. In this study, TEM was employed to investigate the droplet size and structure of the emulsions prepared with experimental SEA1 (Chapter 5, 6) and commercial Montanide^{TM} ISA 206 adjuvants. According to the manufacturer, the Montanide^{TM} ISA 206 (ISA 206, Seppic, France) adjuvant produces water-in-oil-in-water emulsions with a droplet diameter of around 1 μm after a gentle mixing with a water phase *(2)*. The experimental SEA1 adjuvant diluted with aqueous phase forms emulsion with droplets ranging from 43.8 to 140 nm (Chapter 6). The goal of this study was to investigate and confirm multiple (water-in-oil-in-water) morphology of emulsion droplets obtained from the SEA1 adjuvant.

Two different sample preparation protocols, routine and liquid-cell TEM, were examined and compared for visualization of emulsions with TEM. The routine "dry-on-the-grid" method involves the placement of emulsion samples on the carbon coated, copper grid followed by drying and imaging. In addition, negative staining with uranyl acetate (UA) was employed in some experiments to create the contrast between the emulsion droplets and background.

On the contrary, the application of liquid TEM cells helps to avoid drying and visualize samples in their natural state. This method became popular for characterization of nanoparticles, electrochemical deposition, lithiation for batteries, and imaging of biological samples such as cells and viruses *(3)*. In this project, emulsion samples were loaded into the liquid TEM carriers with a

silicon nitride window and a microchannel inside followed by imaging with and without negative staining. The feasibility of liquid-cell TEM for imaging of the emulsions was explored in this study.

Methods

Preparation of emulsion samples for imaging

The experimental oil-surfactant mixture #2 (SEA1 adjuvant) was prepared as described previously in Chapter 5. The emulsion from commercial Montanide ISA 206 oil-based adjuvant was made by mixing 1 volume of warmed PBS (31°C) with 1 volume of adjuvant (31°C) at 350 rpm for 5 min.

Imaging with liquid-cell TEM

TEM imaging was performed with freshly prepared emulsions. A total of three TEM imaging experiments were performed with application of the liquid cells. The sample preparation was performed following the procedure described elsewhere *(4, 5)* and utilizing a K-kit Complete Toolbox Set purchased from Ted Pella Inc (USA). Briefly, emulsion samples were diluted with PBS (1:10 for experimental emulsion and 1:30 for emulsion made with commercial adjuvant) and loaded into the K-kit carriers (0.2 or 2 μm channel heights) using a designated holder and loading stand. In one experiment, emulsions were mixed with UA before loading into the K-kit carriers. Next, carriers were sealed, mounted inside a standard grid for TEM, and vacuum-dried for 30 min. A Tecnai^{TM} G2 Spirit BioTWIN electron microscope (FEI, USA) housed in the Nanotechnology Innovation Center of Kansas State (NICKS) at Kansas State University (Manhattan, KS, USA) was employed to visualize emulsion droplets after applying 80 kV of accelerating voltage.

Imaging with routine sample preparation method

The routine "dry-on-the-grid" TEM sample preparation was performed with two different approaches. For the first approach, the drops of emulsions diluted with PBS (1:10 for SEA1 emulsion and 1:30 for ISA 206 emulsion) were deposited on 200 mesh formvar-carbon coated grids (Electron Microscopy Sciences, USA) and vacuum-dried for 30 min without negative staining. Imaging was performed with a Tecnai^{TM} G2 Spirit BioTWIN electron microscope (FEI, USA) at 80 kV accelerating voltage.

For the second, and more gentle, approach, droplets of the emulsion samples (~5 µl) were placed on a glass slide and a 200 mesh formvar-carbon coated grid was positioned on the top of the droplet using forceps. After 20 seconds, the grid was removed from the droplet and a small piece of paper was used to eliminate the excess of the emulsion sample from the grid. Next, the same grid was placed on top of the uranyl acetate droplet for negative staining. After 20 s, a small piece of paper was used to remove any excess uranyl acetate from the grid. Finally, the grid was placed into the TEM holder without additional drying. The visualization of emulsion drops was done at an accelerating voltage of 100 kV by utilizing a CM100 transmission electron microscope (FEI, USA) equipped with an AMT digital image capturing system at the Department of Biology at Kansas State University (Manhattan, KS, USA).

Results

Liquid cell TEM

Figures A 1 and A 2 demonstrate TEM images of the emulsions prepared with SEA1 and ISA 206 adjuvants with application of 0.2 µm height K-kit carriers and without UA staining. Figure 1 depicts the microscopic pictures of the SEA1 emulsion taken at different magnifications and shows most of the droplets being less than 100 nm in diameter. Considerable overlapping between

the emulsion droplets was observed, while their multiple morphology could not be established (Fig. A. 1).

Very poor contrast was observed in images of ISA 206 emulsion (Fig. A. 2). The emulsion droplets appeared to be around 1 μm or less in size with substantial coalescence of the droplets (Fig. A. 2).

Figures 3 and 4 represent pictures of emulsions imaged with the help of 2 μm carriers for liquid TEM. When UA negative staining was applied, none of the droplets could be visualized in the SEA1 emulsion sample (Fig. A. 3). However, droplets around 500 nm or less were observed in TEM pictures of emulsion made with commercial ISA 206 adjuvant, however, the multiple structure of the droplets could not be confirmed (Fig. A. 4).

Finally, 0.2 μm carriers were employed again to image SEA1 emulsion without UA staining (Fig. A. 5). The presence of round droplets was detected, however, several of them were significantly bigger than expected (350-860 nm) (Fig. A. 5).

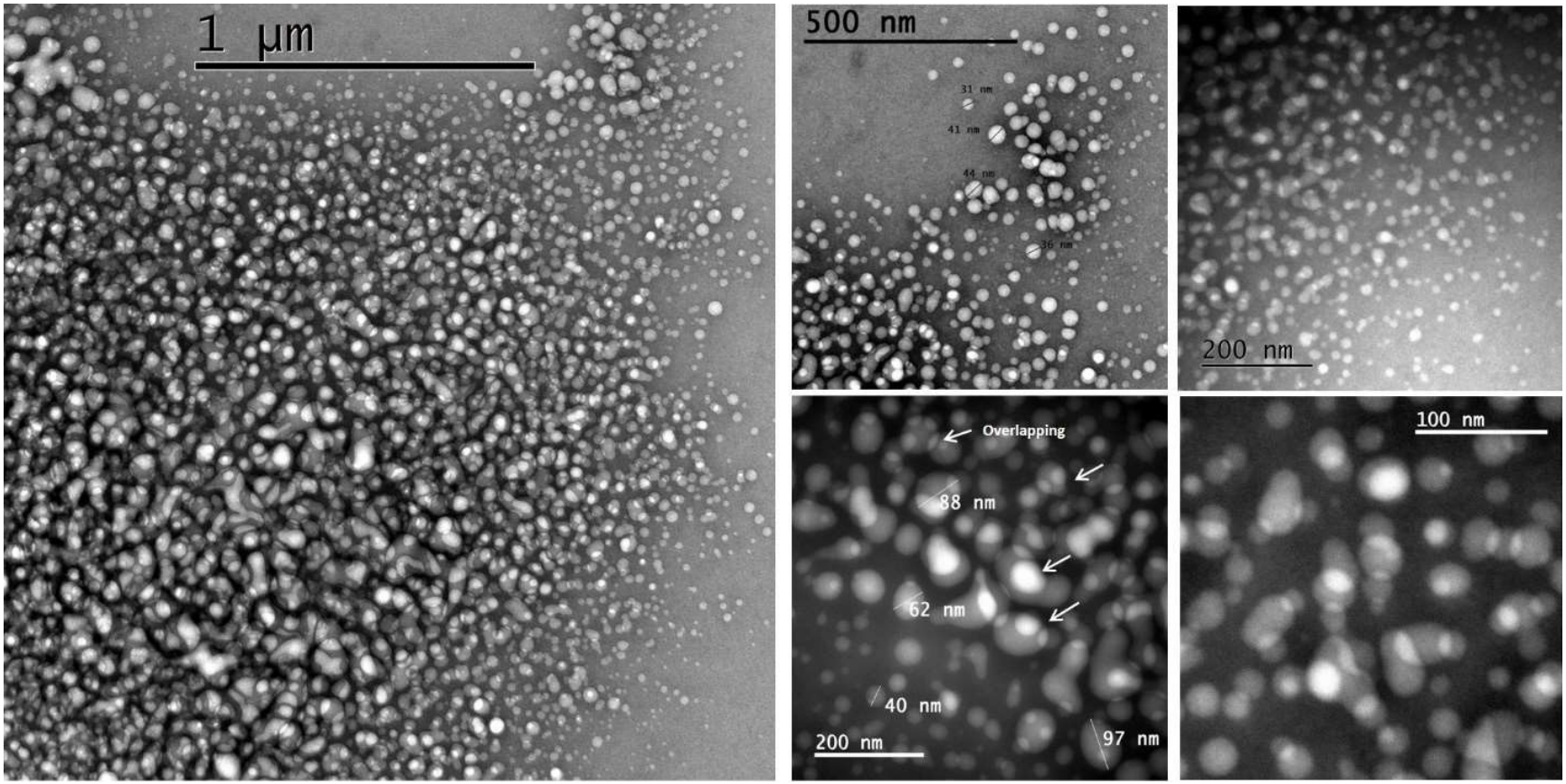

A. 1 TEM images of emulsion sample prepared from experimental SEA1 adjuvant. Experiment was performed with application of 0.2 µm height K-kit carrier without negative staining of the sample at different magnifications. September 1, 2017.

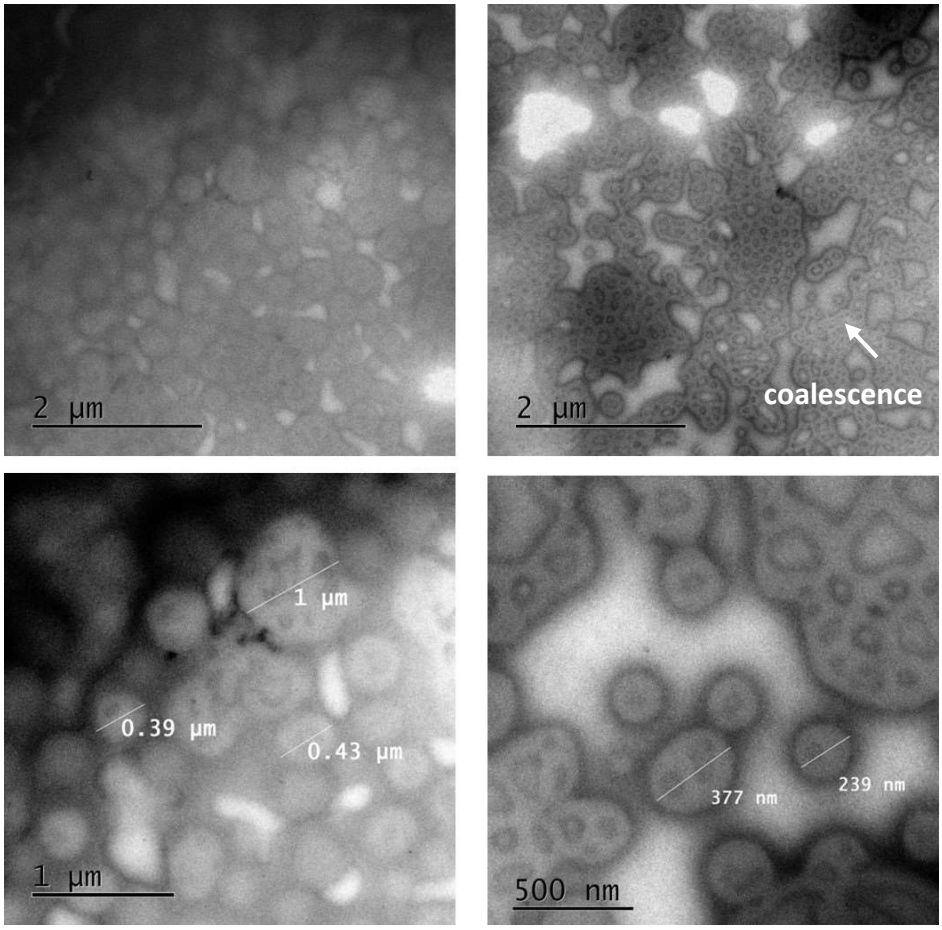

A. 2 TEM images of emulsion made from MontanideTM ISA 206 adjuvant. Imaging was performed with no staining using 0.2 µm K-kit carriers for liquid TEM at different magnifications. September 1, 2017.

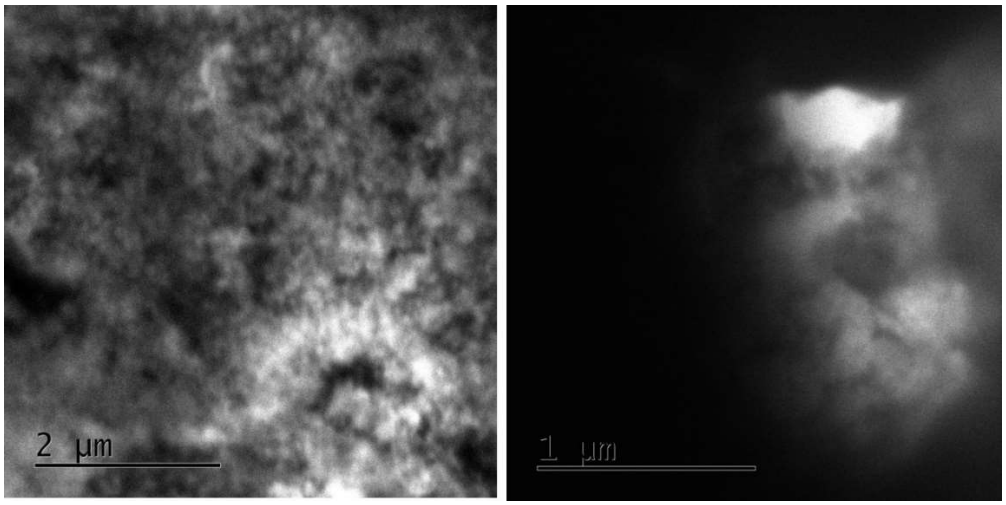

A. 3 TEM images of SEA1 emulsion sample stained with uranyl acetate and taken using 2 µm K-kit carriers for liquid TEM. September 11, 2017.

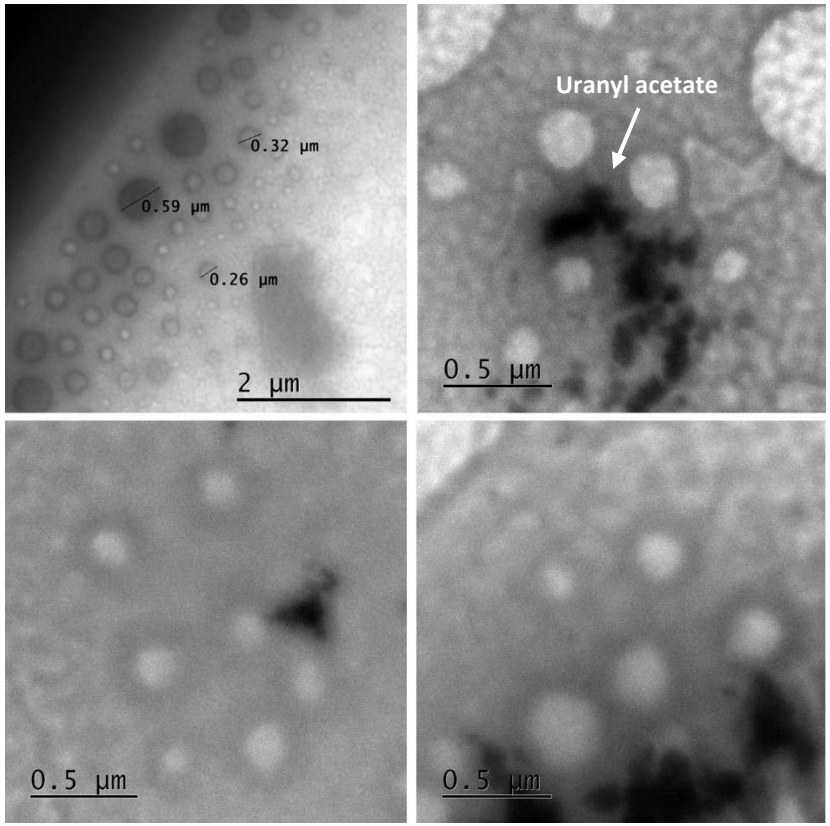

A. 4 TEM images of MontanideTM ISA 206 emulsion performed using 2 µm liquid K-kit carriers and uranyl acetate negative staining. September 11, 2017.

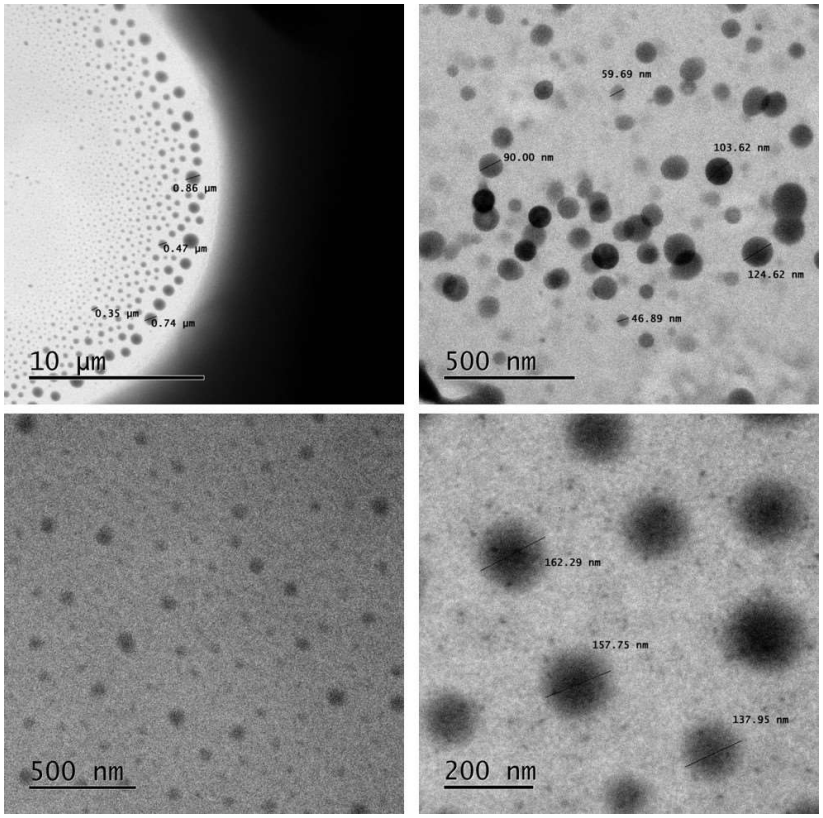

A. 5 TEM images of SEA1 emulsion performed with application of 0.2 µm-height carriers and no uranyl acetate staining. October 5, 2017.

Routine sample preparation

After a pre-imaging 30-minute vacuum-dry of the TEM grids with SEA1 emulsion, the droplets collapsed, forming a film-like structure (top two in Fig. A. 6). Similarly, distorted droplets were observed in images of emulsion prepared with ISA 206 (bottom two in Fig. A. 6).

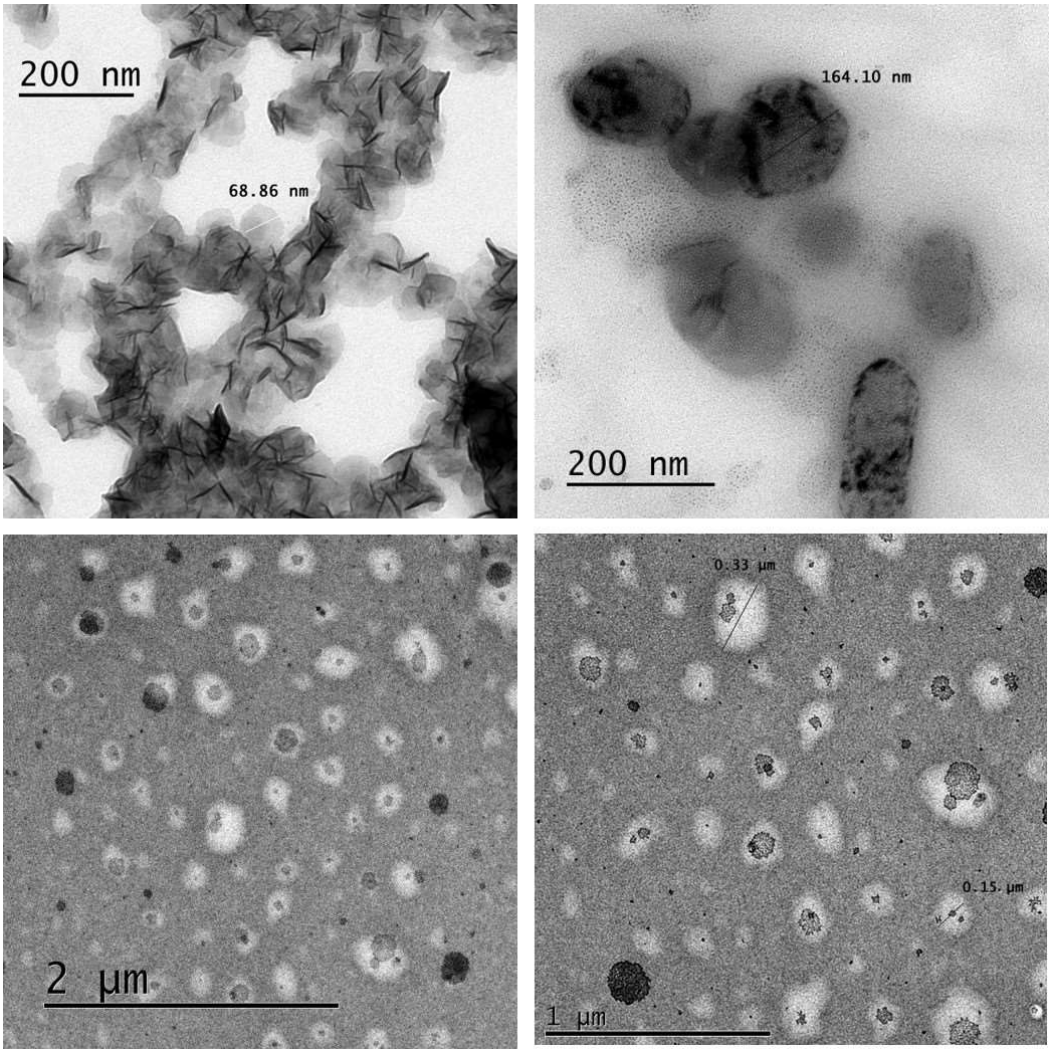

A. 6 TEM images of emulsion samples made with application of routine sample preparation method and without negative staining. The TEM grids with sample were vacuum-dried for 30 min before imaging. The top two images are emulsion prepared with experimental SEA1 adjuvant and bottom two are emulsion made with Montanide™ ISA 206 adjuvant. September 1, 2017.

Emulsions were visualized with greater success when the gentler, “dry-on-the-grid”, sample preparation method was utilized (Fig. A. 7-9). According to Figure 7, the SEA1 emulsion had a majority of the droplets at less than 100 nm in diameter and very few were 200 nm sized droplets. Higher magnifications revealed the multiple (water-in-oil-in-water) structure of the observed emulsion drops (Fig. A. 8). The oil droplets appeared darker than the background due to UA staining, while small internal water droplets had lighter color (Fig. A. 8). Similarly, with ISA 206 emulsion, UA staining dyed the oil droplets a darker color, while small water droplets inside them had lighter appearance (Fig. A. 9).

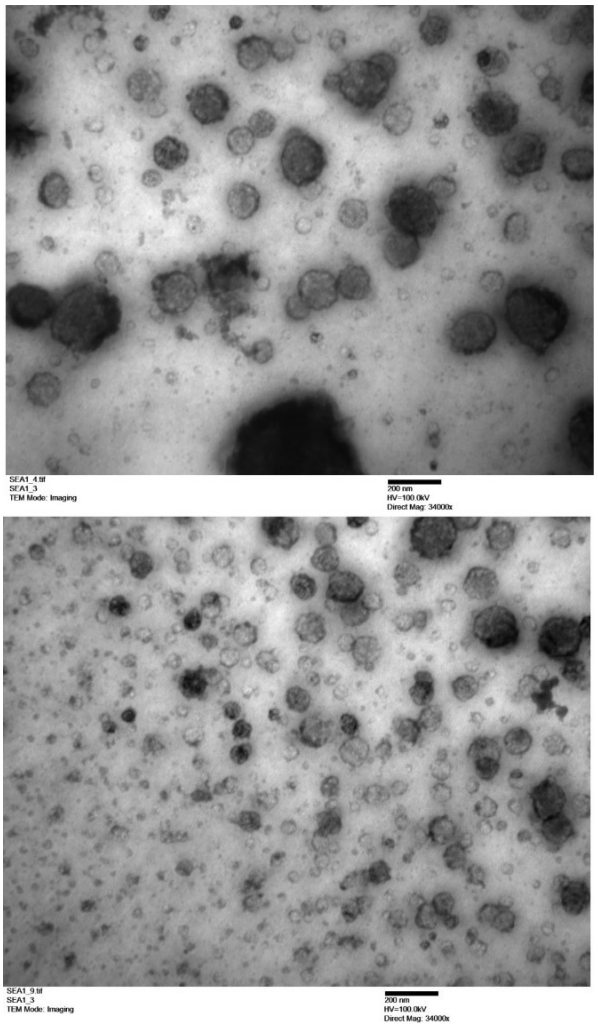

A. 7 TEM images of emulsion made from SEA1 adjuvant with application of gentle dry-on-the-grid protocol, uranyl acetate staining, and taken at magnification of 34,000. October 12, 2017.

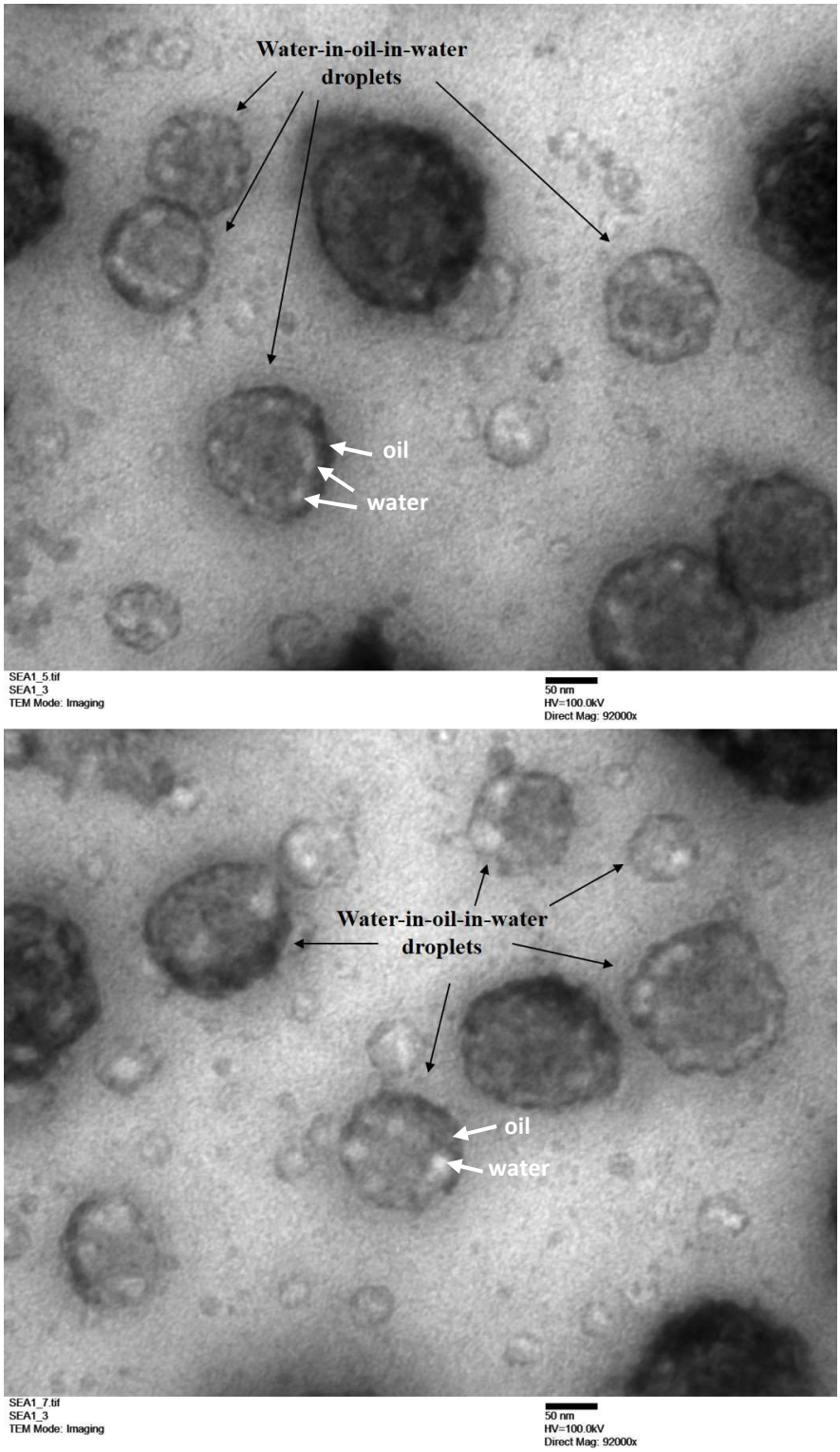

A. 8 TEM images of emulsion prepared with SEA1 experimental adjuvant with application of gentle dry-on-the-grid method, stained with uranyl acetate, and taken at magnification of 92,000. Droplets with multiple water-in-oil-in-water structure can be observed. October 12, 2017.

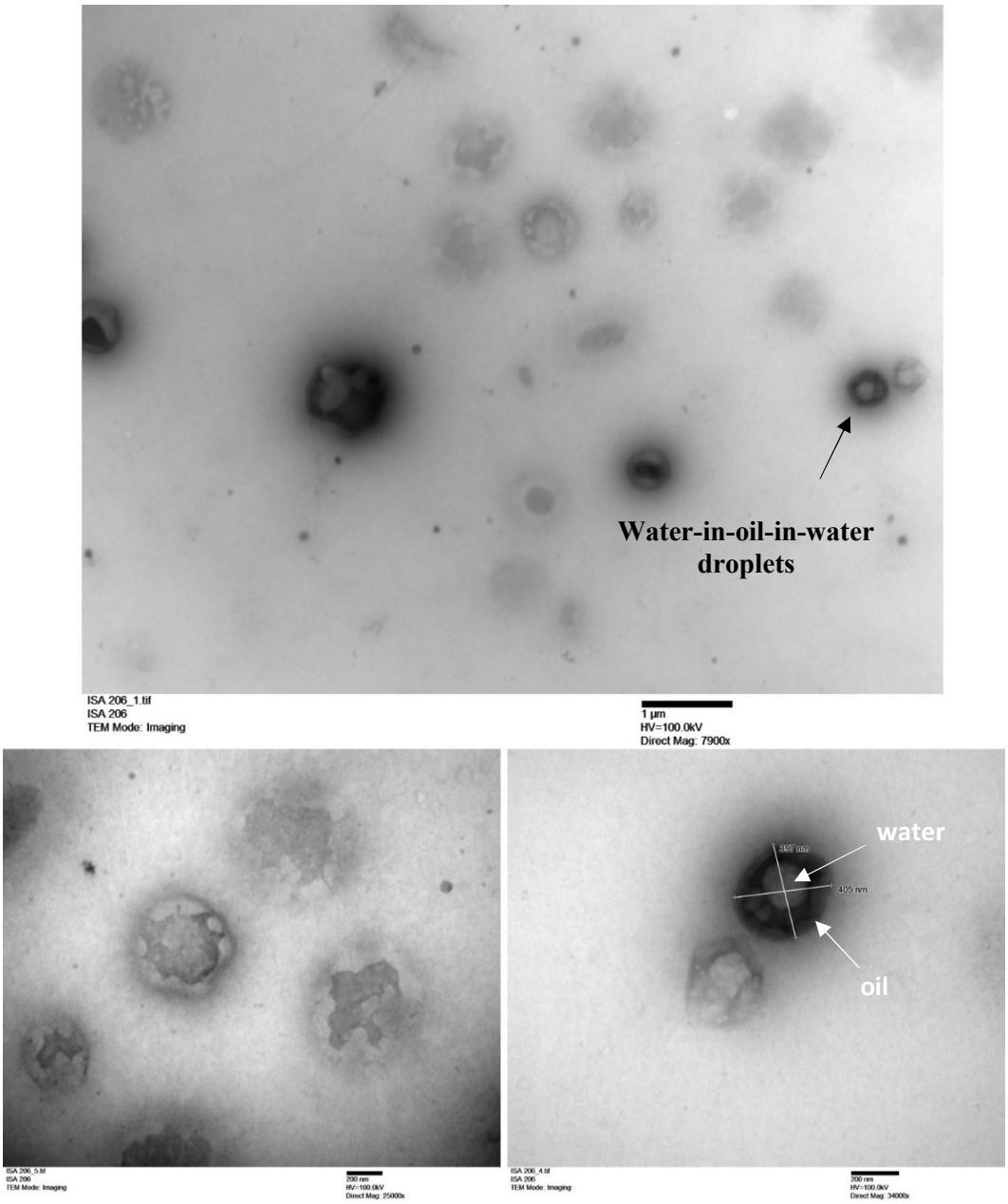

A. 9 TEM images of MontanideTM ISA 206 emulsion with application of gentle dry-on-the-grid sample preparation method and uranyl acetate negative staining, taken at different magnifications. October 12, 2017.

Discussion

When emulsion droplets are in a nanometer size range, only TEM can provide sufficient resolution for viewing their structure. However, the sample preparation is a critical part for

emulsion imaging with TEM. Due to the high-water content, emulsions need to be completely dried out on the grid before placement into a high-vacuum TEM chamber. This can completely distort or destroy the original structure of the emulsion drops. Thus, when the grids with emulsions were vacuum-dried before imaging, only collapsed droplets were observed in TEM pictures, preventing the characterization for the original size or morphology of the droplets (Fig. A. 6). However, when the gentler approach was employed involving the removal of the excess of liquid from the grid with a small piece of paper and no additional drying, emulsion droplets were visualized with better quality and both the size and multiple structure of emulsion droplets were established (Fig. A. 7-9).

The application of liquid cells for viewing the emulsions with TEM was also investigated in this project. Images of SEA1 emulsion with 0.2 μm K-kit carriers revealed the emulsion droplets in their natural state (overlapping each other) and the size of the drops agreed with the dynamic light scattering analysis reported in Chapters 5 and 6 (Fig. A. 1). However, the images could not be reproduced again when another TEM experiment was performed in the same conditions and with the same type of carriers (Fig. A. 5). The electronic beam has been shown to produce radiolysis after contact with water in the liquid cell, which can lead to strong pH changes that result in colloidal instability *(3, 6)*. Thus, some of the SEA1 emulsion droplets depicted in Figure 5 were significantly bigger in contrast to droplets observed in Figure 1. In addition, the substantial coalescence between ISA 206 emulsion droplets viewed in Figure 2 can be also attributed to the electron beam effect on the sample. Furthermore, the use of 2 μm carriers and UA staining did not produce a successful TEM experiment (Fig. A. 3-4). Apparently, the thickness of the sample and the addition of uranyl acetate attributed to the difficulties for permeation of the electronic beam resulting in appearance of blackened areas on the images (Fig. A. 3). Although the use of liquid-cell TEM can be attractive by promising the viewing of emulsion droplets in their native state, the

irradiation of the electron beam can affect the stability of the emulsion droplets. Therefore, experimental conditions such as the electron beam voltage and the microchannel height in the liquid cells should be selected very carefully for successful liquid-cell TEM imaging of the emulsions.

Conclusions

Two different sample preparation methods were used in this project to visualize emulsions with TEM. The liquid-cell TEM technique was explored with application of sample carriers of different heights. The use of carriers with short microchannel height (0.2 μm) and the absence of negative staining produced a more successful outcome in viewing the nanometer emulsion droplets in contrast to the carriers of 2 μm height. However, the TEM experiments with liquid cells were not reproducible, presumably due to the impact of the electron beam radiation on the aqueous emulsion samples. The most successful imaging was done when the gentle, "dry-on-the-grid" protocol was used, allowing the opportunity to confirm the nanoscale size of the droplets and establish water-in-oil-in-water structure of the emulsion made with experimental SEA1 adjuvant.

References

1. Klang, V.; Matsko, N. B.; Valenta, C.; Hofer, F. Electron microscopy of nanoemulsions: An essential tool for characterisation and stability assessment. *Micron* **2011**, *43*.

2. SEPPIC Montanide™ ISA - W/O/W. Ready-to-use adjuvants for water-in-oil-in-water emulsions. *https://www.seppic.com/montanide-isa-w-o-w* (accessed 05/16, 2018).

3. Liao, H.; Zheng, H. Liquid Cell Transmission Electron Microscopy. *Annu. Rev. Phys. Chem.* **2016**, *67*, 719-747.

4. Bio MA-Tek Sample loading for liquid TEM: K-kit. *https://www.youtube.com/watch?v=kFExQtwnjVo* (accessed 8/15, 2018).

5. Liu, K.; Wu, C.; Huang, Y.; Peng, H.; Chang, H.; Chang, P.; Hsu, L.; Yew, T. Novel microchip for in situ TEM imaging of living organisms and bio-reactions in aqueous conditions. *Lab on a Chip* **2008**, *8*, 1915-1921.

6. Schneider, N. M. In *Electron beam effects in liquid cell TEM and STEM;* Ross, F. M., Ed.; Liquid cell electron microscopy; Cambridge University Press: Cambridge, United Kingdom, 2017; pp 140-161.

Appendix B - Hydrogen Peroxide Inactivation of Porcine Reproductive and Respiratory Syndrome Virus for Vaccine Preparation

Abstract

Porcine reproductive and respiratory syndrome virus (PRRSV) is an economically important animal virus that causes reproductive failure and respiratory tract illness in pigs. Current inactivated vaccines have low efficacy against PRRSV. Here, hydrogen peroxide (H_2O_2) was studied as a suitable alternative for inactivated vaccine preparation. The inactivation procedure involved incubation of the North American PRRSV strain NADC-20 solution with different concentrations of H_2O_2 at various temperature conditions followed by evaluation of its viricidal efficacy at two different time points. *In-vitro* studies with Marc-145 cells, inoculated with inactivated viral solutions, demonstrated successful inactivation of virus with the absence of cytopathic effect (CPE) even at very low H_2O_2 concentration of 1% after 1 hour of inactivation procedure. A Western blot experiment was performed to study the effect of H_2O_2 treatment on antibody binding sites of the virus. It has been suggested that an H_2O_2-inactivated virus can be a promising candidate for further *in-vivo* investigation to confirm its efficacy in creating the required protective immunity against PRRSV.

Introduction

Porcine reproductive and respiratory syndrome (PRRS) causes dramatic reproductive failure, pneumonia, and reduced pig growth *(1)* leading to $664 million of economic losses in the US porcine industry annually *(2)*. In 1991, the causative agent, a positive-sense single-stranded enveloped RNA virus of the Arteriviridae family, was discovered *(3)*. The virus infects

macrophages and dendritic cells suppressing the immune system resulting in numerous secondary bacterial infections responsible for high mortality rates in swine *(4)*.

Current efforts to control this disease include the vaccination of pigs with modified-live vaccines (MLV) *(5)*. However, the risk of the reversion to virulence, recombination between wild-type strains and MLV, and the absence of flexibility towards emerging virus strains make MLV insufficient to prevent the disease and completely protect the animals *(6)*. On the contrary, inactivated or killed-virus (KV) vaccines offer safety, but fail to induce the required level of PRRSV-specific antibodies *(7)*. In addition to low efficacy, current KV vaccines have complicated and time-consuming production procedures that require the application of hazardous reactants such as formaldehyde, β-propiolactone, or binary ethylenimine (BEI) *(8)*. Moreover, several studies have demonstrated that these conventional inactivation agents have disadvantages such as strong effects on the immunogenic epitopes of the viruses, high cost, or toxicity *(8, 9)*. Therefore, there is an unmet need to find new suitable inactivation agents that can improve the performance of KV vaccines.

Here, hydrogen peroxide (H_2O_2) was studied as an alternative inactivation agent for PRRS vaccine preparation. Hydrogen peroxide is widely used as an antiseptic and oxidizing agent. In addition, studies with West Nile, Influenza, and Ebola have demonstrated that H_2O_2 treatment inactivates the viruses without affecting their immunogenicity *(10-12)*. In the present research, H_2O_2 was used to inactivate North American PRRSV strain NADC-20. The inactivation procedure was performed at different temperatures and durations. The validation of virus inactivation was confirmed by observing the structural changes caused by invasion of the virus (cytopathic effect) in monkey kidney MARC-145 cells, which are commonly used for PRRSV isolation and vaccine production *(13)*.

In addition, it has previously been demonstrated that most of the protective antibodies and cell-mediated immunity generated against PRRSV are associated with the membrane (M) protein (19-20 kDa) and major envelope glycoprotein (GP) 5, (26-28 kDa) of the virus *(14-16)*. Therefore, the effect of H_2O_2 treatment on these viral proteins was investigated utilizing Western blot analysis.

Materials and methods

Materials

NADC-20 PRRSV was obtained from Dr. Kelly Lager (National Animal Disease Center, USDA-ARS, Ames, USA). The virus was prepared and titrated in MARC-145 cells and stored in aliquots at −80 °C until use. Hydrogen peroxide, H_2O_2 (30%), was purchased from Fisher Scientific (USA). Catalase from bovine liver (38160 units/ml), pH indicator beta-naphthol violet and 2-bromoethylamine hydrobromide 99% were obtained from MP Biomedicals. Sodium thiosulfate was purchased from Sigma Aldrich (USA).

Preparation of inactivation agents

Hydrogen peroxide was used for inactivation procedures as received. Binary ethylenimine (BEI) was synthesized according to the procedure described by Bahnemann *(17)*. Briefly, 2-bromoethylamine hydrobromide (BEA) was diluted in 0.175 M NaOH containing pH indicator to obtain 0.1 M solution. The conversion of BEA to BEI was performed at 37°C for 1 h and confirmed by visual observation of color change of solution from purple to orange (pH drops from ~12.5 to ~8.5). The obtained BEI solution was stored at 4°C until further use.

Virus inactivation

All inactivation procedures were performed in a biosafety cabinet (Biosafety Level 2). PRRSV stock was quickly thawed using a 37°C water bath. Virus was diluted to a titer of ~10^6

$TCID_{50}$/ml using Minimum Essential Medium (MEM, Gibco®) supplemented with 1% Fetal Bovine Serum (FBS, Atlanta Biologicals, USA) before inactivation.

H_2O_2

H_2O_2 was added from a 30% stock solution into the tubes with PRRS virus to obtain three different final concentrations 3 v/v %, 1 v/v %, and 0.1 v/v % H_2O_2 (H_2O_2-PRRSV). A vortex was used for complete mixing of virus with H_2O_2 followed by incubation for 1 and 4 hours at 37°C. Finally, catalase was added to the virus solutions to remove residual H_2O_2 and stop the inactivation.

BEI

PRRS virus was inactivated in 1.5 mM BEI (BEI-PRRSV). A vortex was utilized to ensure the complete mixing of virus with BEI. The virus was incubated with BEI for 24 hours at 37°C. Sterile sodium thiosulfate (1M) was added at 10% of BEI volume to stop the inactivation followed by incubation for 2 hours at 37°C. Validation of viral inactivation was performed using MARC-145 cells.

Validation of inactivation

MARC-145 cells (10^4 cells/well) were propagated in 96-well plates until 70% confluency according to standard protocol. H_2O_2- and BEI-PRRSV solutions were added to cells at 100µl/well followed by incubation for 3 days at 37ºC (5% CO_2). Cells inoculated with untreated virus served as positive controls while and media-only was the negative control.

Cells were observed under light microscope (Axiovert 40 CFL, Carl Zeiss, Germany) to detect the presence of a cytopathic effect (CPE). Images were taken with Axiocam digital camera (Carl Zeiss, Germany).

Western blot experiment with porcine anti-PRRSV serum

The Western blot experiment was performed according to standard procedure. Briefly, 40 µl samples of inactivated and untreated virus were boiled for 5 min with 4x Laemmli Sample buffer (Bio-Rad, USA), supplemented with a or without (if stated) reducing agent, 10% 2-mercaptoethanol (Sigma-Aldrich, USA). Samples were then loaded to the gel cassette and run at 200V for 35 min. Next, the viral proteins were transferred from the gel to a membrane at 100V for 1h in an ice bath. After that, non-specific sites were blocked with 5% milk in phosphate buffered saline (PBS) with 0.05% of Tween 20 (PBST) for 1 h at room temperature. Serum collected from MLV immunized and NADC-20 challenged pigs served as the primary antibody. The membrane was incubated with a 1/5,000 dilution of the pig serum in 1% milk in PBST overnight, at 4°C, with shaking followed by washing three times in PBST. Next, the membrane was incubated with goat anti-swine IgG-HRP antibodies (Santa Cruz Biotechnology, USA, dilution 1/5,000) for 1 h at room temperature followed by washing three times with PBST. SuperSignal^{TM} West Femto Maximum Sensitivity Substrate (Fisher Scientific, USA) was used to image protein bands.

Results

Determination of required concentration of H_2O_2 and time for virus inactivation

The microscopic observation of MARC-145 cells revealed the absence of a cytopathic effect in cells inoculated with virus treated with 0.1% H_2O_2 for 4 hrs. and with 1% and 3% H_2O_2 for 1 h (Fig. B. 1). However, CPE was observed in cells incubated with 0.1% H_2O_2-PRRSV (1-hour inactivation) and in control cells incubated with untreated NADC-20 PRRSV (Fig. B. 1). No CPE was detected in cells inoculated with BEI-PRRSV and negative control cells (Fig. B. 1).

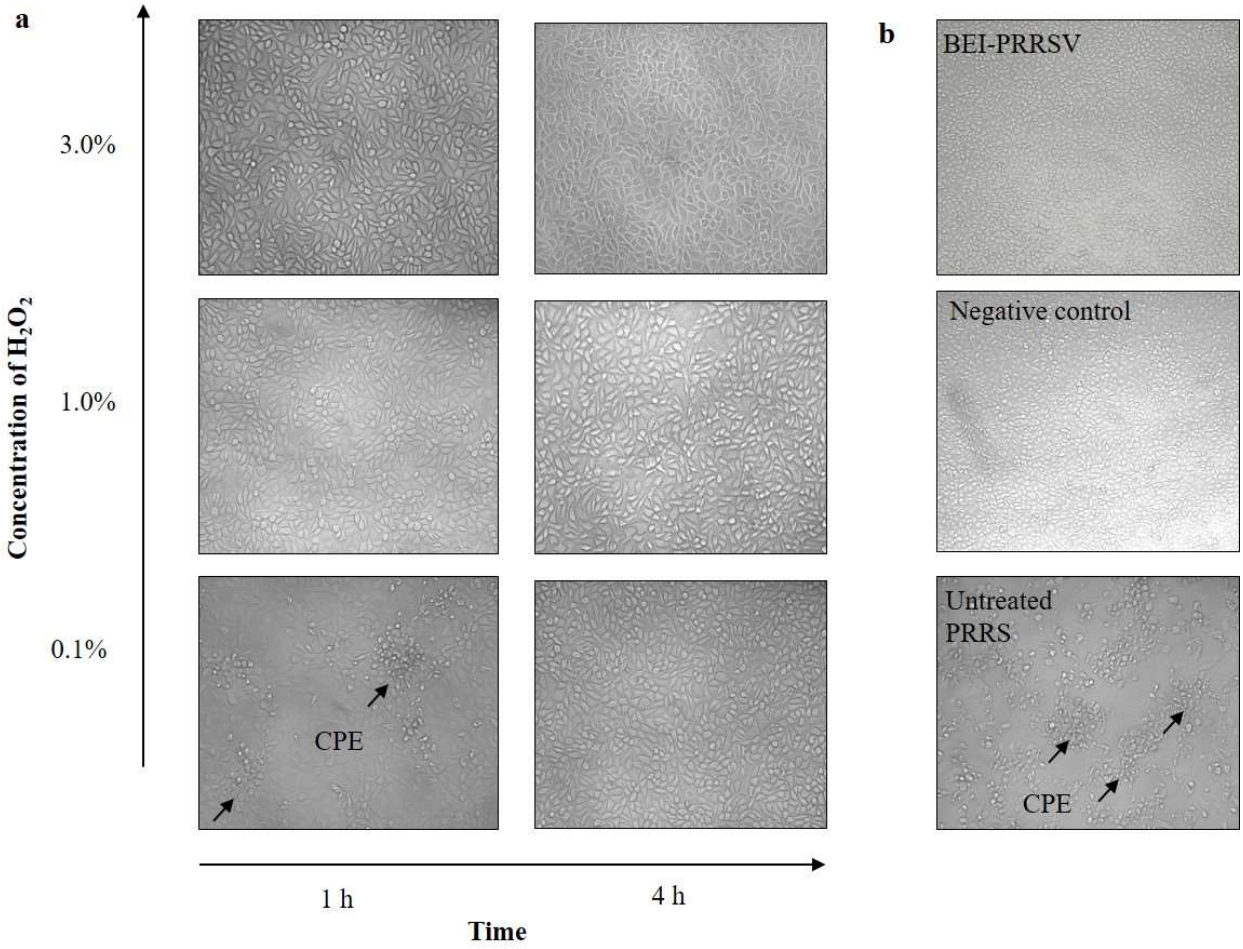

B. 1 Microscopic images of MARC-145 cells. (a) H2O2 treatment of the PRRSV demonstrates the absence of cytopathic effect (CPE) in cells incubated with virus treated with 0.1% H2O2 for 4 hours and with 1% and 3% H2O2 for 1 hour and 4 hours. CPE is observed in cells incubated with 0.1% H_2O_2-PRRSV (1-hour treatment); (b) Cells incubated with BEI-PRRSV and negative control do not have CPE, while it is observed in cells incubated with untreated PRRSV.

Effect of H_2O_2-treatment on antibody bonding sites of the virus

From Figure B. 2a, BEI-treated virus sample (line 3) had a faint M protein band. No significant changes were observed in protein bands of the virus treated with 1% H_2O_2 for 1h (line 7) in comparison with the untreated virus (line 2). Western blotting revealed gradual dissapearance of the M protein band in samples inactivated with increased concentration of H_2O_2 and/or duration of inactivation (lines 6, 5, 4). When a western blot experiment was performed

under nonreducing conditions (Fig. B. 2b), the complete dissappearance of one band and extreme fading of three other bands were observed in the BEI-inactivated sample (line 3) in comparison with untreated the virus sample (line 2). However, samples inactivated with 3% H_2O_2 and 1% H_2O_2 still had one bright and three faint bands (lines 4 and 5, respectively).

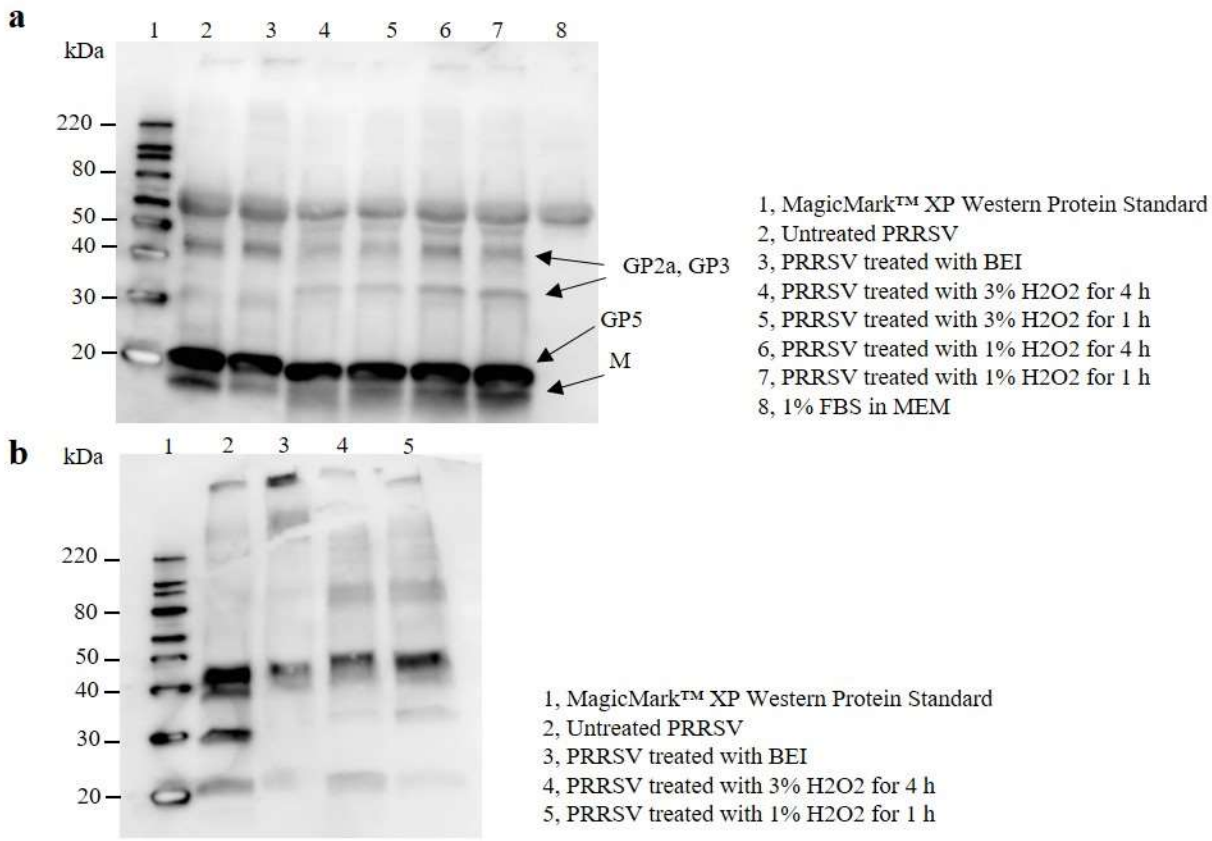

B. 2 Images from Western blotting demonstrate the effect of H2O2 and BEI treatments on membrane protein M and glycoproteins GP5, GP2 and GP3 of PRRSV with application of reducing agent (a) and without (b). The blots were probed with serum of MLV immunized pig as primary antibody and goat anti-swine IgG-HRP secondary antibody.

Discussion

PRRSV causes devastating damages to the porcine industry all over the world *(18)*. At this time, there is no reliable vaccine that is safe to use and effective in inducing protective immunity *(6)*. Commercial MLV vaccines are unsafe, while killed-virus vaccines do not induce the required

level of protective antibodies *(7, 19)*. Therefore, there is a need to improve the efficacy of the vaccines against the PRRS virus.

This study investigates hydrogen peroxide as an inactivation agent for production of KV vaccines for PRRS. First, the ability of H_2O_2 to inactivate the virus was determined and validated using MARC-145 cells. The absence of CPE was observed in cells incubated with PRRSV treated with 0.1% H_2O_2 for 4 hours, 1% H_2O_2 and 3% H_2O_2 for 1 hour (Fig. B. 1) indicating that even very low H_2O_2 concentrations will be enough to kill the virus. In addition, the impact of H_2O_2 treatment on the antigenicity of the virus was studied and compared with BEI, a commonly used inactivation agent *(19, 20)*. Western blot analysis demonstrated that treatment with 1% H_2O_2 preserves the structure of M and GP5 proteins of the virus, as it still can be recognized by the antibodies from the serum of MLV vaccinated pigs (Fig. B 2a). However, the BEI-inactivated viral sample had a faint M protein band signifying structural damage of this important antigenic protein (Fig. B. 2a). A similar result was observed when western blotting was performed under nonreducing conditions (Fig. B. 2b). One protein band completely disappeared, and three others faded in the BEI treated virus sample, while all four bands were visible in H_2O_2-PRRSV samples (Fig. B. 2b). These findings suggest that H_2O_2 is a better choice for preparation of KV vaccines in comparison with BEI, as it causes fewer changes in the conformation of viral proteins that are important for recognition by antibodies generated against PRRSV. In addition, BEI has needed to be synthesized before the inactivation procedure, while hydrogen peroxide was utilized as received. For future research, an H_2O_2-inactivated vaccine should be studied *in-vivo* to confirm its efficacy in creating adequate immune protection against PRRS virus.

Conclusions

In-vitro studies with MARC-145 cells, infected with inactivated viral solutions demonstrate successful inactivation of virus with the absence of a cytopathic effect, even at very low H_2O_2 concentrations of 0.1% after 4 hours of an inactivation procedure and a concentration of 1% after 1 hour of inactivation. In addition, western blot analysis reveals that inactivation of virus with 1% H_2O_2 is less damaging to the antibody binding sites in comparison with a BEI inactivation agent. Therefore, the H_2O_2-inactivated vaccine is a promising candidate for further *in-vivo* investigation to confirm its efficacy in creating protective immunity against PRRSV.

References

1. Goyal, S. M. Porcine Reproductive and Respiratory Syndrome. *J Vet Diagn Invest* **1993***, 5*, 656-664.

2. Holtkamp, D. J.; Zimmerman, J. J.; Yoder, T. K.; Wang, C.; Mowrer, C. L.; Kliebenstein, J. B.; Neumann, E. J.; Rotto, H. F.; Yeske, P. E.; Haley, C. A. Assessment of the economic impact of porcine reproductive and respiratory syndrome virus on United States pork producers. *JSHAP* **2013***, 21*, 72-84.

3. Collins, J. E.; Benfield, D. A.; Christianson, W. T.; Harris, L.; Hennings, J. C.; Shaw, D. P.; Goyal, S. M.; McCullough, S.; Morrison, R. B.; Joo, H. S.; Gorcyca, D.; Chladek, D. Isolation of Swine Infertility and Respiratory Syndrome Virus (Isolate ATCC VR- 2332) in North America and Experimental Reproduction of the Disease in Gnotobiotic Pigs. *J Vet Diagn Invest* **1992***, 4*, 117-126.

4. Murtaugh, M. P.; Xiao, Z.; Zuckermann, F. Immunological responses of swine to porcine reproductive and respiratory syndrome virus infection. *Viral Immunol.* **2002***, 15*, 533.

5. Renukaradhya, G. J.; Meng, X.; Calvert, J. G.; Roof, M.; Lager, K. M. Live porcine reproductive and respiratory syndrome virus vaccines: Current status and future direction. *Vaccine* **2015***, 33*, 4069-4080.

6. Nan, Y.; Wu, C.; Gu, G.; Sun, W.; Yan-Jin Zhang; En-Min Zhou Improved Vaccine against PRRSV: Current Progress and Future Perspective. *Front Microbiol* **2017***, 8*.

7. Charerntantanakul, W. Porcine reproductive and respiratory syndrome virus vaccines: Immunogenicity, efficacy and safety aspects. *WJV* **2012***, 1*, 23.

8. Stauffer, F.; El-Bacha, T.; Da Poian, A.,T. Advances in the development of inactivated virus vaccines. *Recent patents on anti-infective drug discovery* **2006**, *1*, 291.

9. Brown, F. Review of accidents caused by incomplete inactivation of viruses. *Dev. Biol. Stand.* **1993**, *81*, 103.

10. Pinto, A. K.; Richner, J. M.; Poore, E. A.; Patil, P. P.; Amanna, I. J.; Slifka, M. K.; Diamond, M. S. A hydrogen peroxide- inactivated virus vaccine elicits humoral and cellular immunity and protects against lethal West Nile virus infection in aged mice. *J. Virol.* **2013**, *87*, 1926.

11. Dembinski, J. L.; Hungnes, O.; Hauge, A. G.; Kristoffersen, A.; Haneberg, B.; Mjaaland, S. Hydrogen peroxide inactivation of influenza virus preserves antigenic structure and immunogenicity. *J. Virol. Methods* **2014**, *207*, 232-237.

12. Marzi, A.; Halfmann, P.; Hill-Batorski, L.; Feldmann, F.; Shupert, W. L.; Neumann, G.; Feldmann, H.; Kawaoka, Y. An Ebola whole- virus vaccine is protective in nonhuman primates.(VACCINES)(Report)(Author abstract). *Science* **2015**, *348*, 439.

13. Kim, H.; Kwang, J.; Yoon, I.; Joo, H.; Frey, M. Enhanced replication of porcine reproductive and respiratory syndrome (PRRS) virus in a homogeneous subpopulation of MA- 104 cell line. *Arch. Virol.* **1993**, *133*, 477-483.

14. Loemba, H.; Mounir, S.; Mardassi, H.; Archambault, D.; Dea, S. Kinetics of humoral immune response to the major structural proteins of the porcine reproductive and respiratory syndrome virus. *Arch. Virol.* **1996**, *141*, 751-761.

15. Bautista, E.; Suárez, P.; Molitor, T. T cell responses to the structural polypeptides of porcine reproductive and respiratory syndrome virus. *Arch. Virol.* **1999**, *144*, 117-134.

16. Bastos, R. G.; Dellagostin, O. A.; Barletta, R. G.; Doster, A. R.; Nelson, E.; Zuckermann, F.; Osorio, F. A. Immune response of pigs inoculated with Mycobacterium bovis BCG expressing a truncated form of GP5 and M protein of porcine reproductive and respiratory syndrome virus. *Vaccine* **2004**, *22*, 467-474.

17. Bahnemann, H. G. Inactivation of viral antigens for vaccine preparation with particular reference to the application of binary ethylenimine. *Vaccine* **1990**, *8*, 299-303.

18. PRRS Control Economic impact in swine industry. *https://www.prrscontrol.com/prrs-the-disease/economic-impact-in-swine-industry/* (accessed 6/28, 2018).

19. Renukaradhya, G. J.; Meng, X.; Calvert, J. G.; Roof, M.; Lager, K. M. Inactivated and subunit vaccines against porcine reproductive and respiratory syndrome: Current status and future direction. *Vaccine* **2015**, *33*, 3065-3072.

20. Bahnemann, H. Binary ethylenimine as an inactivant for foot-and- mouth disease virus and its application for vaccine production. *Arch. Virol.* **1975**, *47*, 47-56.